BAW-1648
November 1980

# THERMAL-MECHANICAL REPORT — EFFECT OF HPI ON VESSEL INTEGRITY FOR SMALL BREAK LOCA EVENT WITH EXTENDED LOSS OF FEEDWATER



Babcock & Wilcox

BAW-1648

November 1980

# THERMAL-MECHANICAL REPORT — EFFECT OF HPI ON VESSEL INTEGRITY FOR SMALL BREAK LOCA EVENT WITH EXTENDED LOSS OF FEEDWATER

Applicable to

Babcock & Wilcox 177-Fuel Assembly
Nuclear Steam Systems

BABCOCK & WILCOX
Nuclear Power Group
Nuclear Power Generation Division
P. O. Box 1260
Lynchburg, Virginia 24505

Babcock & Wilcox

Babcock & Wilcox
Nuclear Power Group
Nuclear Power Generation Division
Lynchburg, Virginia

Report BAW-1648

November 1980

# Thermal-Mechanical Report — Effect of HPI on Vessel Integrity for Small Break LOCA Event With Extended Loss of Feedwater

Key Words: Brittle Fracture, Small Break, Reactor Vessel Downcomer, High Pressure Injection

## ABSTRACT

This report has been prepared to address issues raised in a letter from D. F. Ross of the U. S. Nuclear Regulatory Commission to J. H. Taylor of Babcock & Wilcox. The letter, dated July 12, 1979, is entitled "Information Request on Reactor Vessel Brittle Fracture." The investigation reported herein addresses the possibility of exceeding the fracture mechanics acceptance criteria of the reactor vessel in a nuclear steam system caused by excessive cooling by high-pressure injection flow (without reactor coolant loop flow) during small breaks (or total loss of feedwater events where the operator opens the power-operated relief valve) where the reactor coolant pressure is kept relatively high owing to choked flow out the small break (or open PORV).

CONTENTS

CONTENTS (Cont'd)



List of Tables



List of Figures

## Figures (Cont'd)

## Figures (Cont'd)

## Figures (Cont'd)

# 1. INTRODUCTION AND DISCUSSION

The investigations described in this report were performed to evaluate the concern of brittle fracture during recovery from a small LOCA with extended loss of feedwater in response to NRC's information request dated July 12, 1979.[2] This report describes the analyses performed and the results obtained.

## 1.1. The Brittle Fracture Concern

The concern associated with brittle fracture during a small LOCA with the required assumption of extended loss of feedwater can best be understood through the use of simple schematics of the system. Figure 1-1 shows the reactor coolant flows within the reactor coolant system during normal operation.

Figure 1-2 shows the system flows a few minutes after a small break typical of a stuck-open power-operated relief valve (PORV). During this phase, the reactor coolant system (RCS) pressure and temperature are dropping and RCS flow is decreasing as a result of an operator requirement to trip the RC pumps on ESFAS actuation. The temperature in the RCS is higher than in the secondary side of the steam generator; thus, the generators assist in removing heat and circulating the RCS coolant. Assuming no feedwater is available, the RCS must be cooled by injecting coolant from the high-pressure injection (HPI) system. The warm RCS loop water is well mixed with the cold HPI flow as it passes the HPI nozzle; thus, relatively warm water enters the vessel and downcomer.

If the transient proceeds unhindered, RCS temperature and pressure continue to fall and steam voids will form in the system. The rate of temperature and pressure decrease and the volume of voids is primarily a function of the break size. At this point, natural circulation loop flow can cease. For the larger small breaks assuming an extended loss of feedwater and no forced RC flow, loss of natural circulation could occur in 8 to 15 minutes and is partly the result of voids at the top of the hot leg and partly the result of heat removal capability by the steam generators. Loss of steam generator heat removal occurs when the RCS temperature falls below the secondary system temperature.

When loop flow ceases, the cold HPI water will begin to cool the cold leg and subsequently flow into the reactor vessel (RV) downcomer. There it will mix with the warm vent valve return flow as shown in Figure 1-3. The system will stay in this condition, with the downcomer fluid temperature gradually decreasing as decay heat decreases, until reactor coolant loop flow is initiated. Reactor coolant pumps are normally restarted once 50F subcooled conditions are re-established around the entire loop. No credit is taken for this in the analysis. Instead, it is assumed that reactor coolant pumps are not started. If RC pressures remain high enough and there is insufficient vent valve flow or mixing, the RV wall temperatures may decrease to the point where cracks in the RV could initiate if flaws exist in the RV metal.

The potential for brittle fracture of the reactor vessel is dependent upon RV material properties, flaw size from which the brittle fracture initiates, temperature, and stress. The main components of stress are usually the RC pressure and vessel thermal gradients due to cooling. Transients that exhibit high vessel stress at a low RV temperature must be evaluated to ensure that the fracture mechanics acceptance criteria will not be violated during the transient considering the vessel irradiated material properties and postulated flaw sizes.

## 1.2. Investigations

The analyses presented in this report can be divided into four areas:

1. LOCA analysis.
2. Reactor vessel downcomer mixing.
3. Reactor vessel cooldown analysis.
4. Linear elastic fracture mechanics.

The LOCA analyses provided all the information necessary for performing the linear elastic fracture mechanics (LEFM) analyses except the RV downcomer temperature next to the RV wall and the RV wall temperature versus time. The LOCA analyses determined the RV downcomer temperature assuming complete mixing of the HPI and vent valve flows entering the downcomer. The extent to which mixing occurs is uncertain; therefore, various RV downcomer mixing calculations were made using different assumptions. Next, temperature gradients in the RV versus time are determined.

Finally, LEFM analyses were conducted for different LOCA events assuming different amounts of downcomer mixing. The analyses performed are summarized below.

The combination of LOCA, mixing, vessel cooldown, and LEFM analyses which will be emphasized in this report are summarized as cases 1 through 4 in Table 1-1.

### 1.2.1. LOCA Analyses

Several LOCA analyses were performed. Three breaks (0.007, 0.015, and 0.023 $ft^2$) were analyzed assuming no feedwater to the steam generators. They were located at the top of the pressurizer. The analyses were performed both with and without operator action to throttle back the HPI flow. For the three cases with operator action (cases 2-4, Table 1-1), the assumed action was to reduce HPI flow when the core outlet temperature reached 100F subcooled and then maintain approximately 100F subcooling at the core outlet. The primary purpose of the LOCA analyses was to determine the HPI flow rate, vent valve flow rate and temperature, RCS pressure, and RV downcomer temperature. The 0.007-$ft^2$ pressurizer break with no operator action (case 1, Table 1-1) was analyzed in detail using the CRAFT computer code[1] for 10 hours real time in response to the NRC-requested analysis.[2] The other LOCA analyses used the CRAFT code only during the blowdown stage of the transient. After the RCS refilled with water a steady-state analysis was performed to determine the reactor vessel conditions. The steady-state analytical method was benchmarked against the CRAFT analysis for the 0.007-$ft^2$ pressurizer break with no operator action. The LOCA analyses are described in detail in section 2 of this report.

### 1.2.2. RV Downcomer Temperature Evaluation

Fracture mechanics analyses require calculation of the RV wall temperature, which in turn depends on the downcomer fluid temperature. It is expected that there will be significant mixing, both in the cold leg piping in the area of HPI injection and in the downcomer, but because of the complex geometry of the downcomer region, quantifying this effect represents the principal uncertainty in the investigation. For this reason, very conservative bounding calculations were also performed. The analyses performed to evaluate potential mixing are discussed in section 3.

### 1.2.3. RV Cooldown Analyses

Once the downcomer fluid temperature at the vessel wall is determined, the temperature gradients versus time through the wall must be determined. The reactor vessel cooldown analyses are described in detail in section 4.

### 1.2.4. Linear Elastic Fracture Mechanics Analyses

Linear elastic fracture mechanics analyses were performed for each of the break cases and for a range of mixing assumptions. These analyses are described in section 5.

## 1.3. Assumptions and Conservatisms

Assumptions are used throughout this report as necessary to address the items contained in the Staff's July 12, 1979 information request. Three fundamental assumptions which have been made to address the requested information are (1) an extended loss of all feedwater, (2) subsequent extended loss of both forced and natural circulation, and (3) combining worst case plant parameters in order to perform a generic analysis which conservatively envelops the operating B&W plants.

Since the issuance of the Staff request, programs have been undertaken or completed which significantly reduce the potential of these situations occurring. Extensive upgrades underway to increase the reliability of the emergency feedwater systems decrease the probability of ever experiencing an extended loss of feedwater and the need to cool the core via the HPI system.

In addition, as mentioned above, current instructions to plant operators call for restarting reactor coolant pumps once 50F subcooled fluid conditions are re-established throughout the system. This is also ignored in the analysis.

The main conservatisms and assumptions used throughout this report are summarized below.

1. All feedwater is lost for an extended period of time.
2. All reactor coolant pump forced flow is lost for an extended period of time.
3. Core flow into the downcomer is assumed to pass through four vent valves rather than the eight valves existing on all but one plant. This reduces the amount of warm water entering the downcomer.

4. A hypothetical maximum HPI flow capacity is assumed over the entire RCS pressure range analyzed. No single plant can achieve this hypothetical capacity over the entire pressure range.

   This assumption affects all the analyses, including those which assume operator action to throttle HPI, since the initial reactor vessel cool-down prior to achieving 100F subcooling at the core outlet is maximized, resulting in increased thermal stresses during the transient.

5. The MIX2 mixing analyses (section 3) assume little HPI-vent valve flow mixing in the downcomer. The HPI flow was assumed to enter the downcomer and essentially stream down the RV wall and mix with the vent valve flow, which is assumed to be circumferentially distributed.

6. In addition to HPI flow mixing with the hot water coming from the vent valves, several other mechanisms are available for heating the HPI flow

   a. Upstream mixing in the cold leg piping.
   b. Heating by the reactor vessel walls.
   c. HPI pump energy.
   d. Heating by the cold leg piping.

   These effects, however, were conservatively ignored in all the analyses. The heat available from items a and b above is expected to be significant. The hotter fluid from the vent valves is expected to travel into the cold leg piping beyond the 2 feet which were modeled. The vent valve flow will mix with and heat the HPI fluid in the cold leg before it enters the downcomer. This is the gravity effect discussed in section 3. The reactor vessel wall also will provide heat to the downcomer fluid. However, a more important feature of this heating is the inherent tendency to reduce the wall to fluid heat transfer. This is because the fluid next to the vessel wall is heated up locally. The buoyancy force due to the density gradient tends to oppose the downward flow and as a result, the velocity of the fluid near the vessel wall could be slowed or even reversed. This mixed convection phenomenon would tend to reduce heat transfer from the vessel wall into the fluid and maintain the vessel wall temperature higher than predicted by these calculations.

7. A worst-case HPI fluid temperature of 40F is assumed.

8. Linear elastic fracture mechanics (LEFM) methods were used in the brittle fracture analysis. No credit was taken for warm prestressing.

Table 1-1. Analysis Summary - Cases 1 Through 4

| | Case 1 | Case 2 | Case 3 | Case 4 |
|---|---|---|---|---|
| LOCA analysis | 0.007-$ft^2$ pressurizer break, no HPI throttling | 0.007-$ft^2$ pressurizer break with HPI throttling | 0.023-$ft^3$ pressurizer break with HPI throttling | 0.023-$ft^2$ pressurizer break with HPI throttling |
| Mixing analysis | Complete, perfect mixing (CRAFT) | Distributed vent valve flow, streaming HPI flow (MIX2) | Distributed vent valve flow, streaming HPI flow (MIX2) | No mixing |
| Reactor vessel cooldown analysis | Constant heat transfer (BEFRAM) | More detailed analysis (see section 4) | More detailed analysis (see section 4) | More detailed analysis (see section 4) |
| LEFM (fracture analysis) | LEFM at 6 EFPY | LEFM at 3.8 EFPY | LEFM at 3.8 and 4.8 EFPY | LEFM at 3.8 EFPY |

Figure 1-1. RCS Flow During Normal System Operation

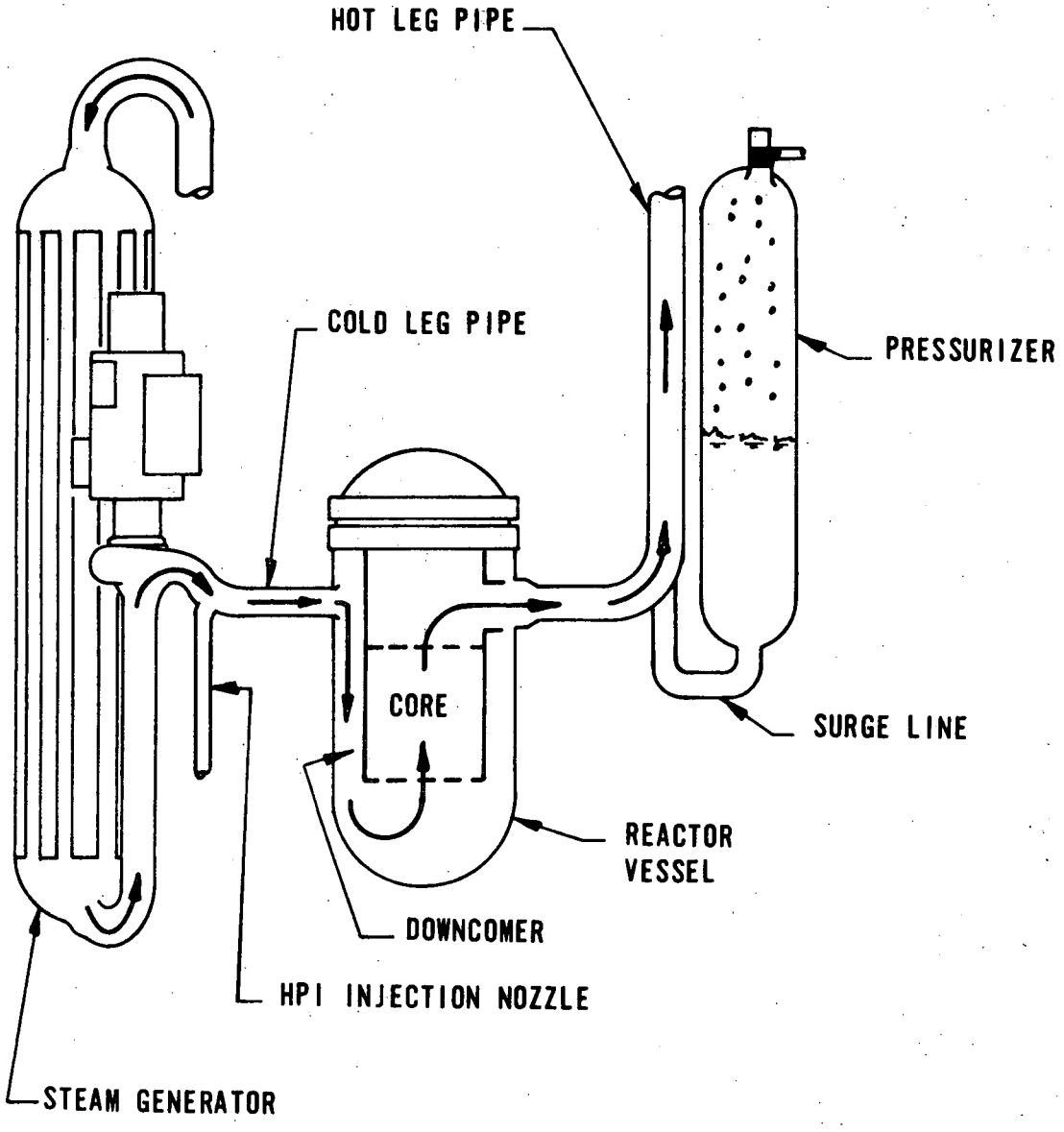

Figure 1-2. RCS Flow During Total Loss of Feedwater Event With a Small Break

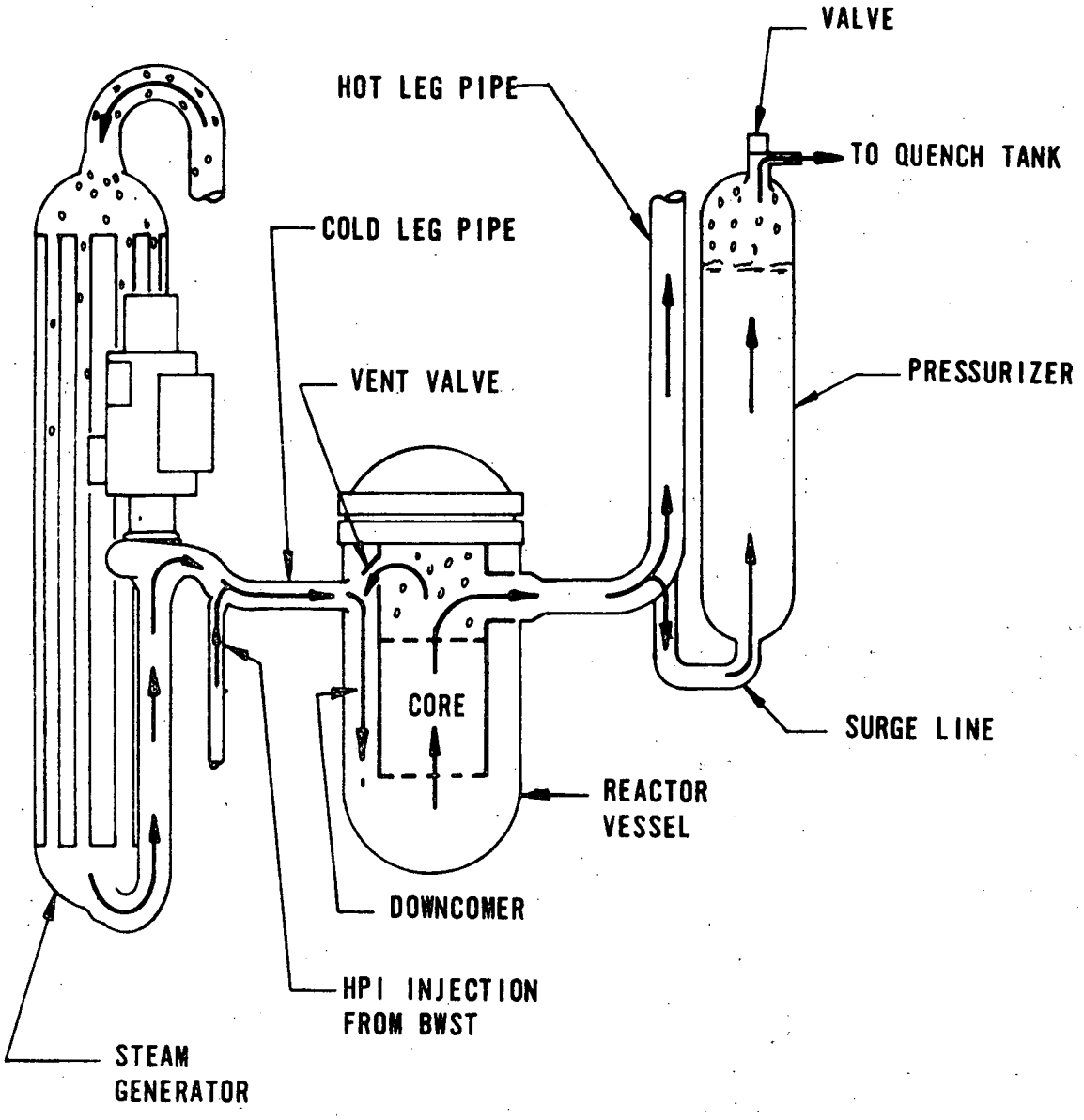

Figure 1-3. Reactor Vessel Flow During Small Break

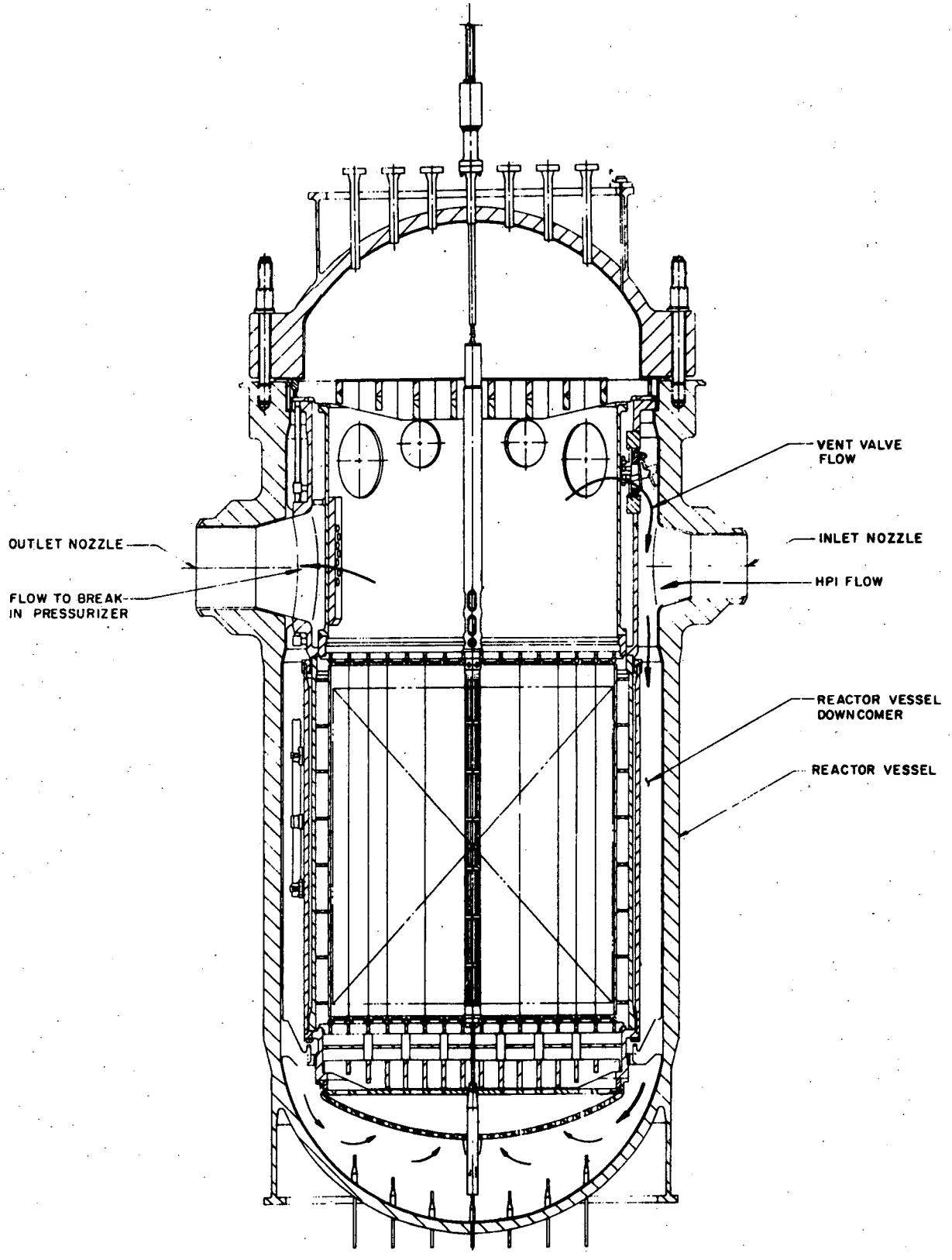

# 2. SMALL BREAK ANALYSIS

In order to bound the brittle fracture concern, a number of evaluations and small-break LOCA analyses were performed; these included (1) evaluating worst-case inputs for the analyses, (2) running one break size out 10 hours, (3) analyzing a spectrum of breaks using worst-case HPI flow to help define the worst-case break size, and (4) analyzing the spectrum of breaks assuming operator action to throttle HPI based on subcooling at the core outlet.

## 2.1. Evaluation of Worst-Case Parameters

The most limiting transient is considered to be the one that produces a system pressure coming closest to the maximum allowable pressure as determined by a linear elastic fracture mechanics analysis (LEFM). The maximum allowable pressure is a function of three parameters — temperature, rate of temperature change, and material properties. Of these three parameters, only temperature and rate of temperature change are affected by the transient variables of HPI flow, break location, and break size. Therefore, an investigation was undertaken to define the worst-case parameters (HPI flow, break location, and break size) for use in ECCS/brittle fracture analyses. The results of the investigations are provided below.

### 2.1.1. HPI Flow Effect

HPI flow rate has a significant impact on RCS pressure and downcomer temperature. When HPI flow increases, the RV downcomer water temperature decreases and the RCS pressure increases. Both of these changes increase the potential for reactor vessel brittle failure. Therefore, the worst condition from the standpoint of brittle fracture mechanics is the condition of maximum HPI flow into the RCS. Except where operator action is explicitly modeled, the analyses assumed the maximum HPI system flow allowed by the piping configuration with three HPI pumps operating at pressures above ∿1500 psig and the flow from two HPI pumps and two makeup pumps (as on Davis-Besse) for RCS pressures below ∿1500 psig (see Figure 2-1 for the pump head curves used in the analyses).

This means that the unthrottled analysis (case 1, Table 1-1) encompasses the maximum HPI flow injection capability of all 177-FA plants. This also means that for the throttled analyses (cases 2-4, Table 1-1) the initial cooldown prior to achieving 100F subcooling at the core outlet and beginning to throttle HPI is maximized. This is conservative with respect to the thermal shock concern.

### 2.1.2. Break Location Effect

A small unmitigated LOCA with prolonged total loss of feedwater and RC pump trip will eventually result in a loss of primary loop circulation. Under this condition, mixing of cold HPI water with the water in the RV downcomer is primarily dependent on the capability of the vent valves to provide circulation of hot water into the downcomer.

For cold leg breaks, the hot water leaving the core flows (1) through the hot leg, steam generator, and broken cold leg to the break, and (2) through the vent valve, downcomer, and broken cold leg to the break. The latter path has the least flow resistance and thus allows a large portion of the hot water to enter the downcomer for mixing. Furthermore, the diversion of HPI water to the break reduces the total amount of HPI water entering the downcomer. For hot leg or pressurizer breaks, more HPI water is available to enter the downcomer. In addition, less vent valve flow occurs in a hot leg or pressurizer break, thus decreasing the amount of hot water available for downcomer mixing. As a result, the most severe downcomer conditions will result from a break in the hot leg or pressurizer. The analyses that follow use a pressurizer break to evaluate system conditions.

### 2.1.3. Break Size Effect

Because of the combination of parameters that influence brittle fracture susceptibility, the worst break size cannot be determined a priori. As the break size increases, the downcomer temperature decreases due to a lower system pressure and increased HPI flow. However, the lower system pressure tends to offset the effect of the lower temperature. In addition, the initial cooldown rate increases as the break size increases. Because these effects tend to offset each other, a spectrum of breaks was analyzed to show the effect of the break size. Three pressurizer break sizes — 0.007, 0.015, and 0.023 $ft^2$ — were analyzed. The 0.007-$ft^2$ corresponds to the PORV orifice area, the

0.023-$ft^2$ break corresponds to that of the safety valve, and 0.015-$ft^2$ is an intermediate-size break. The bounding break sizes were chosen by the following logic:

1. The 0.007-$ft^2$ break was the smallest break size considered for this investigation because the operator is instructed by procedures to open the PORV during a loss-of-feedwater event.

2. Break sizes larger than 0.023 $ft^2$ result in more rapid depressurization to pressures at which the LPI system provides makeup (with little or no repressurization). The transient response of these larger breaks is similar to that of the large break LOCA being considered under NRC Task Action Plan A-11. Therefore, 0.023-$ft^2$ is the largest break size that was considered in this investigation.

While the discussion above indicates that break sizes can be adequately bounded, the worst break with respect to thermal shock cannot be defined a priori because of the interation of HPI flow, pressure, and temperature on the brittle failure concern. Therefore, the PORV case was chosen for the detailed 10-hour CRAFT run since it represents the most probable event.

## 2.2. LOCA Analyses Without Operator Action to Throttle HPI Flow

### 2.2.1. 0.007-$ft^2$ Pressurizer Break (Case 1, Table 1-1)

A 10-hour CRAFT analysis was conducted to determine the system response for an extended total-loss-of-feedwater accident.[1] The break size chosen was 0.007 $ft^2$ at the top of the pressurizer. This corresponds to an open PORV, which is the most likely small break to accompany an assumed total-loss-of-feedwater event.

#### 2.2.1.1. Model Development

In response to the NRC request to provide an analysis of the thermal-mechanical conditions in the vessel for 10 hours, an eight-node CRAFT model, as shown in Figure 2-2, was developed to determine the thermal-hydraulic conditions in the vessel.[2] This model was compared with the 22-node model developed for the small break LOCA analysis. A comparison of the results from both models (as shown in Figures 2-3 and 2-4) shows that the simplified model can adequately predict the thermal-hydraulic conditions in the vessel. A sudden drop in the downcomer temperature is caused by the initiation of HPI. The system noding is described below.

Node 1: Reactor vessel downcomer and lower plenum.

Node 2: Reactor core and upper plenum.

Node 3: Cold legs between RC pumps and reactor vessel.

Node 4: Hot legs.

Node 5: Primary side of steam generators and cold legs between steam generators and RC pumps.

Node 6: Secondary side of steam generators.

Node 7: Pressurizer.

Node 8: Containment.

The CRAFT code assumes homogeneous mixing of the liquids in a node and determines its thermodynamic conditions based on the thermal equilibrium between the steam and liquid phases. This assumption will result in complete mixing of the cold and hot fluids entering the downcomer region from the cold legs and vent valves, so the downcomer node temperatures calculated by CRAFT are mixed mean temperatures.

2.2.1.2. Assumptions Used for 0.007-$ft^2$ Break

The 0.007-$ft^2$ pressurizer break size (PORV throat area), without operator action to throttle HPI flow, was chosen for the 10-hour CRAFT analysis since operator guidelines call for opening the PORV and HPI injection if all feedwater is lost. The following key assumptions were made in this analysis:

1. Reactor and RC pumps trip at time zero. Mixing of cold HPI water with the hot fluid in the RCS is minimized when no flow circulation around the primary loop is assumed, i.e., RC pump trip and loss of steam generator heat removal capability.

2. Loss of main and emergency feedwater is assumed to occur simultaneously at time zero.

3. PORV is opened at 20 minutes by operator action.

4. HPI is actuated at 20 minutes — HPI system flow without operator action is assumed as described in section 2.1.1. This HPI flow and the coldest BWST temperature (40F) will promote a colder downcomer temperature.

5. Four vent valves are modeled. The vent valve flow enhances mixing. The most severe case would be no vent valve flow since this produces lower downcomer temperatures. However, the system is self-compensating with

respect to vent valve flow; decreasing the vent valve flow promotes a higher $\Delta P$ across the vent valve, which will increase flow through the valve. Four vent valves were modeled although all plants except Davis-Besse have eight.

6. A Moody discharge model with a discharge coefficient of 0.75 was used to calculate flow through the open PORV. This valve is based on the normalization of the Moody choked flow to the design steam flow through the PORV.

7. Initial operating power level is 102% of 2772 MWt.

8. Decay heat is based on 1.2 times the ANS standard.

Modeling of the piping and quench tank downstream of the PORV was treated as a part of the containment since flow choking always occurs at the PORV.

For purposes of this analysis, the HPI has been injected directly into the downcomer at the inlet elevation. HPI flow into the cold leg pipe volume (node 3) between the reactor vessel and the RC pumps will reduce the node temperature below the lower bound of the steam table used in CRAFT. In order to avoid this difficulty, the HPI flow was injected directly into the downcomer.

The vent valve flow area is based on four vent valves in a fully open position. As the differential pressure across the vent valve falls below 0.25 psi, the valve opening angle decreases. The flow reduction due to the partial opening of the vent valve is accomplished by increasing the flow resistance in accordance with the $\Delta P$ across the vent valve as shown in Table 2-2.

2.2.1.3. PORV Relief Line Choking Evaluation

An evaluation was performed to determine whether choking flow ever occurs downstream of the PORV. If choked flow occurs in the downstream piping, mass accumulation and pressure buildup in the pipe will result. This may create an unchoking condition of the PORV. The upper and lower boundary conditions in the pressurizer were used to examine the flow characteristics in the downstream piping to demonstrate that downstream choking will not occur. The calculations are provided below.

1. Upper Bound Condition

The Moody choked flow through the PORV is calculated for an upstream condition of $P_o$ = 2500 psia and $h_o$ - 731.7 Btu/lbm as follows:

Mass flux $G_{Moody}$ = 11,369 lbm/ft$^2$-s,

Throat pressure $P_t$ = 1500 psia,

Exit quality x = 15%,

Flow through PORV $W_{porv} = AxG_{Moody} = 0.007 \times 11{,}369 = 97.6$ lbm/s.

Using the throat pressure and the exit quality, the enthalpy of the mixture is 695.4 Btu/lbm. The choked flow in the downstream pipe is calculated using the PORV exit condition, i.e., $P_o$ = 1500 psia and $h_o$ = 695.4 Btu/lbm:

Mass flux $G_{Moody}$ = 7543 lbm/s-ft$^2$

Throat pressure $P_t$ = 885 psia,

Flow rate $W_{pipe} = AxG_{Moody} = 0.051 \times 7543 = 384.7$ lbm/s.

2. Lower Bound Condition

With pressurizer pressure $P_o$ = 1400 psia and enthalpy $h_o$ = 598.8 Btu/lbm, the choked flows through the PORV and the downstream pipe are determined similarly:

$W_{porv} = 0.007 \times 9064 = 63.4$ lbm/s,

$P_t$ = 830 psia,

x = 5%,

$h_o$ = 549.2 Btu/lbm.

The choked flow in the downstream pipe for P = 280 psia and h = 549.2 Btu/lbm is

$W_{pipe} = 0.051 \times 6383.1 = 325$ lbm/s.

The Moody discharge model was used to calculate steam and saturated water flow through the PORV. The orifice equation was used to calculate subcooled water flow. The pressure in the quench tank was assumed to reach equilibrium with the containment within 20 minutes; the maximum pressure drop between the PORV and the quench tank will be 200 psi.

The calculations above indicate that the flow in the downstream pipe is always greater than that through the PORV. Therefore, choked flow will occur only through the PORV during the transient.

2.2.1.4. Results

The sequence of events for the 0.007-$ft^2$ case is tabulated in Table 2-1. The main events can be summarized as follows:

| Sequence of events | Time, s |
|---|---|
| • Reactor trip, RC pump trip, turbine trip, and loss of all feedwater. | 0.0 |
| • Secondary side boils dry. | 420.0 |
| • RCS repressurizes and exceeds safety valve setpoint pressure of 2515 psia, and safety valves open. | 780.0 |
| • PORV is open and HPI is initiated (operator action). | 1,201.0 |
| • Loop flow essentially stops. | 2,300.0 |
| • HPI flow matches leak flow, and system reaches a subcooled state at approximately 1500 psia. | 5,300.0 |
| • End of analysis. | 36,000.0 |

Following reactor trip, the steam generator provided sufficient cooling and the system depressurized. The system repressurized and exceeded the safety valve setpoint pressure after steam generator cooling was lost at 420 seconds. The loop flow continued until approximately 2300 seconds into the transient. Loop flow was maintained because both the hot and cold legs were filled with water during this period and the density gradient between the cold and hot legs was enough to maintain the loop circulation. Figures 2-5 through 2-8 show the liquid levels in cold legs, hot legs, pressurizer, and reactor vessel. The fluid temperature plots, shown in Figures 2-9 through 2-11, indicate that the primary system reached a subcooled state at approximately 5300 seconds. The flow rates and qualities as a function of time for the core exit, PORV, vent valve, and HPI are provided in Figures 2-12 through 2-18. Limited steam flows were observed during the early part of the transient. The water inventory in the primary system is presented in Figure 2-19, and the pressure in the core as a function of time is shown in Figure 2-20. The system pressure stabilized at 1500 psia. The vent valve flow continued for the entire 10 hours. Pressurizer fluid/metal temperature, upper head metal temperature, and cold leg water temperature as a function of time are presented in Figures 2-21 through 2-23.

2.2.1.5. Conservatisms

1. Because this analysis is generic, maximum achievable HPI flow was considered. As indicated in section 2.2, this involved the combination of two different HPI systems.
2. No operator action was assumed to reduce the HPI flow.
3. HPI flow was assumed to be directly and totally injected into the downcomer. If the actual piping configuration were modeled whereby the HPI is directed into the cold leg pipe, a fraction of the total HPI flow injected tends to flow backward through the steam generator resulting in less HPI flow into the downcomer and a less severe temperature degradation.
4. Four vent valves are also used in the analysis to envelop the Davis-Besse raised-loop plant. The lowered-loop plant with eight vent valves will have vent valve flow equal to or greater than that of the raised-loop plant. One of the key factors affecting downcomer temperature is the amount of hot water flowing through the vent valves. Greater vent valve flow results in a warmer downcomer temperature.

2.2.2. 0.015- and 0.023-$ft^2$ Pressurizer Breaks

In addition to the 0.007-$ft^2$ pressurizer break, 0.015- and 0.023-$ft^2$ breaks were analyzed to determine the effect of break size on the reactor vessel downcomer temperature and system pressure. These additional analyses were not as comprehensive as the 0.007-$ft^2$ analysis. They used simpler calculational methods and only determined the RV conditions.

2.2.2.1. Analytical Method

The eight-node CRAFT model described in section 3.1 was used for the initial blowdown analysis. The 0.015- and 0.023-$ft^2$ breaks were run for 20 and 45 minutes, respectively. The subsequent transient calculations, performed using a steady-state code, are provided below.

Under the steady-state assumption, the rate of change of mass ($M_{RCS}$) and energy ($E_{RCS}$) in the RCS is zero:

$$\frac{dM_{RCS}}{dt} = \frac{dE_{RCS}}{dt} = 0. \qquad (1)$$

Then the core outlet enthalpy is calculated:

$$h_h = \frac{q}{W_{HPI}} + h_{HPI} \tag{2}$$

where

$h_h$ = core outlet enthalpy, Btu/lbm,
$h_{HPI}$ = enthalpy of HPI water, Btu/lbm,
$W_{HPI}$ = HPI flow, lbm/s,
$q$ = decay heat, Btu/s.

The vent valve flow is determined by performing an energy balance in the downcomer region:

$$W_{vv} = W_{HPI} \frac{h_c - h_{HPI}}{h_h - h_c} \tag{3}$$

where

$h_c$ = core inlet enthalpy, Btu/lbm,
$W_{vv}$ = vent valve flow, lbm/s.

The vent valve flow, which can also be calculated from the elevation pressure drop across the vent valve, is given by

$$W_{vv} = \frac{288 \times g_c \rho_h A_{vv}^2 \Delta P}{K_{vv}} = 96.26\, A_{vv} \frac{\rho_h \times \Delta P}{K_{vv}}. \tag{4}$$

where

$\rho_h$ = core outlet density, lbm/ft$^3$,
$A_{vv}$ = vent valve flow area, ft$^2$,
$K_{vv}$ = loss coefficient,
$\Delta P$ = elevation pressure drop, psi
= $Hx(\rho_c - \rho_h)/144$,
$\rho_c$ = core inlet density, lbm/ft$^3$,
$H$ = elevation head, ft.

Assuming a system pressure and a downcomer water temperature $T_c$, the vent valve flow $W_{vv}$ can be calculated using equations 3 and 4. The downcomer water temperature is determined by iterating on the assumed $T_c$ until equations 3 and 4 predict the same vent valve flow. A benchmark study was performed for the stuck-open PORV case (0.007-ft$^2$ break) assuming a system pressure of 1500 psia. The results indicate that the steady-state code predicts the downcomer temperature approximately 9% above the CRAFT prediction, as shown in Figure 2-24. The

9% deviation in the downcomer temperature was used as an adjustment factor for the two breaks analyzed.

#### 2.2.2.2. Assumptions Used for 0.015- and 0.023-ft$^2$ Breaks

The assumptions used in the CRAFT model are the same as those described in section 2.2.1 except for the following:

1. The break was initiated at time zero. The 0.015- and 0.023-ft$^2$ small break transients assumed that a break occurred simultaneously with the loss of feedwater. The 0.007-ft$^2$ break transient assumed that the break occurred 20 minutes after losing feedwater flow by opening the PORV.
2. HPI was initiated by an ESFAS setpoint of 1365 psia with a 35-second delay. The 0.007-ft$^2$ break transient did not assume an initiating break as do the 0.015- and 0.023-ft$^2$ small break transients, and HPI was assumed to be operator-initiated at 20 minutes for the 0.007-ft$^2$ break.
3. A discharge coefficient of 1.0 was applied to the Moody discharge model instead of 0.75 because these are considered simple breaks that do not have the complex flow geometry of the PORV. The Moody correlation was used for both saturated and subcooled water.

The steady-state analysis was performed using a constant system pressure based on HPI flow equal to leak flow for a given break size. The steady-state system pressures were calculated as 1000 and 600 psia for the 0.015- and 0.023-ft$^2$ breaks, respectively.

#### 2.2.2.3. Results

Table 2-1 provides the sequence of events for the 0.015- and 0.023-ft$^2$ breaks. The downcomer temperature transients predicted by CRAFT and steady-state codes for these breaks are provided in Figure 2-25. The loop circulation ceased early in the transient as shown in Figure 2-26 because of the loss of steam generator cooling and the RCS voiding.

#### 2.2.2.4. Conservatisms

The maximum HPI flow indicated above was used for both the CRAFT and steady-state calculations. No operator action was taken to reduce the HPI flow. The HPI water temperature was assumed to be 40F.

## 2.3. LOCA Analyses With Operator Action to Throttle HPI Flow (Cases 2-4, Table 1-1)

Fracture mechanics analyses performed on the data from the breaks without operator action to throttle HPI flow analyzed above using the techniques of section 5 of this report produce undesirable results after several hours when HPI is not throttled. As a result, the 0.007-, 0.015-, and 0.023-$ft^2$ breaks were analyzed again, now assuming that the operator started throttling back the HPI flow rate when the core outlet temperature reached 100F subcooled. (HPI flow under these conditions is independent of the number of HPI pumps operating.) The operator then maintained the core outlet temperature at 100F subcooled for the remainder of the transient. Maintaining this subcooling margin results in higher downcomer temperatures due to the reduced HPI flow rates. Throttling also results in reduced downcomer pressures. Both of these effects of throttling are beneficial with respect to the thermal shock concern.

### 2.3.1. Assumptions Used

The 100F subcooled conditions were used as the basis for a steady-state calculation to determine the downcomer pressure and temperature. The following assumptions were made:

1. The HPI water temperature is 40F.
2. The system is in a steady-state condition; i.e., HPI flow is equal to leak flow.
3. Leak flow is based on the Moody correlation with a discharge coefficient of 1.0.
4. The core outlet temperature is maintained at 100F subcooled.
5. Decay heat is based on 1.2 times ANS standard.
6. Pressurizer water temperature is equal to core outlet temperature.

### 2.3.2. Analytical Methods

The results of the eight-node CRAFT analyses, as described in section 2.2.2.1, were used to determine the RCS conditions until the core outlet became 100F subcooled. Operator action to reduce HPI flow to maintain 100F subcooling is assumed at this time. The remainder of the transient conditions are calculated using a steady-state analysis as described below.

In a steady-state condition, the relationship of HPI flow to leak flow is defined as

$$W_L = W_{HPI}\left(\frac{\nu_{HPI}}{\nu_L}\right) \quad (5)$$

where

$W_L$ = leak flow, lbm/s,

$W_{HPI}$ = HPI flow, lbm/s,

$\nu_{HPI}$ = specific volume of HPI, $ft^3$/lbm,

$\nu_L$ = specific volume of core outlet water, $ft^3$/lbm.

Assuming a system pressure and 100F subcooling, the leak flow can be calculated by the Moody correlation. Equation 6 is used to determine the HPI flow ($W_{HPI}$) required to maintain 100F subcooling. Equation 5 is used as a convergence criterion for determining the system pressure. If $W_{HPI}$ and $W_L$ fail to satisfy the equation, the system pressure is readjusted until the criterion is satisfied. Once the system pressure is determined, then the equations (3 and 4) in 2.2.2.1 are used in the same manner to determine the vent valve flow.

$$q = W_{HPI}(h_h - h_{HPI}) \quad (6)$$

where

$q$ = decay heat rate, Btu/s,

$h_h$ = enthalpy of core outlet water based on the 100F subcooled state, Btu/lbm,

$h_{HPI}$ = enthalpy of HPI water, Btu/lbm,

$W_{HPI}$ = HPI flow rate, lbm/s.

### 2.3.3. Results

The mixed downcomer temperature was calculated to be equal to the saturation temperature minus 150F. This value is based on the assumption of 100F subcooled at the core outlet plus 50F core $\Delta T$. The downcomer temperature and pressure plots are shown in Figures 2-27 and 2-28 for the 0.007-, 0.015-, and 0.023-$ft^2$ breaks. The vent valve and HPI flows and vent valve fluid temperature versus time (to 3 hours) for the 0.007- and 0.023-$ft^2$ breaks are shown in Figures 2-29 through 2-31. The HPI flow and the vent valve flow and temperature are used for the mixing and reactor vessel temperature analyses as described in sections 3 and 4. Fracture mechanics analyses performed on this data are discussed in section 5 of this report.

Table 2-1. Transient Sequence of Events

| | 0.007 $ft^2$ (cases 1, 2), time-minutes | 0.015 $ft^2$, time-minutes | 0.023 $ft^2$ (cases 3, 4), time-minutes |
|---|---|---|---|
| Reactor, turbine, and feedwater trip | 0 | 0 | 0 |
| Reactor coolant pump trip | 0 | 0 | 0 |
| LOCA initiated | 20 | 0 | 0 |
| Reach saturation at core outlet | Never | 2 | 2 |
| HPI initiated | 20 | 3 | 3 |
| Regain subcooled state at core outlet | NA | 7 | 9 |
| Loss of natural circulation | 40 | 13 | 9 |
| Achieve 50F subcooled at core outlet | 55 | 19 | 17 |
| Achieve 100F subcooled at core outlet | 77 | -- | 30 |

Table 2-2. Vent Valve Opening Vs Resistance

| $\Delta P$ across vent valve, psi | Avg opening angle, degrees | Resistance factor,[a] K |
|---|---|---|
| $\geq 0.25$ | 21 | 4.2 |
| $0.25 > \Delta P \geq 0.2$ | 17.5 | 5.0 |
| $0.20 > \Delta P \geq 0.16$ | 12.0 | 8.8 |
| $0.16 > \Delta P \geq 0.12$ | 8.13 | 16.0 |
| $0.12 > \Delta P \geq 0.08$ | 4.13 | 46.0 |
| $0.08 > \Delta P$ | 0 | $\infty$ |

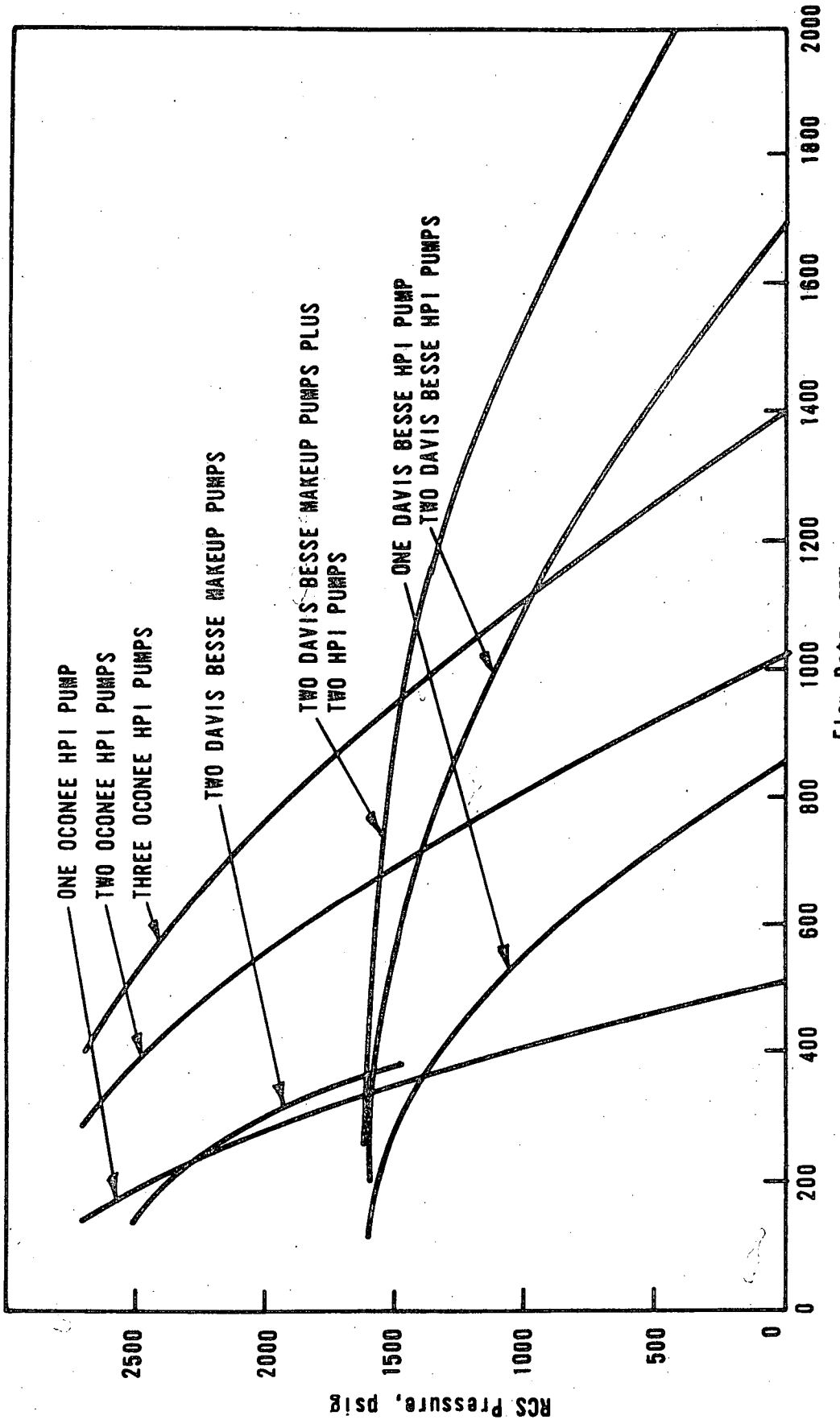


Figure 2-1. HPI Flow Rate Vs RCS Pressure

Figure 2-2. CRAFT Noding Scheme, Eight-Node Model of RCS

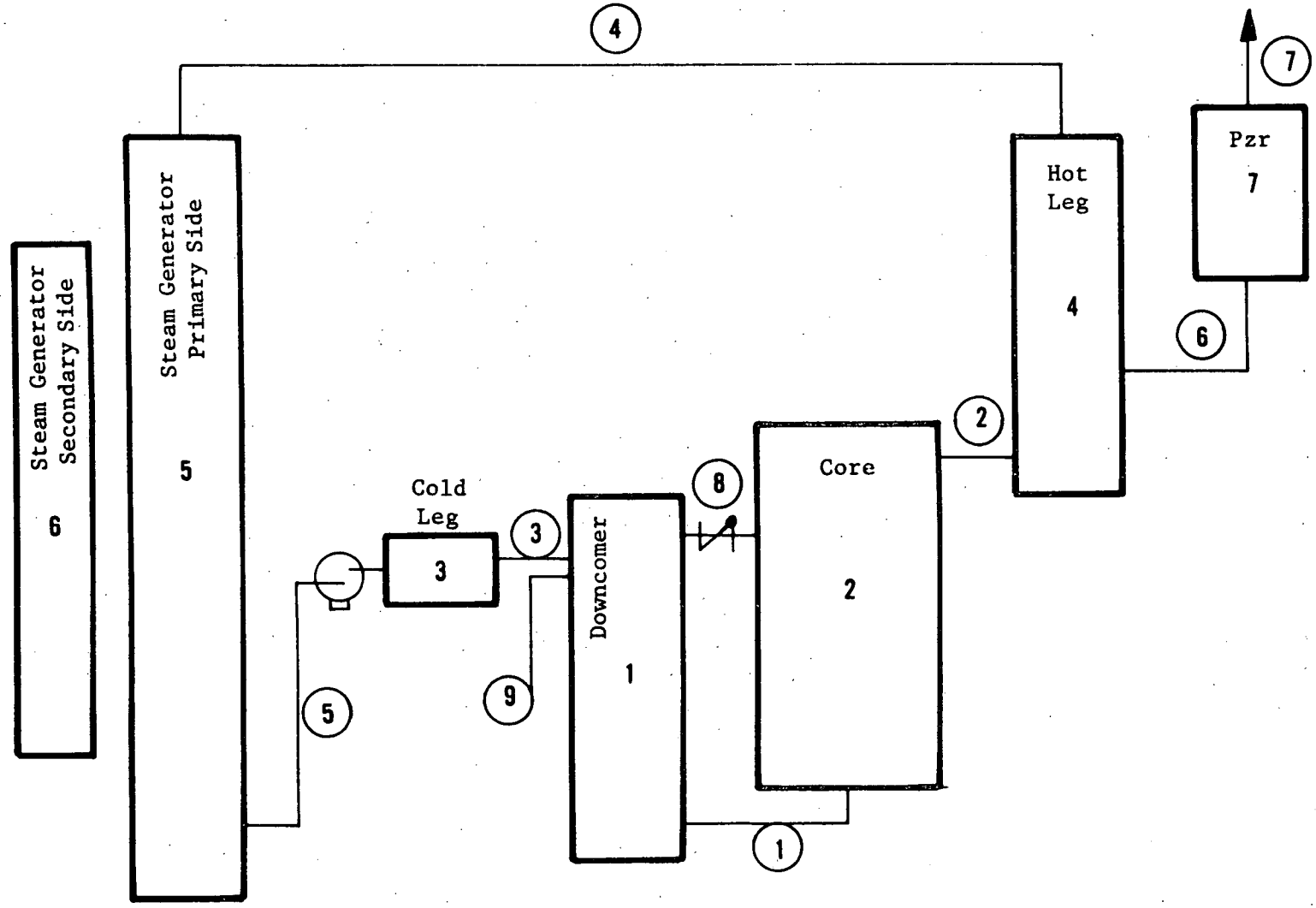

Figure 2-3. Downcomer Temperature Vs Time, Comparison of Multinode and Eight-Node CRAFT Models, Stuck-Open PORV, Two HPI Pumps, AFW @ 40 s

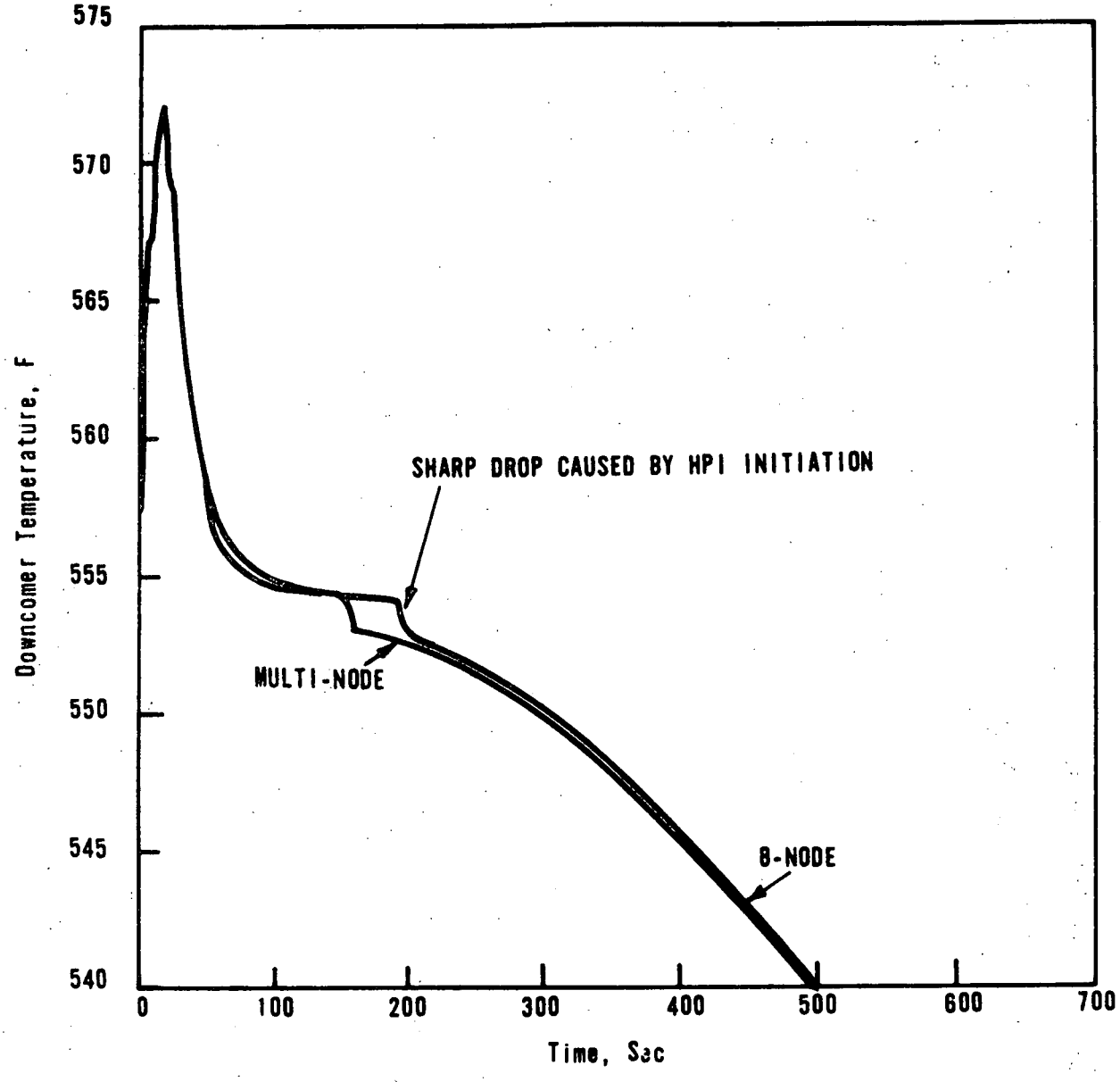

Figure 2-4. Downcomer Pressure Vs Time — Comparison of Multi-node and Eight-Node CRAFT Models, Stuck-Open PORV, Two HPI Pumps, AFW @ 40 s

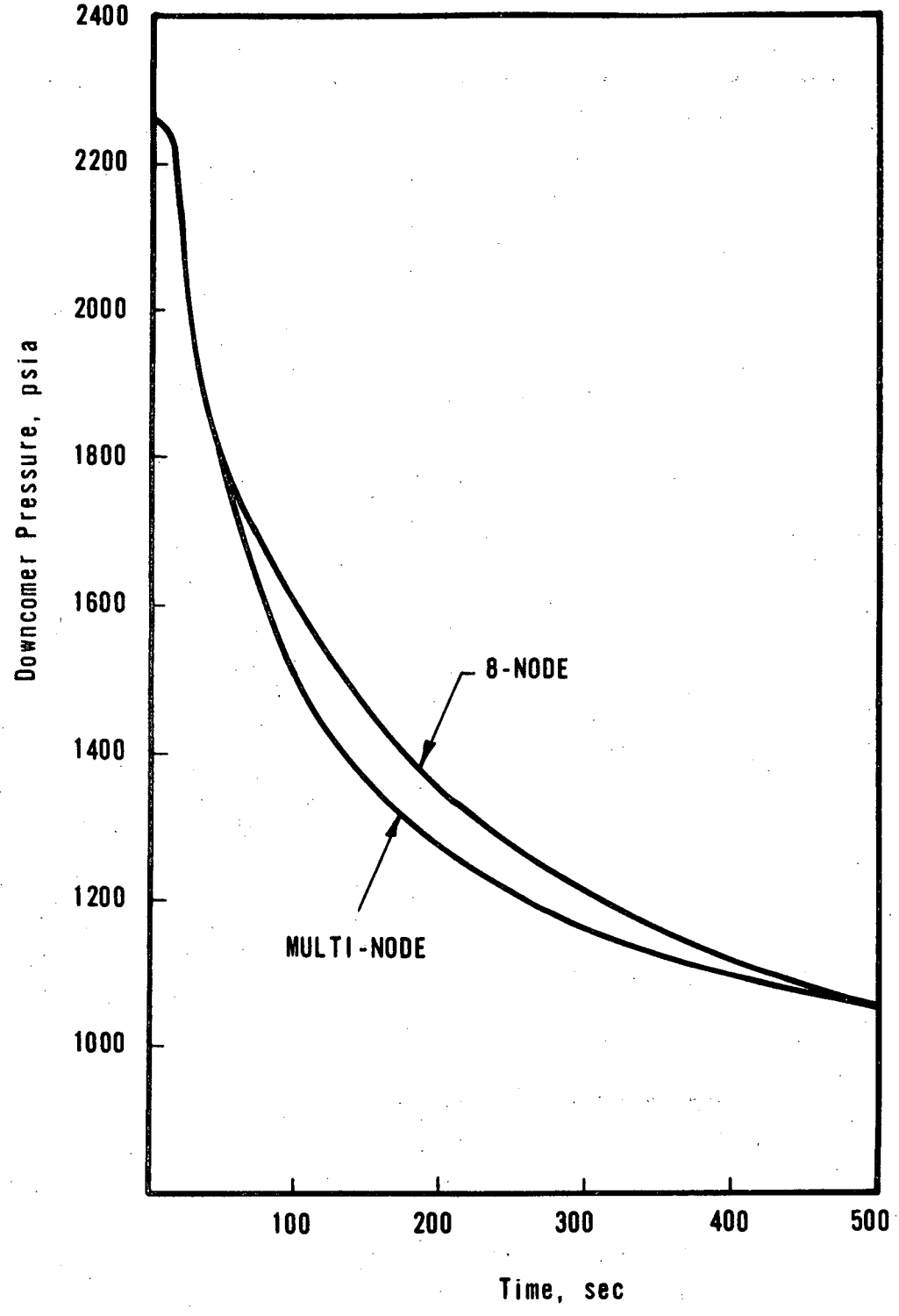

Figure 2-5. Cold Leg Level 0.007-ft$^2$ Pressurizer Break Without HPI Throttling, Node 3

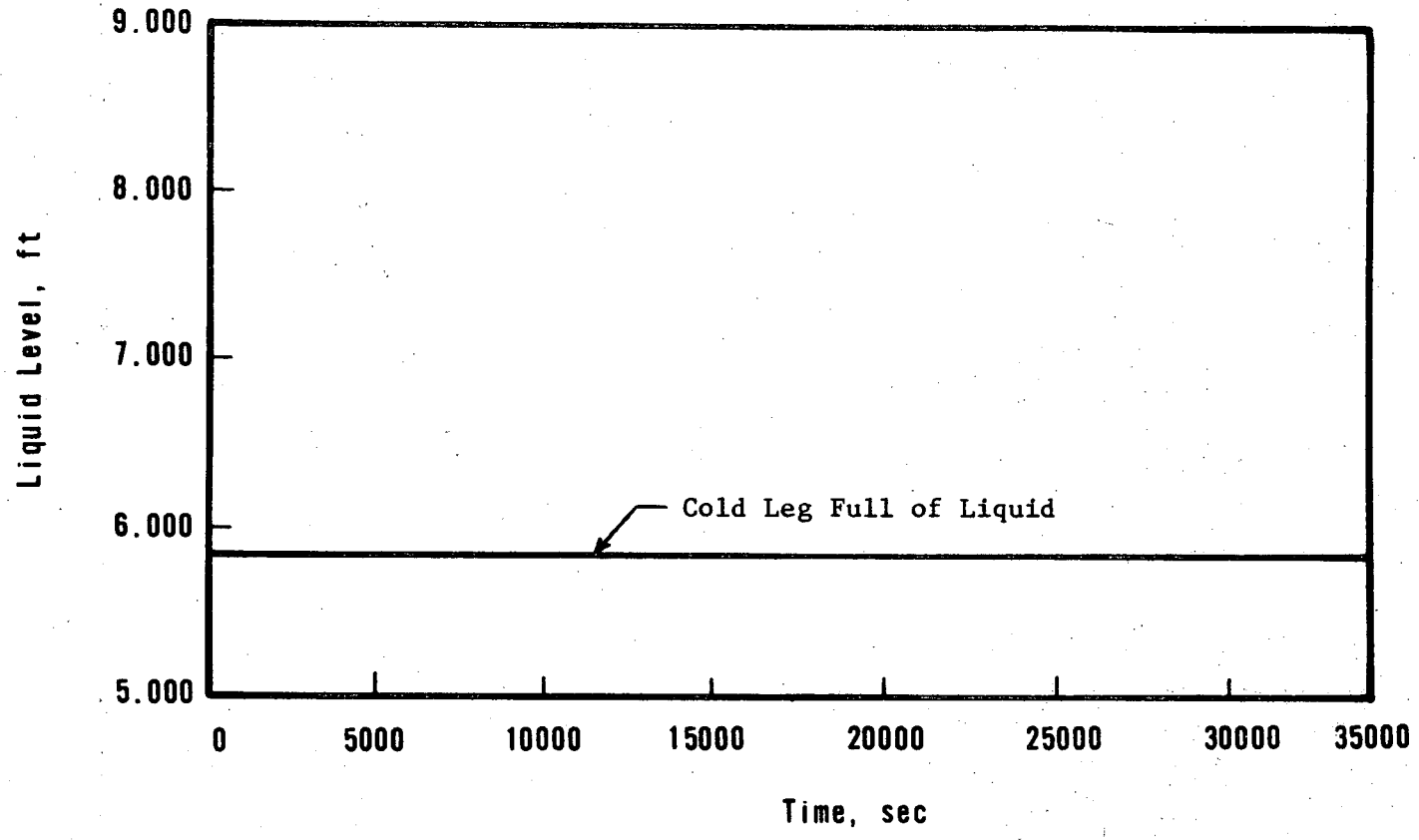

Figure 2-6. Hot Leg Level, 0.007-ft$^2$ Break Without HPI Throttling, Node 4

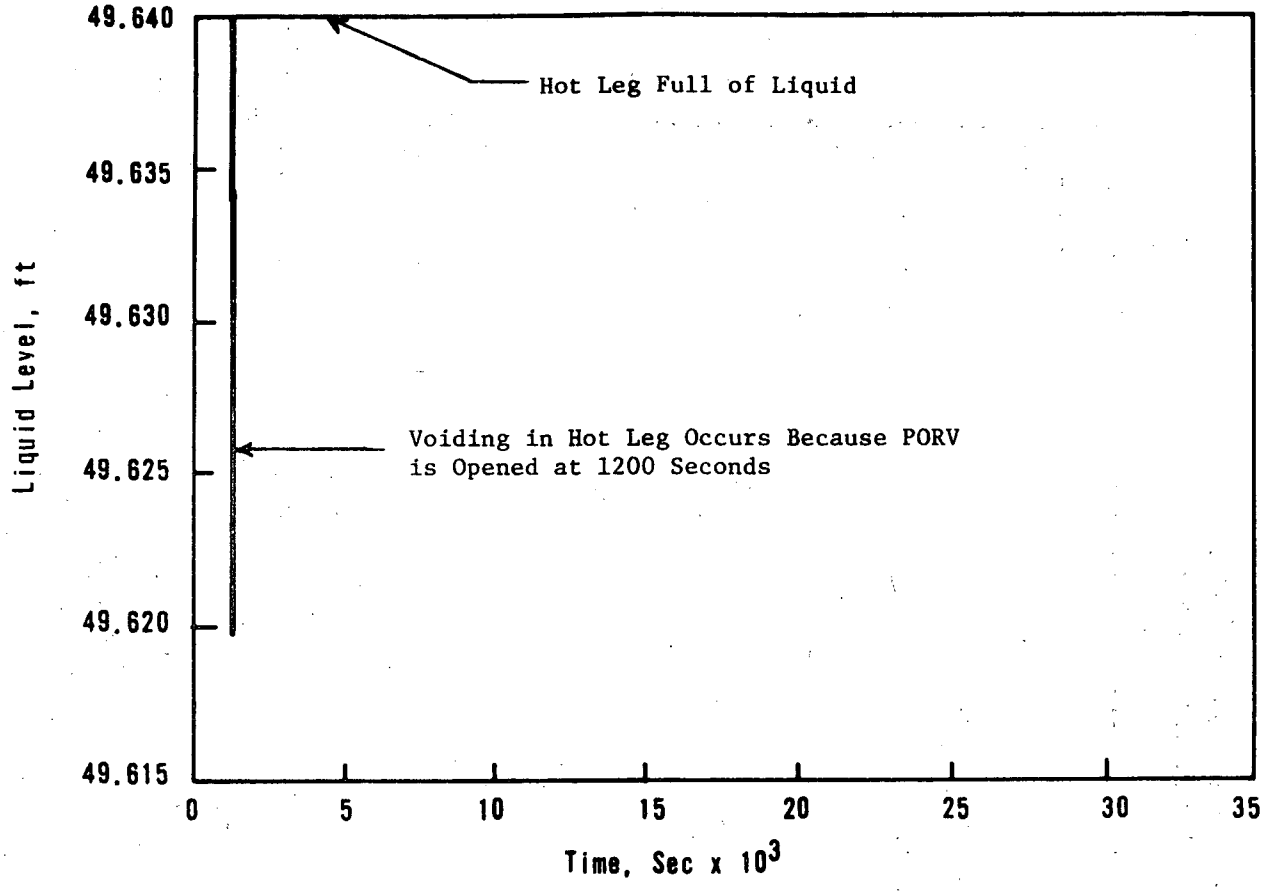

Figure 2-7. Pressurizer Level 0.007-ft$^2$ Pressurizer Break Without HPI Throttling, Node 7

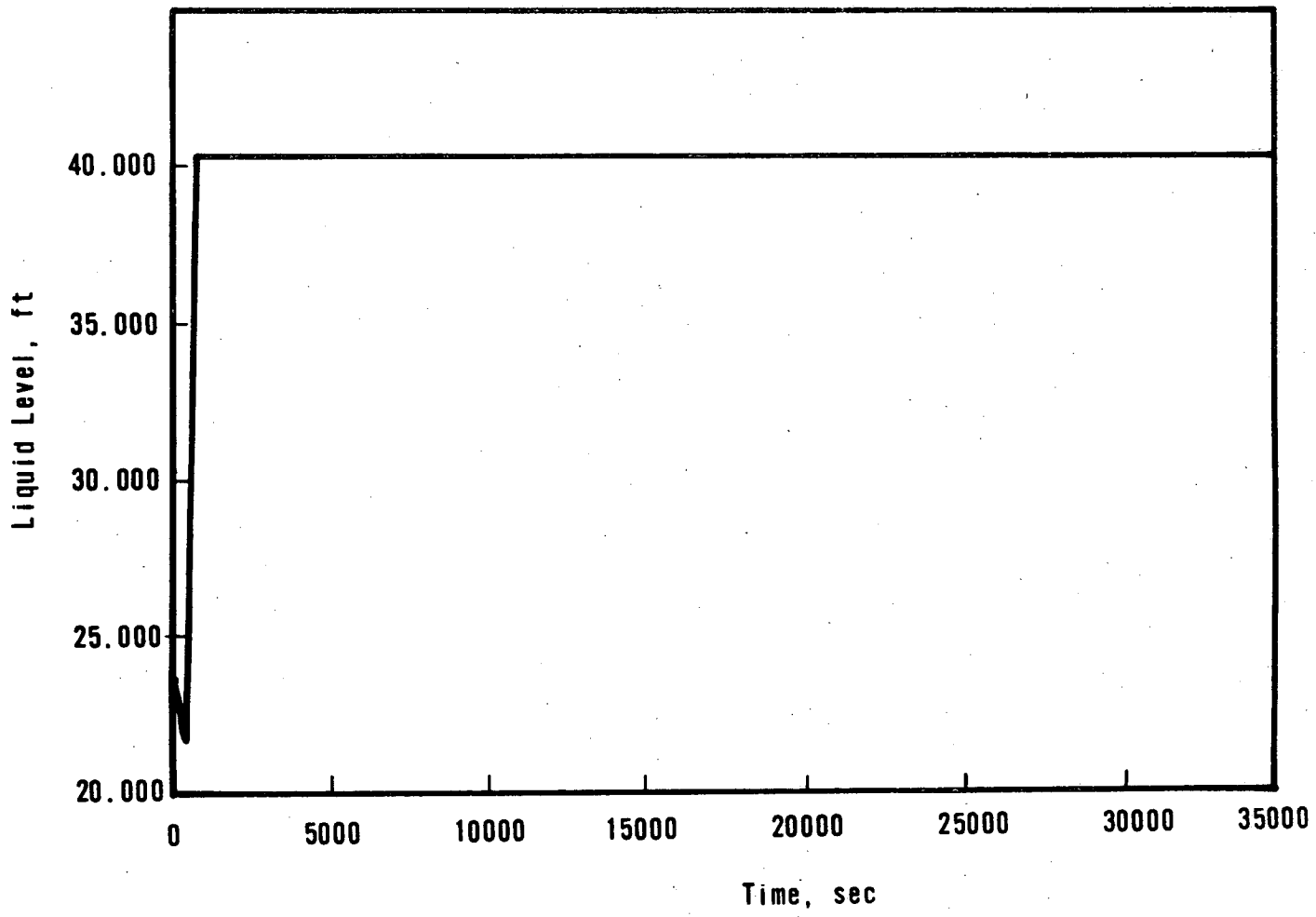

Figure 2-8. RV Liquid Level 0.007-ft$^2$ Pressurizer Break Without HPI Throttling

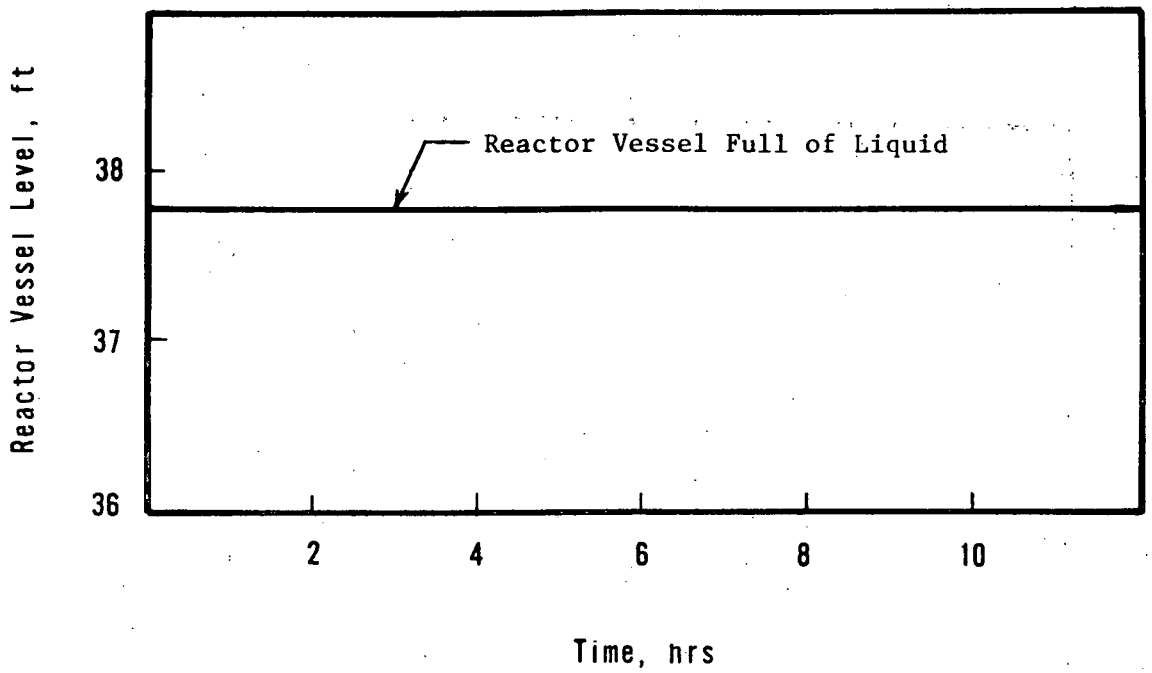

Figure 2-9. Core Outlet Temperature Vs Time, 0.007-ft$^2$ Pressurizer Break Without HPI Throttling, Node 2

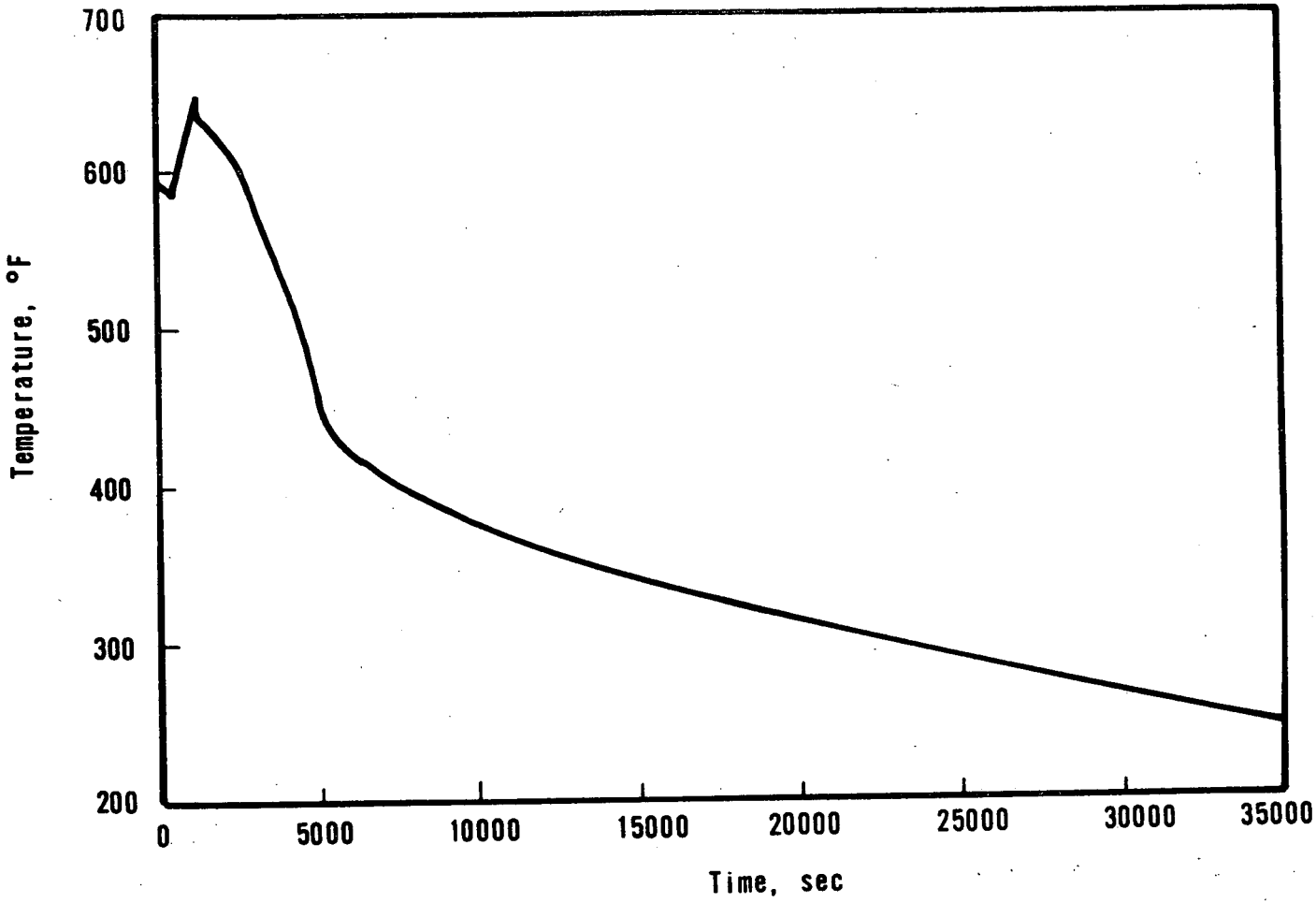

Figure 2-10. Downcomer Temperature Vs Time, 0.007-ft$^2$ Pressurizer Break Without HPI Throttling, Node 1

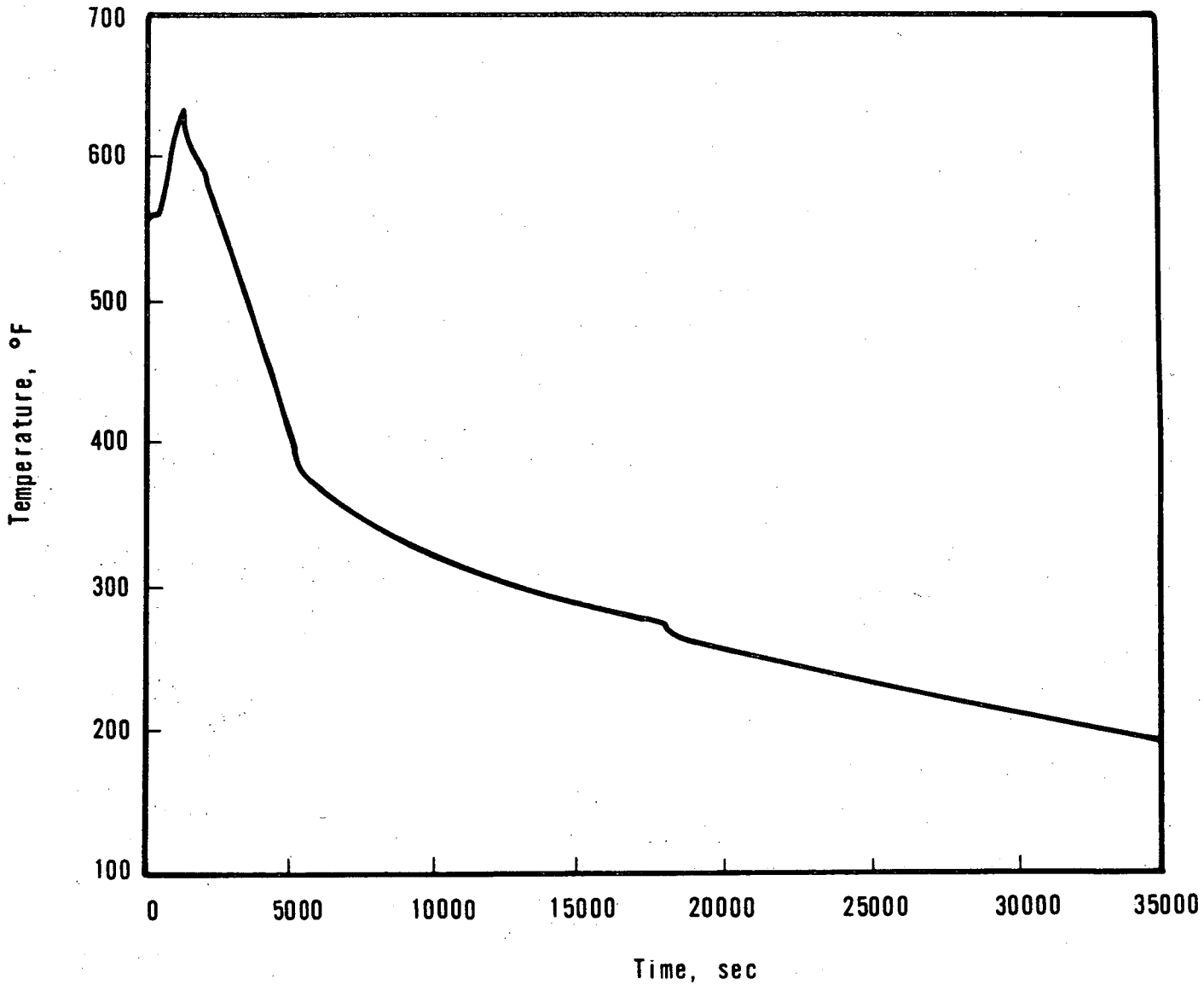

Figure 2-11. Hot Leg Temperature Vs Time, 0.007-ft$^2$ Pressurizer Break Without HPI Throttling, Node 4

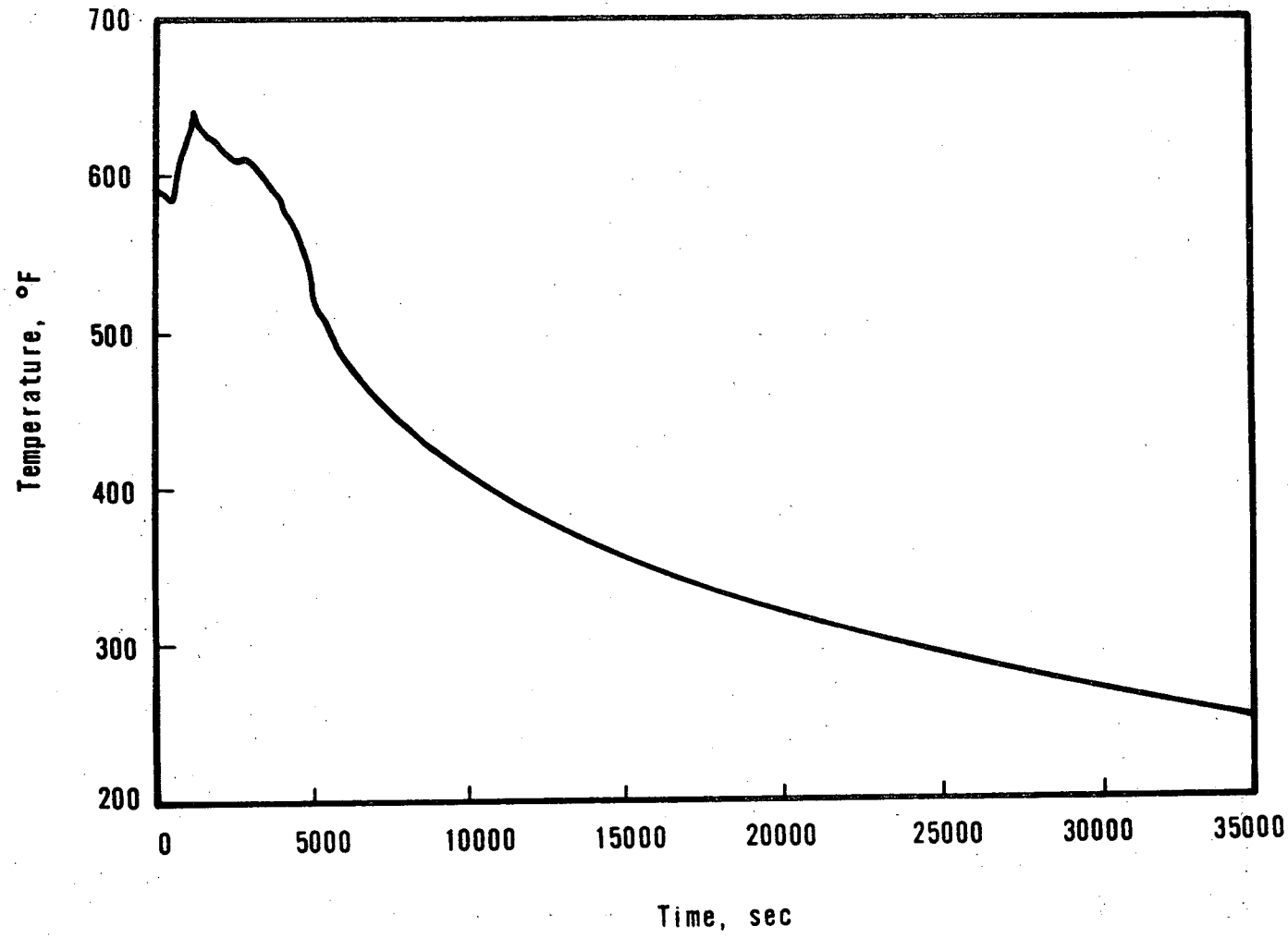

Figure 2-12. Core Exit Flow Vs Time – 0.007-ft$^2$ Pressurizer Break Without HPI Throttling, Path 2

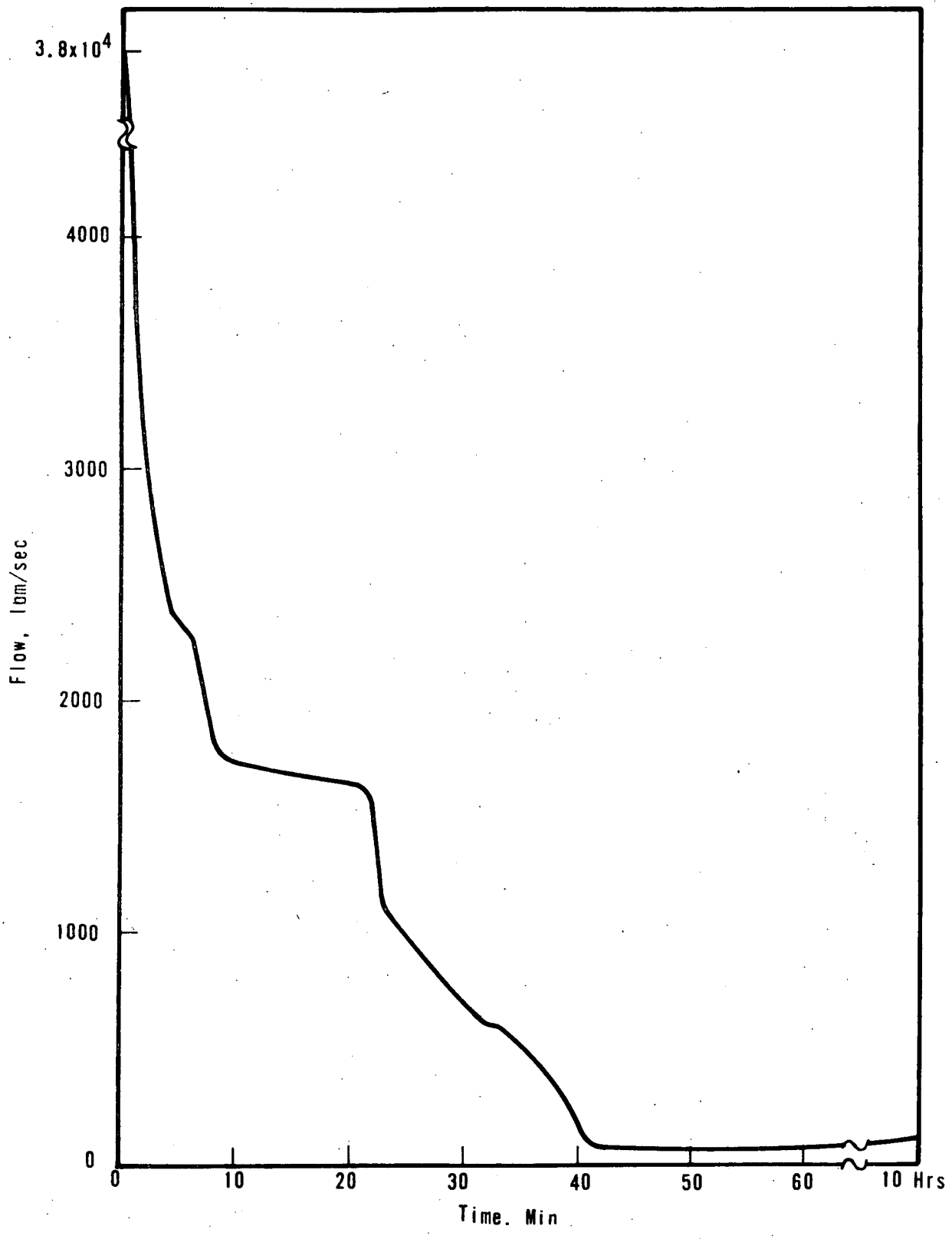

Figure 2-13. Leak Path Flow Vs Time, 0.007-ft$^2$ Pressurizer Break Without HPI Throttling, Path 7

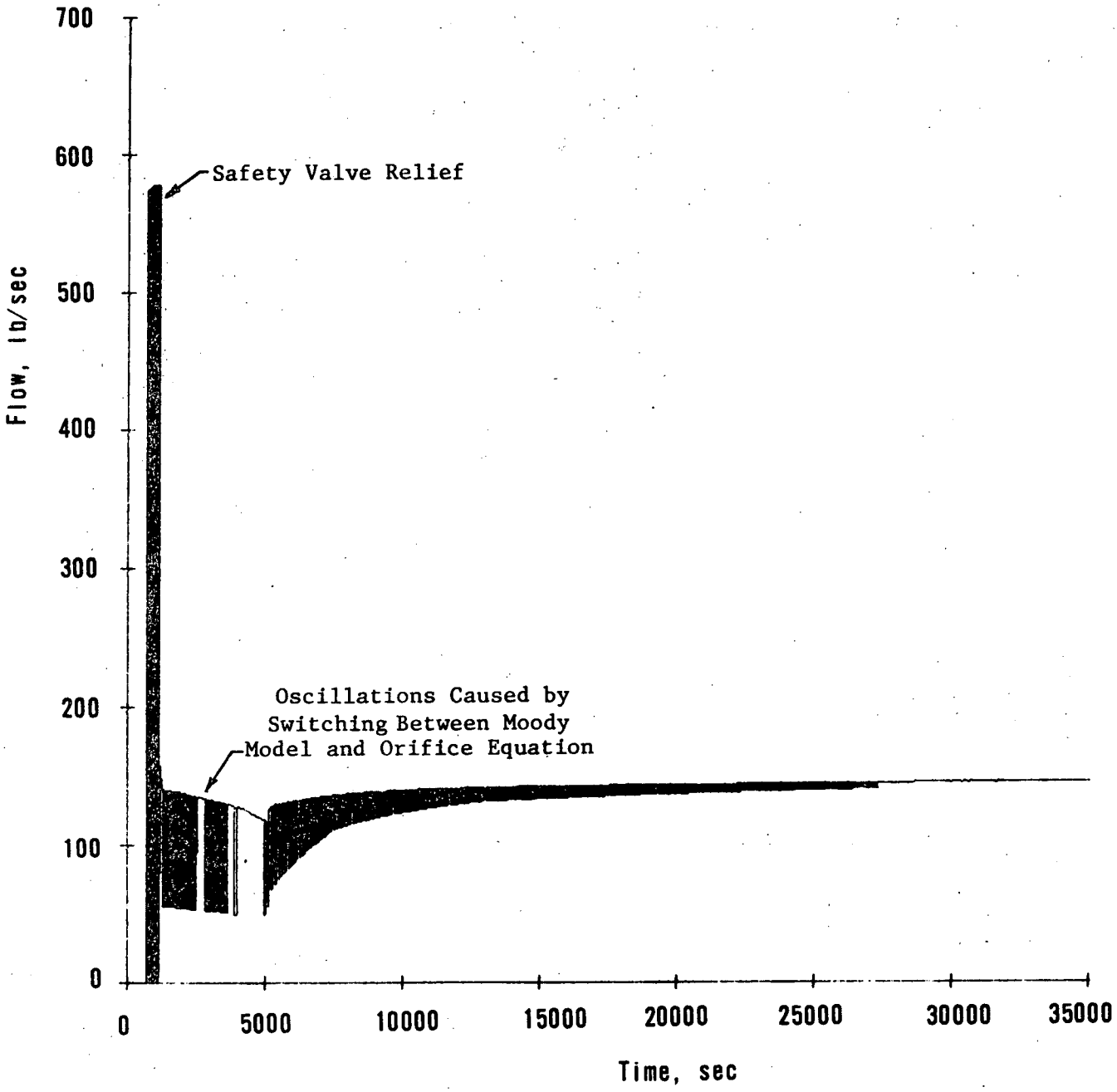

Figure 2-14. Vent Valve Flow Vs Time, 0.007-ft$^2$ Pressurizer Break Without HPI Throttling, Path 8

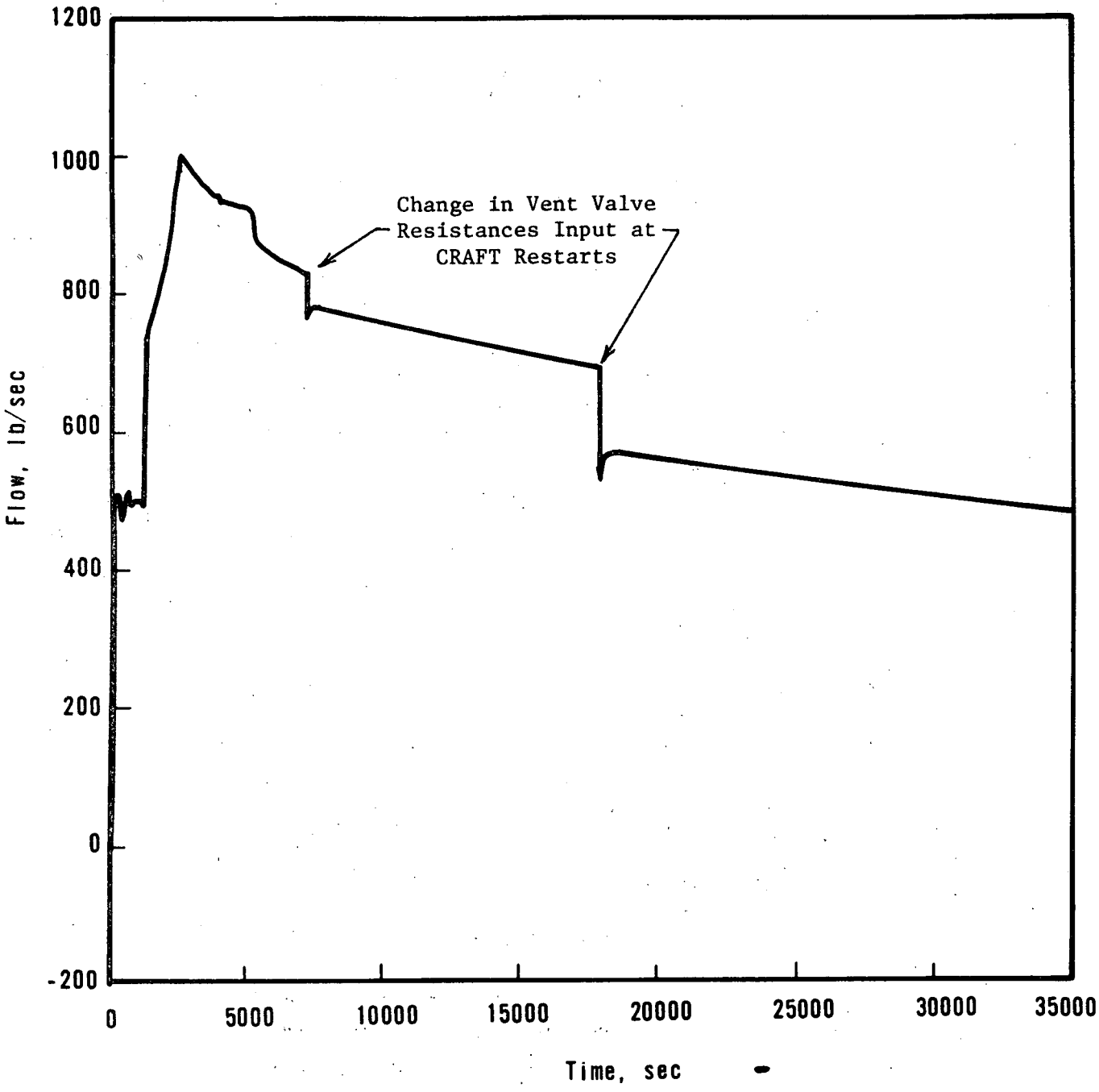

Figure 2-15. HPI Flow Vs Time, 0.007-ft$^2$ Pressurizer Break Without HPI Throttling, Path 9

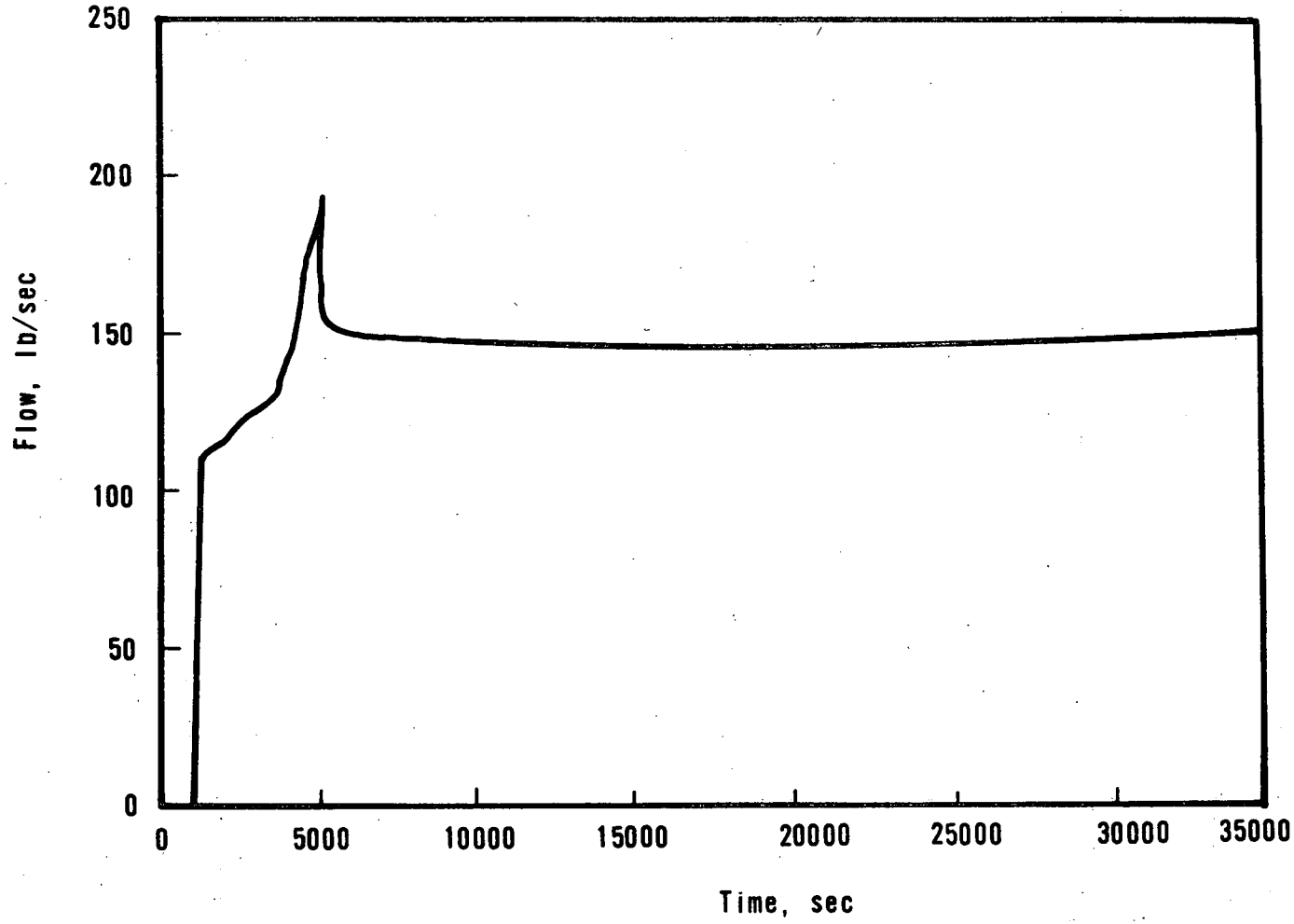

Figure 2-16. Core Outlet Quality, 0.007-ft$^2$ Pressurizer Break Without HPI Throttling, Path 2

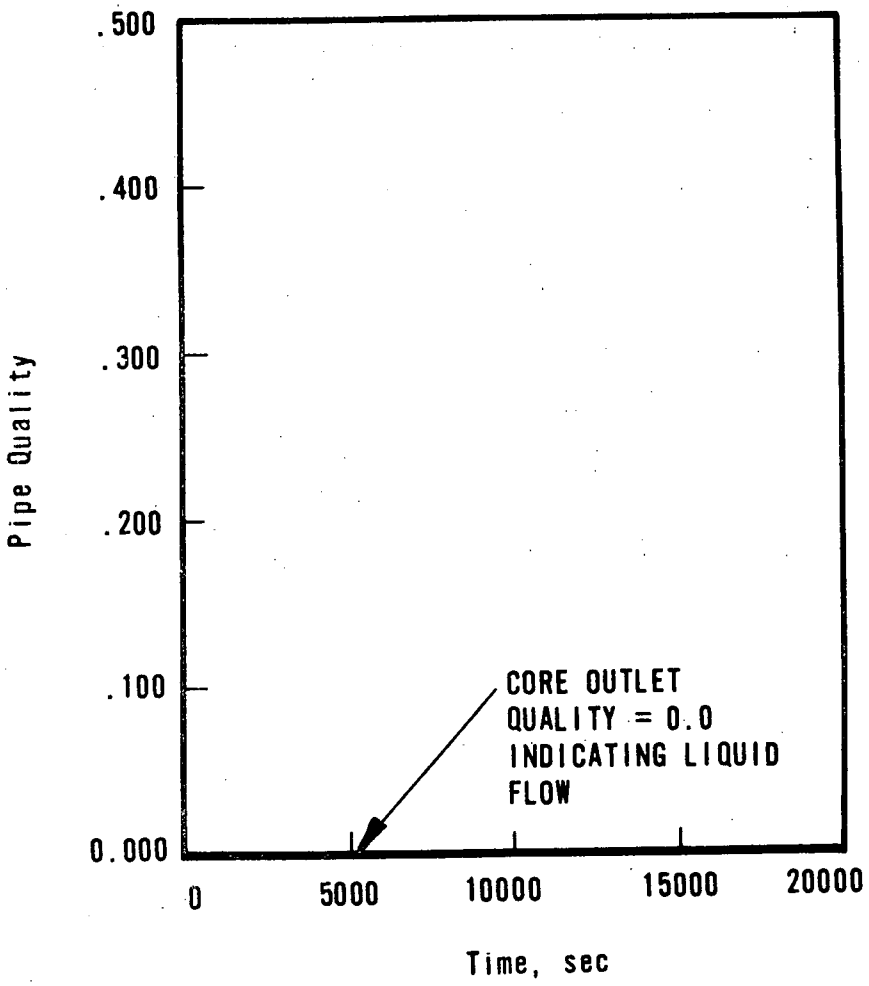

Figure 2-17. Leak Path Quality (PORV), 0.007-ft$^2$ Pressurizer Break Without HPI Throttling, Path 7

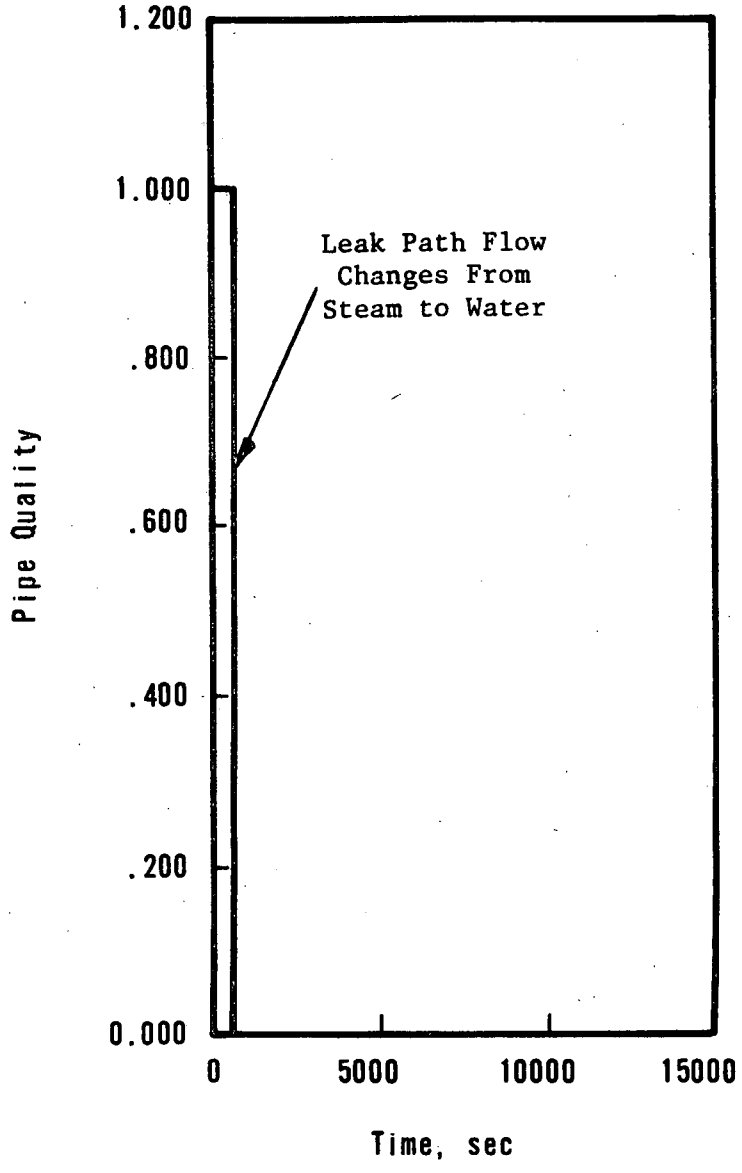

Figure 2-18. Vent Valve Quality, 0.007-ft$^2$ Pressurizer Break Without HPI Throttling, Path 8

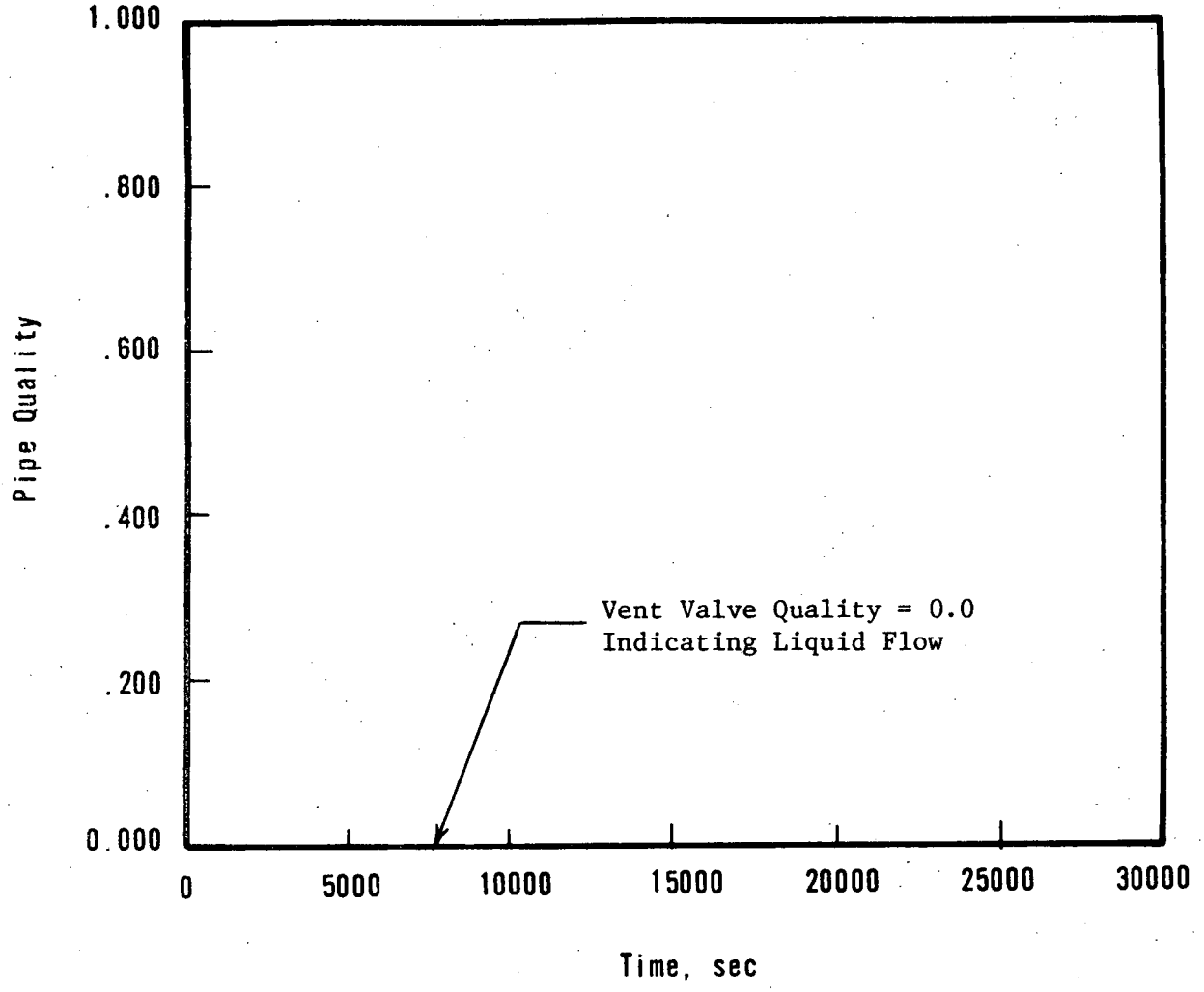

Figure 2-19. Primary System Inventory, 0.007-ft$^2$ Pressurizer Break Without HPI Throttling

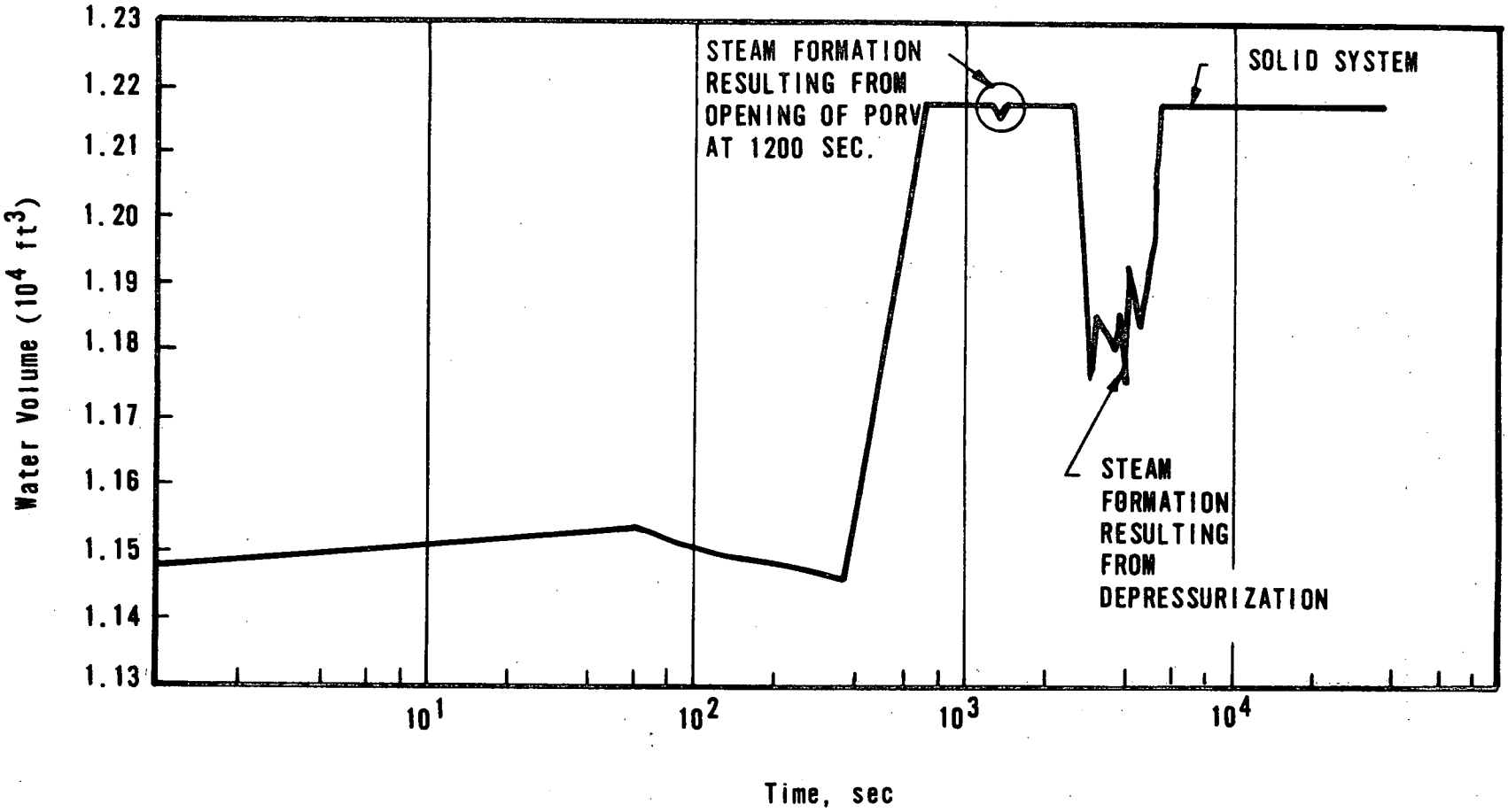

Figure 2-20. Core Pressure Vs Time, 0.007-ft$^2$ Pressurizer Break Without HPI Throttling, Node 2

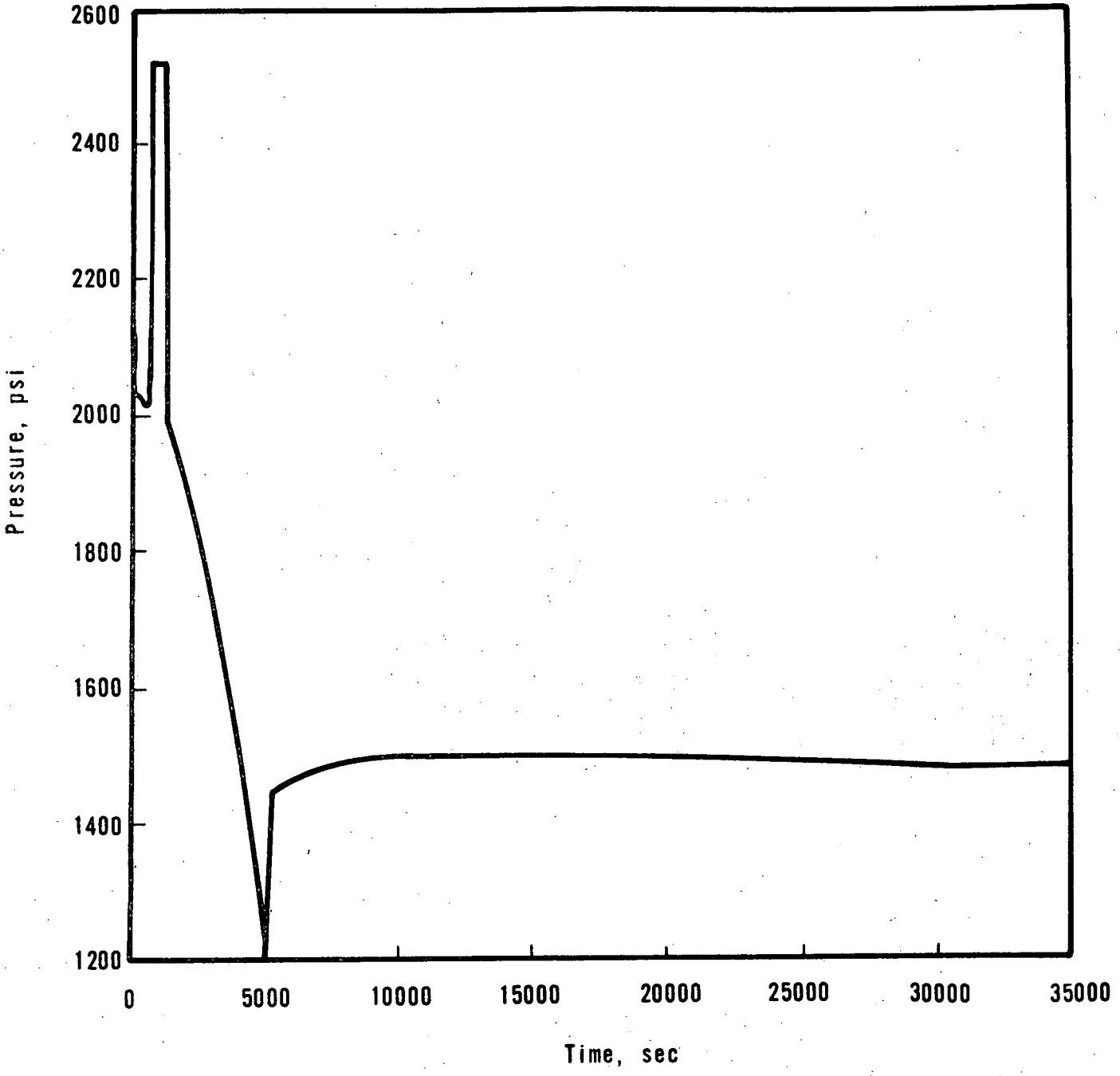

Figure 2-21. Pressurizer Fluid and Metal Temperature Vs Time, 0.007-ft$^2$ Break Without HPI Throttling

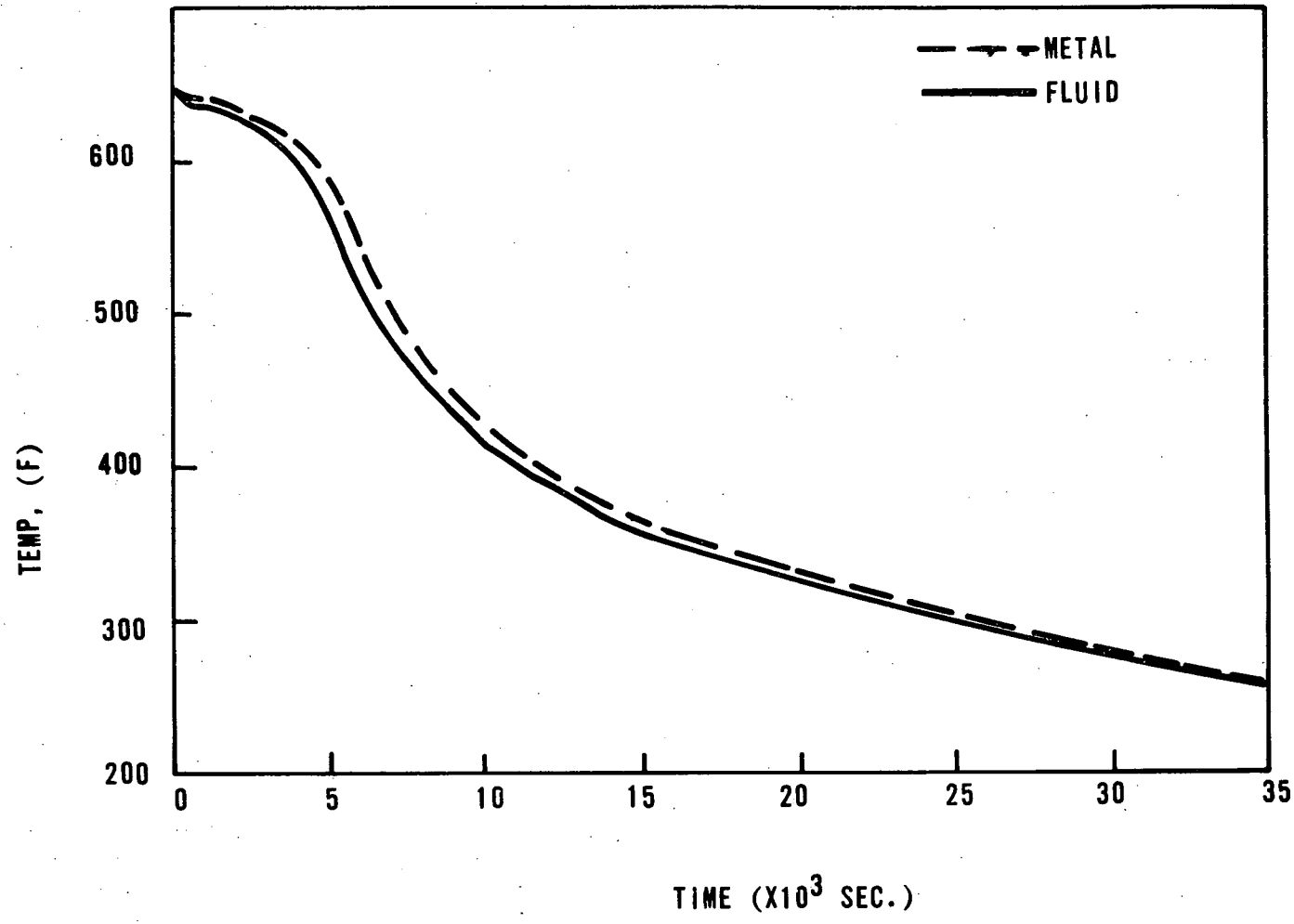

Figure 2-22. Upper Head Metal Temperature Vs Time, 0.007-ft$^2$ Pressurizer Break Without HPI Throttling

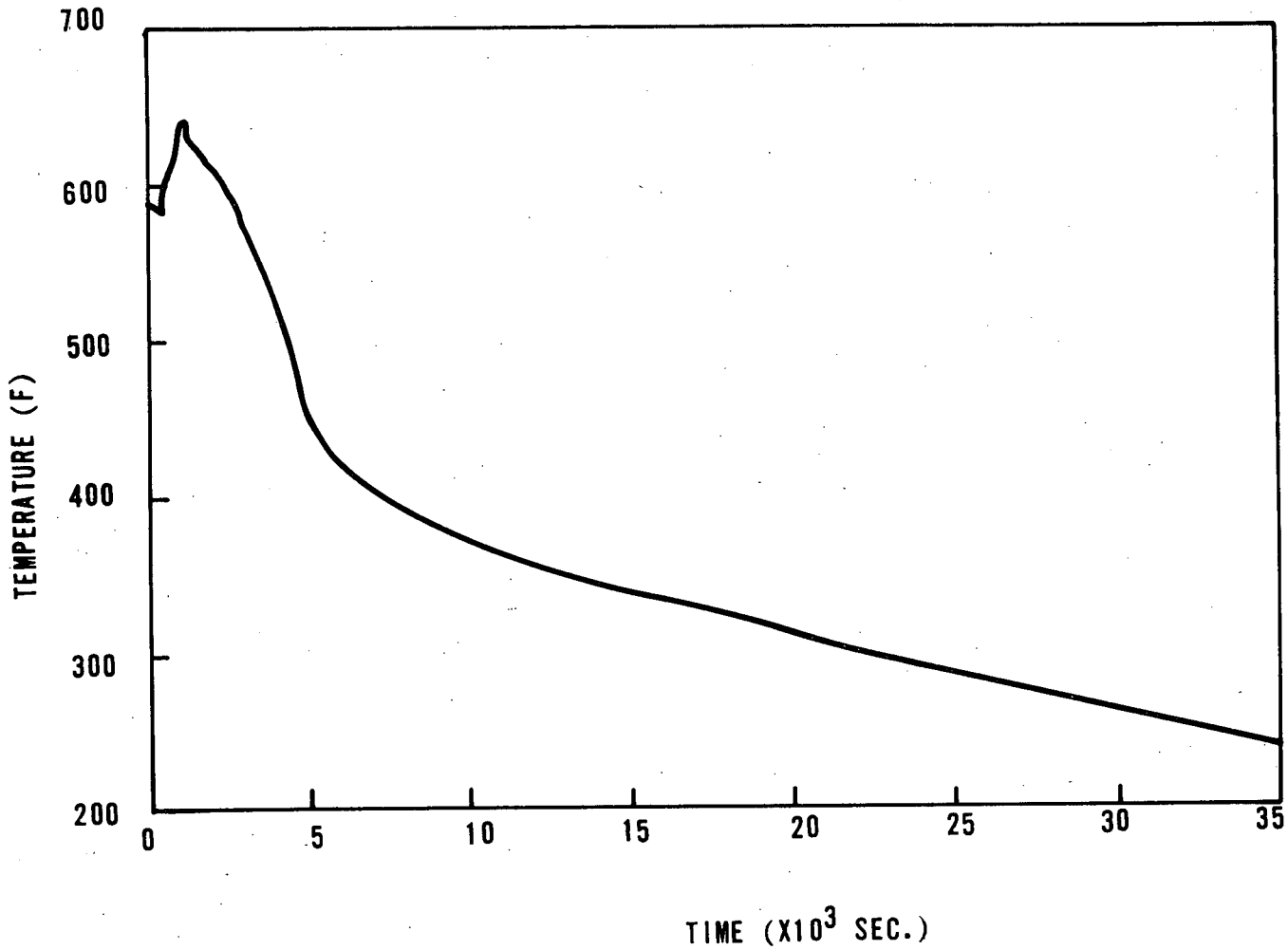

Figure 2-23. Cold Leg Water Temperature Vs Time, 0.007-ft$^2$ Pressurizer Break Without HPI Throttling

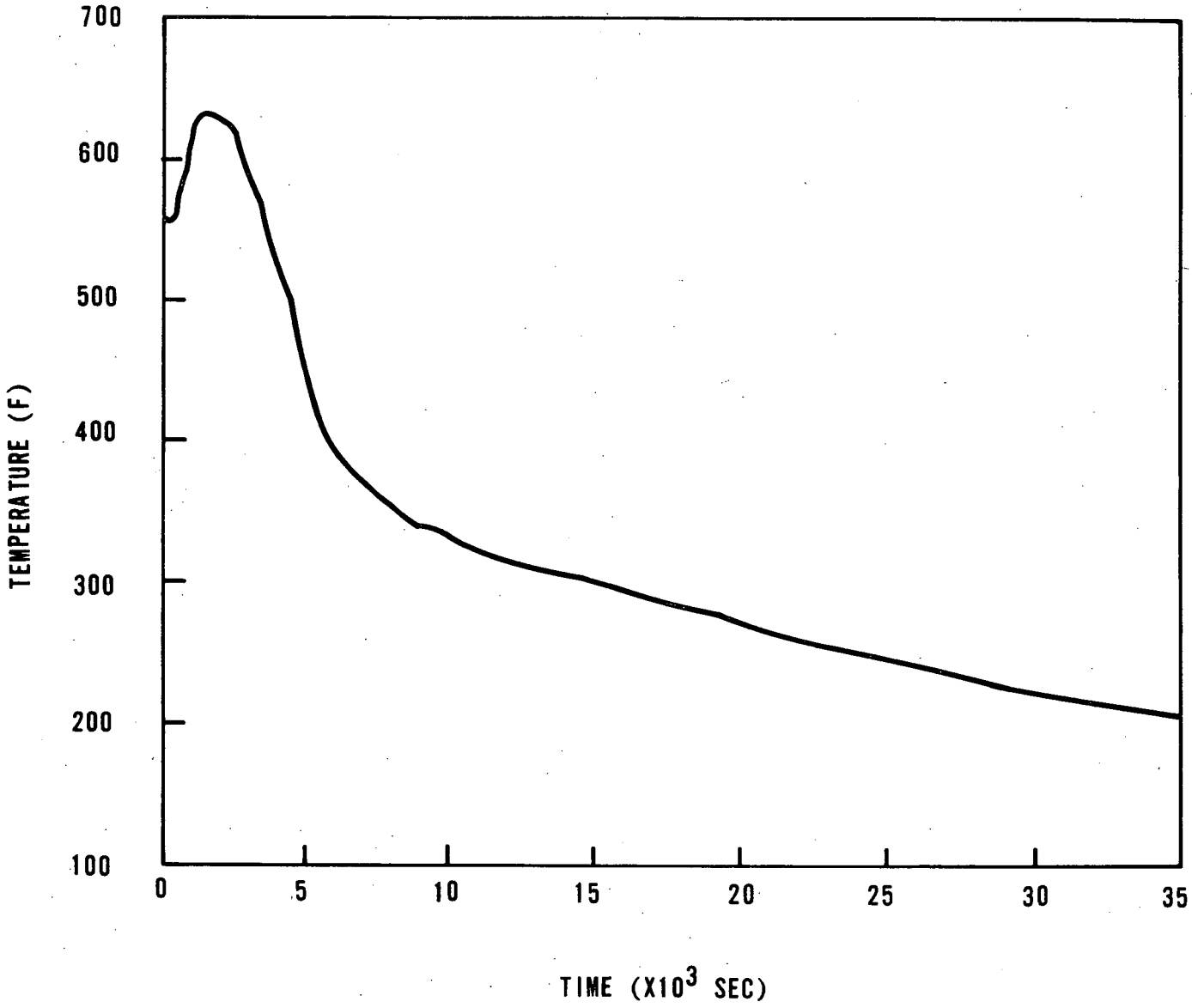

Figure 2-24. Downcomer Temperature Vs Time at 1500 psia, Comparison of Eight-Node CRAFT to Semi-Steady-State Analysis Method

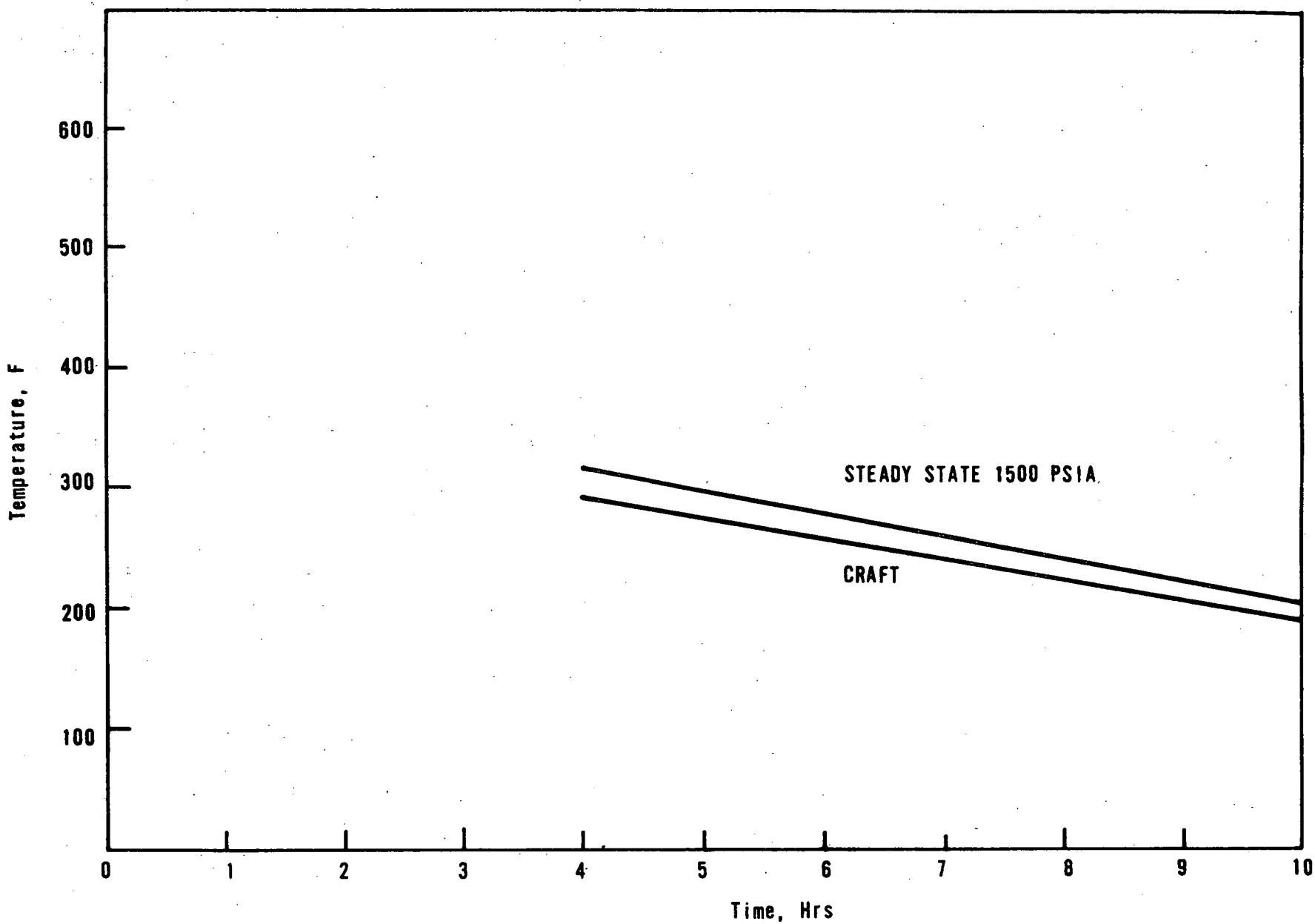

Figure 2-25. Downcomer Temperature Vs Time, 0.015- and 0.023-ft$^2$ Pressurizer Breaks Without HPI Throttling — CRAFT Semi-Steady-State Analysis

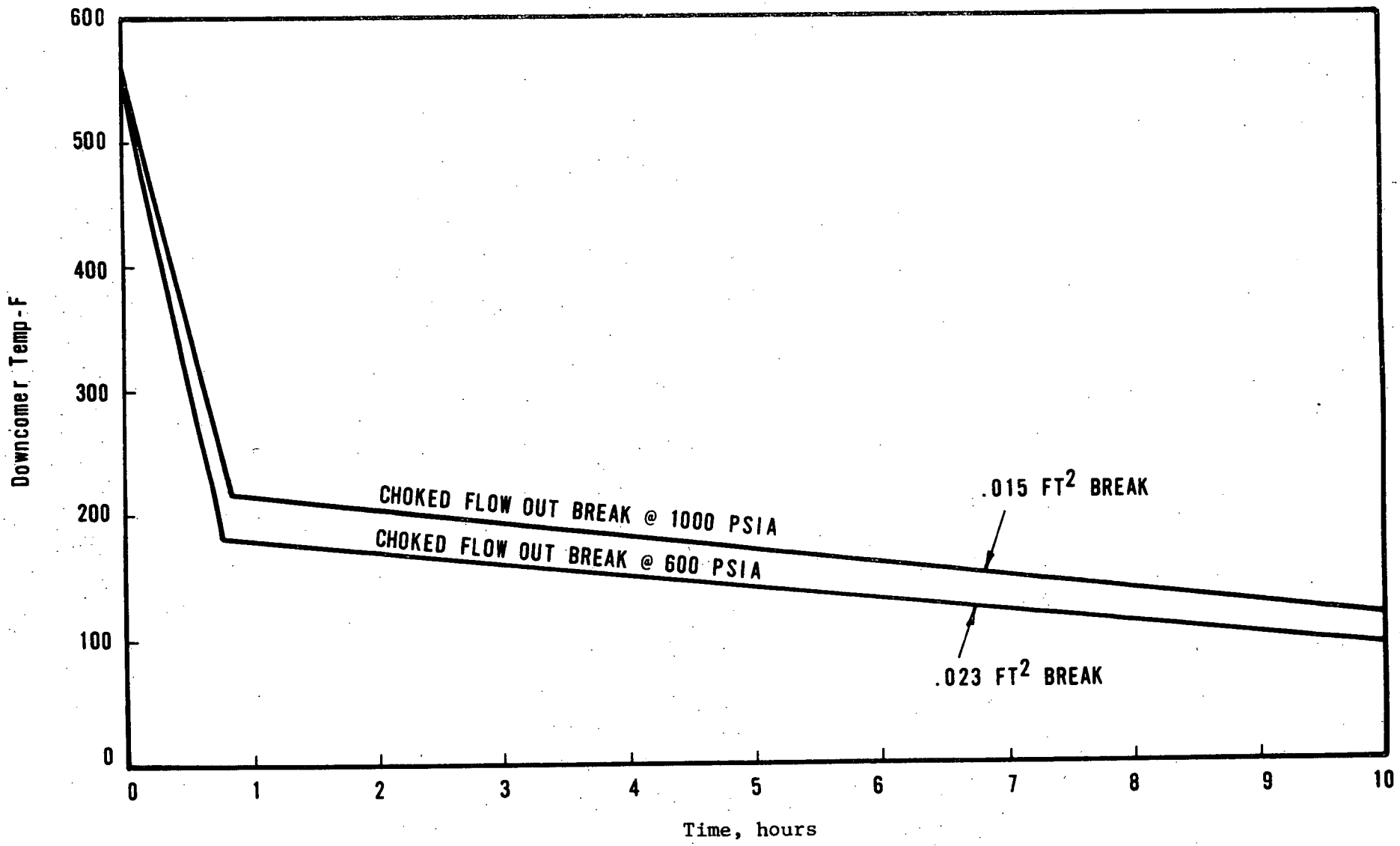

Figure 2-26. RC Loop Flow Vs Time, 0.015- and 0.023-ft$^2$ Pressurizer Breaks Without HPI Throttling, Flow Path 3

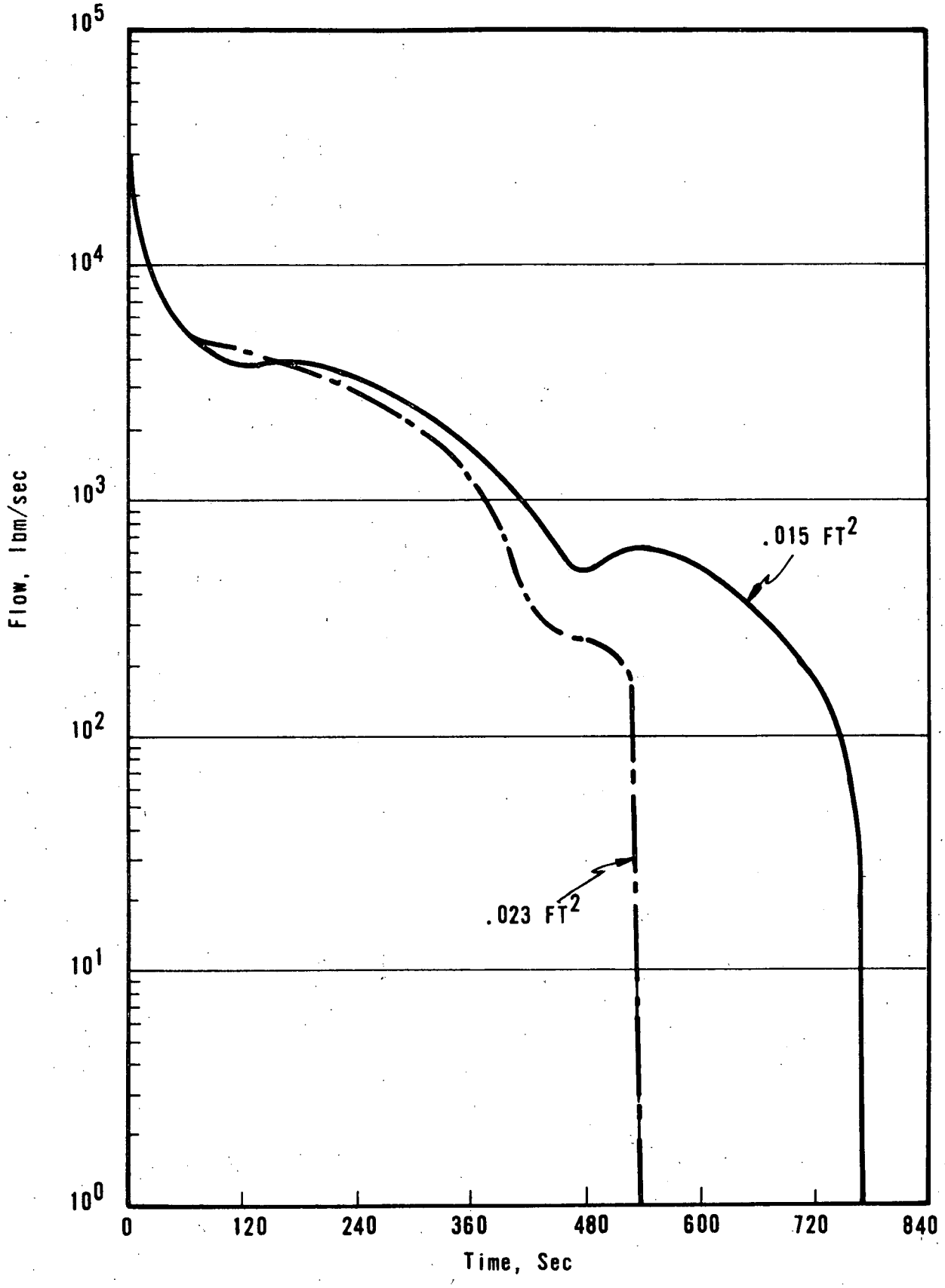

Figure 2-27. Downcomer Temperature Vs Time, 0.007-, 0.015-, and 0.023-ft$^2$ Pressurizer Breaks With HPI Throttling at 100F Subcooled Core Outlet Assuming Moody Discharge Flow for 100F Subcooled Water

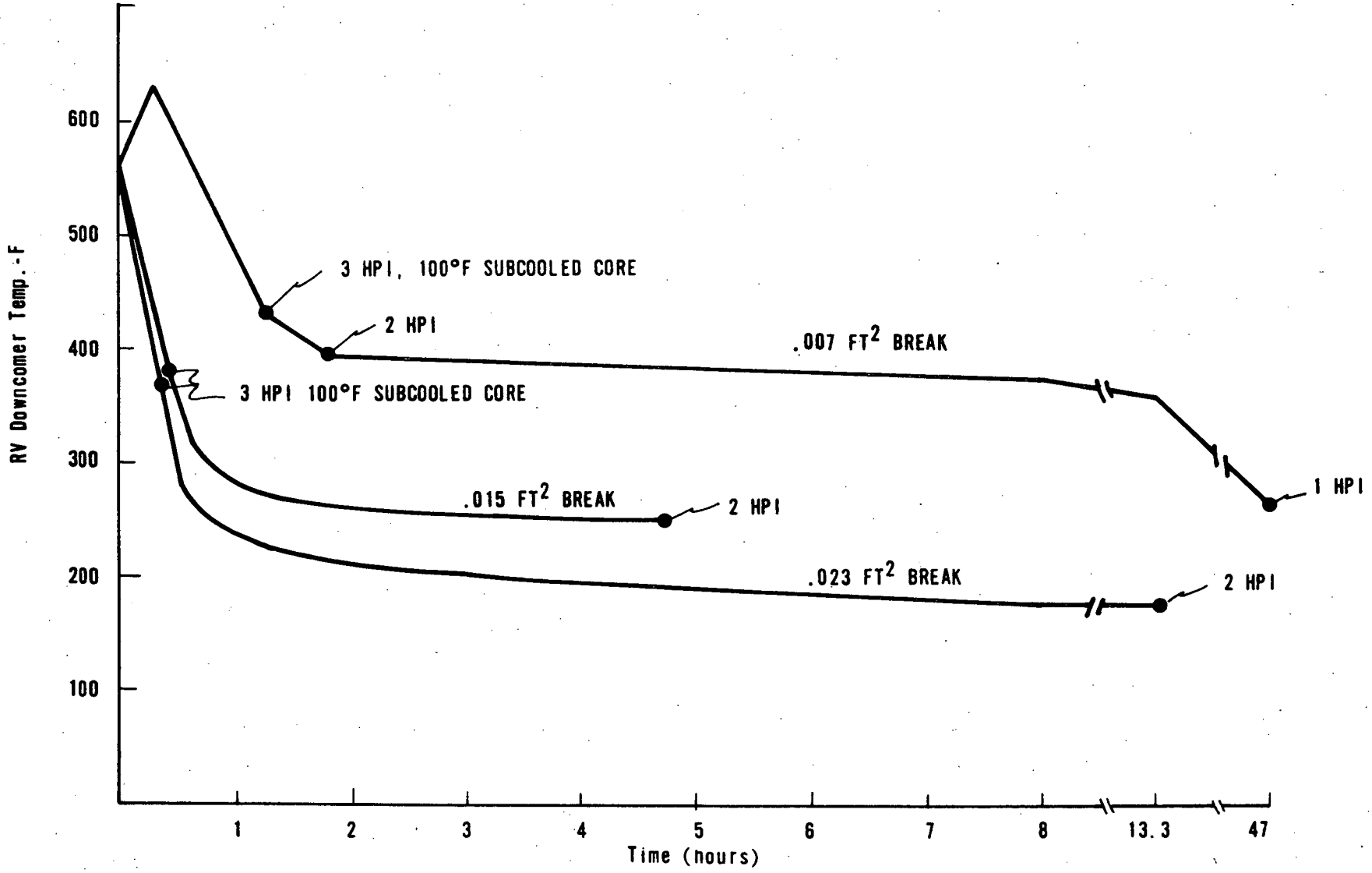

Figure 2-28. RV Pressure Vs Time, 0.007-, 0.015-, and 0.023-ft$^2$ Pressurizer Breaks With HPI Throttling at 100F Subcooled Core Outlet Assuming Moody Discharge Flow for 100F Subcooled Water

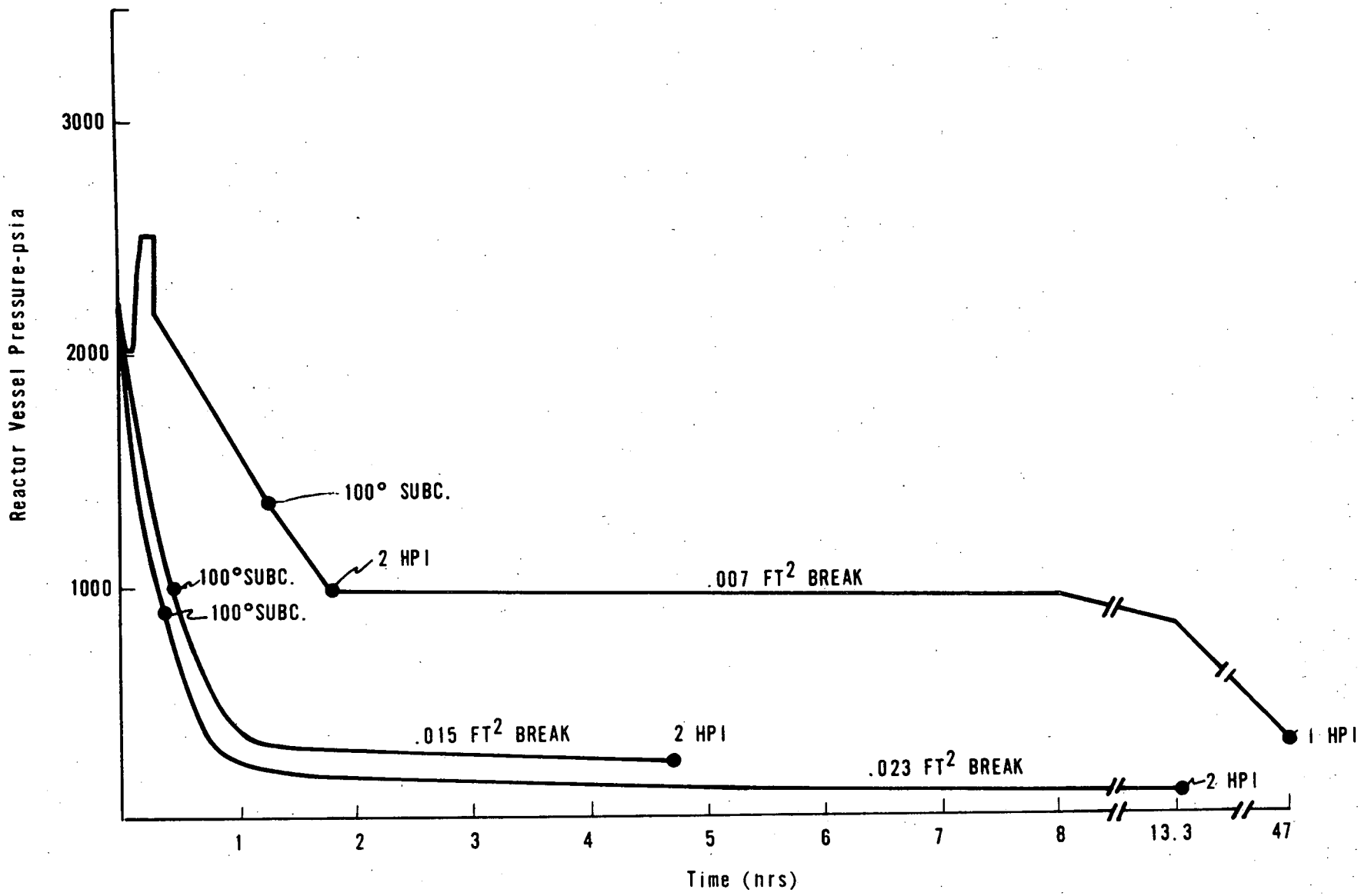

Figure 2-29. HPI Flow Vs Time, 0.007- and 0.023-ft$^2$ Pressurizer Break With Operator Action

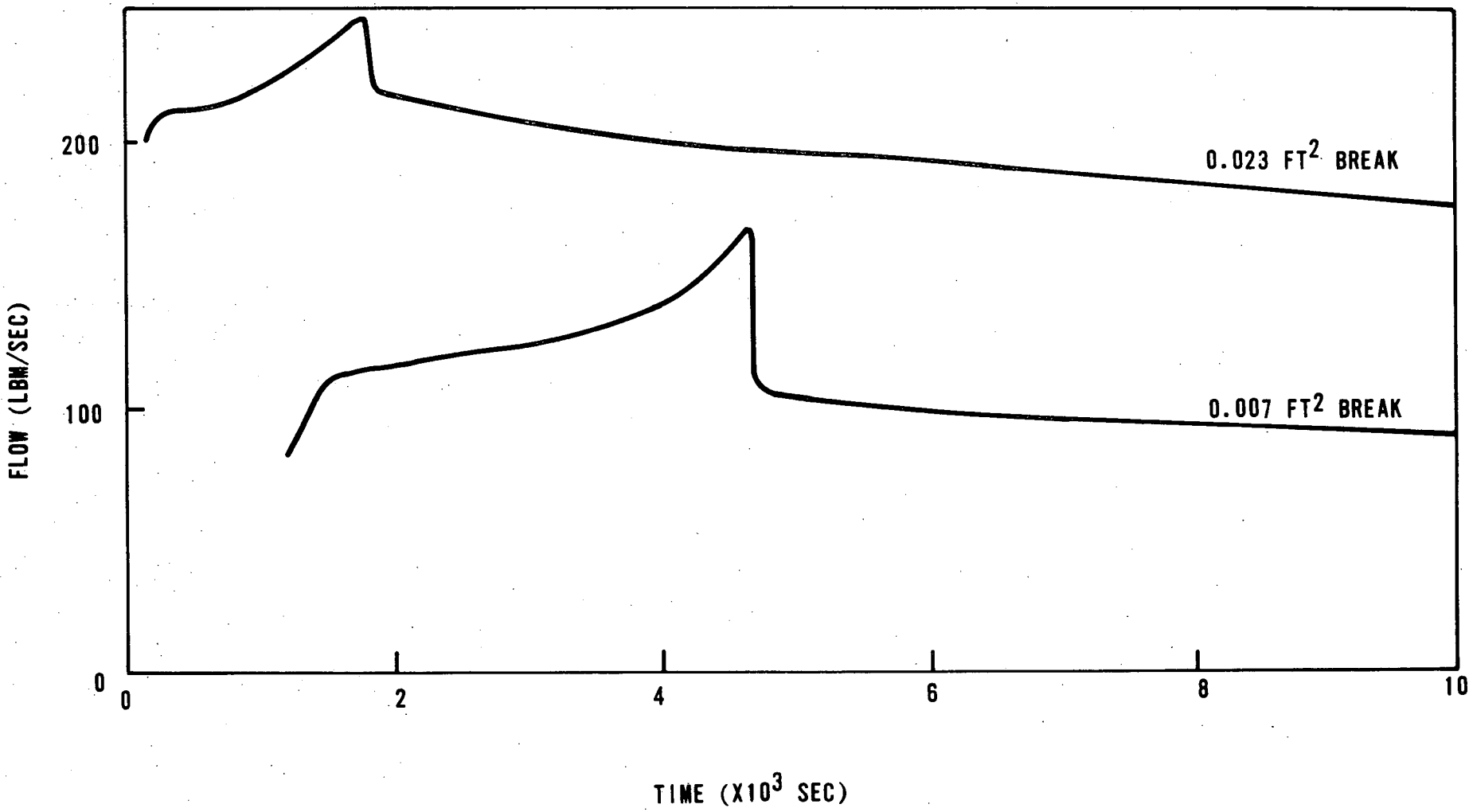

Figure 2-30. Vent Valve Flow Vs Time, 0.007- and 0.023-ft$^2$ Pressurizer Break With Operator Action

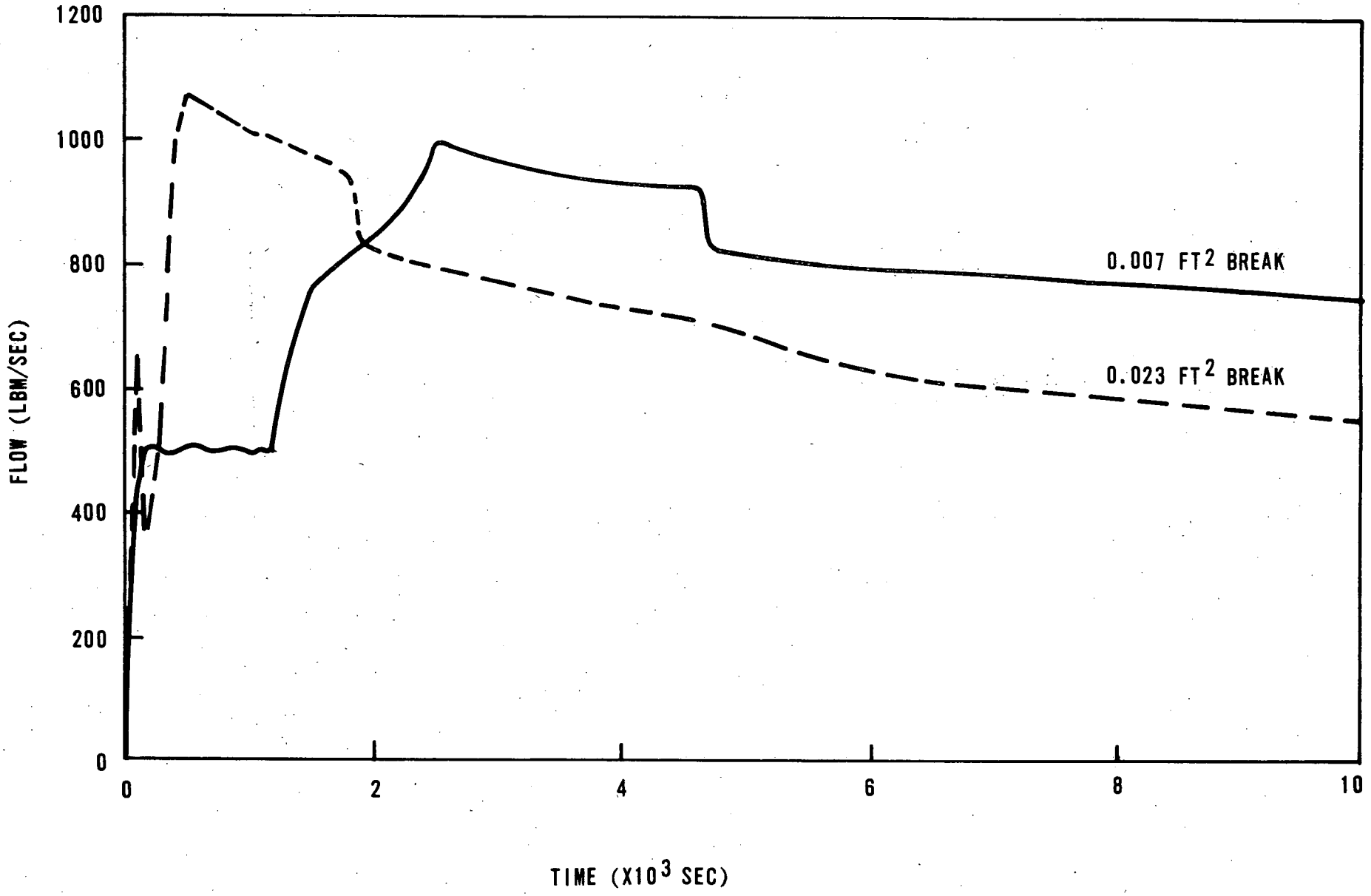

Figure 2-31. Vent Valve Fluid Temperature Vs Time, 0.007- and 0.023-ft$^2$ Pressurizer Break With Operator Action

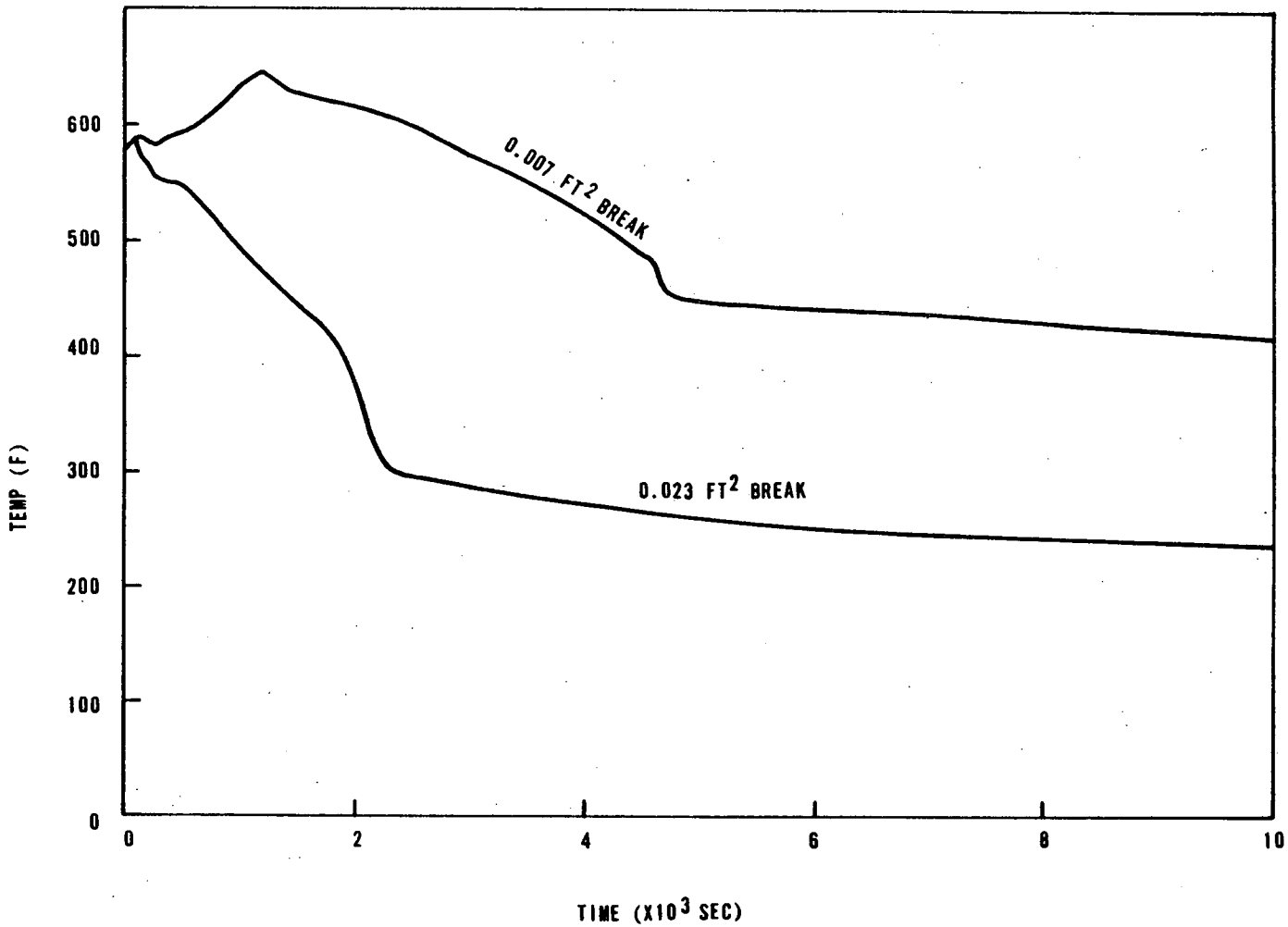

# 3. REACTOR VESSEL DOWNCOMER MIXING

The fracture toughness of the RV is a function of the temperature of the downcomer fluid next to the RV wall. Therefore, to derive the RV fracture toughness, the downcomer fluid mixing must be evaluated to determine the fluid temperature next to the RV wall. The various mixing models used in the analyses are presented below.

## 3.1. CRAFT Mixing (Case 1, Table 1-1)

The LOCA analyses described in section 2 determine mixed mean downcomer temperature. One node (node 1 in Figure 2-2) is used in the CRAFT model for the RV downcomer; it calculates the RV downcomer temperature assuming complete mixing of all fluids in the downcomer. For the extended loss-of-feedwater transients, the fluids entering the downcomer are the cold leg loop flow (only at the very beginning of the event), the HPI flow, and the vent valve flow. After the loop flow stops, only the HPI and vent valve flows remain. The velocities of the flows are very low (less than 1 fps in the cold leg and downcomer); consequently, complete mixing in the downcomer as determined by CRAFT may not occur.

## 3.2. MIX2 Mixing (Cases 2 and 3, Table 1-1)

Because the vent valve flow offers the most benefit with regard to downcomer water heatup, an effort was made to analytically predict the mixing. MIX2, a two-dimensional code under development at B&W, was used to model the region of the downcomer where mixing takes place. MIX2 solves the continuity, momentum, and energy equations in both space and time for single-phase, compressible water flow. The solution method employed is the implicit-continuous-Eulerian technique. The gravity effect is also included in the analysis to handle natural circulation or mixed convection problems. The inputs to MIX2 are the system pressure, inlet flow velocities, and temperatures. The turbulence exchange is modeled by an effective viscosity model. The outputs of MIX2 are the local velocity and temperature fields of the domain being analyzed.

### 3.2.1. Analysis Assumptions

Breaks of various sizes, both with and without operator action, were analyzed. The 0.023-$ft^2$ break with operator action to throttle the HPI to maintain the core outlet 100F subcooled (case 3) is given herein as an example case because loss of natural circulation occurs faster for this break than for the 0.007- or 0.015-$ft^2$ breaks ($\sim$540 seconds). As such, it would be the controlling break for minimum cooldown times for small breaks, which require heating of the HPI flow by hotter vent valve water.

The downcomer and part of the cold leg are modeled by a 18×12 grid system. HPI flow is modeled by a uniform stream going from right to left, and the vent valve flow is modeled by the stream coming from the top (as shown in Figure 3-1). The two streams of different temperatures are mixed in the downcomer region. It must be pointed out that MIX2 is a two-dimensional code, so assumptions must be made to account for the flow distribution in the circumferential direction, i.e., how the HPI and downcomer flows spread out in the downcomer annulus.

An obvious assumption that can be made is that both the HPI water and the vent valve flow spread out quickly and distribute uniformly in the downcomer annulus. Calculational results indicated that the fluid temperature in the downcomer obtained from this analysis is generally quite high, and it provides an optimistic estimate for the vessel wall temperature. Actual conditions may or may not approach this model. On the other hand, we can assume that the HPI water does not spread around the annulus, while the vent valve flow distributes uniformly. This is a much more conservative assumption, and the calculational results given herein as an example and used in cases 2 and 3, Table 1-1 use that assumption.

These calculations were performed with and without accounting for gravity effects. It is also noted that because of modeling limitations, the mixing boundary condition used 40F water in the cold leg approximately 2 feet from the downcomer. If the length of cold leg pipe from the downcomer to the HPI injection point had been modeled, additional mixing would probably occur. The locations of the HPI nozzles on the cold leg pipes and their distance from the downcomer are shown for lowered- and raised-loop plants in Figures 3-2 and 3-3, respectively.

### 3.2.2. Analysis Performed

The following parameters were used for the mixing analysis:

| | |
|---|---|
| Number of cells in X-direction | 18 |
| Number of cells in Y-direction | 12 |
| $\delta X$, ft | 0.139 |
| $\delta Y$, ft | 0.467 |
| Turbulent diffusivity $\nu_T$, $10^{-4}$ $ft^2/s$ | 1.0 |
| HPI temperature, F | 40 |

System pressure, HPI and vent valve flow velocities and temperatures were obtained from the analysis described in section 2.

The results of the MIX2 calculations are fluid temperature profiles in the downcomer immediately below the nozzle. Figure 3-4 illustrates typical downcomer fluid temperature profiles both with and without gravity effects. It can be seen that the case with the gravity effect has a more moderate temperature gradient in the downcomer. This is because the gravity effect tends to cause the HPI flow to settle and flow along the bottom of the cold leg, creating space for the hotter vent valve flow to come in to the upper part of the cold leg pipes. This phenomenon can be illustrated by the two schematic flow maps appearing as Figures 3-5 and 3-6. As a result of the gravity effect, considerable mixing takes place in the cold leg and the stratification effect is less pronounced.

The resulting downcomer fluid temperature at the vessel wall directly beneath the cold leg nozzle for the 0.023-$ft^2$ break with operator action (case 3, Table 1-1) is shown in Figure 3-7.

### 3.2.3. Summary

Based on the results of the mixing analysis, it is concluded that mixing will occur and that the HPI water will be heated by the hotter vent valve water. Quantification of the mixing benefit is more difficult. If the circumferential distribution assumptions of the previous section are accepted (uniform vent valve flow distribution, concentrated HPI), then the analyses show the mixing phenomenon could provide as much as 150F of heatup based upon 540F vent valve water. In addition, the heatup could be greater than 150F if the existing 17 feet of cold leg between the HPI injection point and the downcomer were used

in the analysis rather than 2 feet. However, the uncertainty in the circumferential distribution of flow and in the analytical predictions (both computational and modeling) makes the exact benefit difficult to determine.

### 3.3. Bounding Analyses (Case 4, Table 1-1)

Because of the uncertainty in the degree of HPI-vent valve fluid mixing actually taking place in the downcomer bounding analyses were performed. These analyses assumed essentially no mixing. They are discussed more fully in sections 4 and 5.

Figure 3-1. Numerical Model of MIX2 Analysis

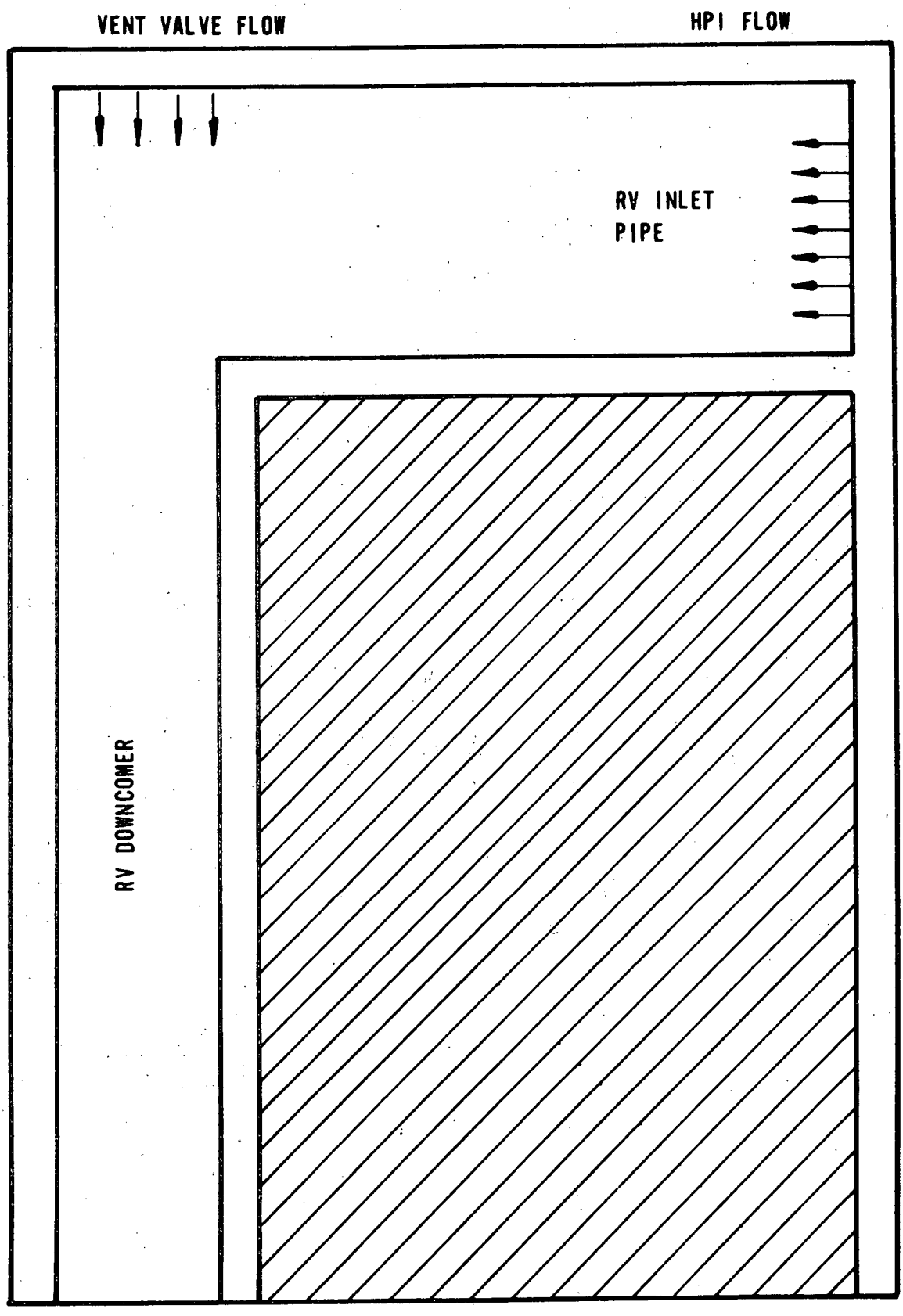

Figure 3-2. Locations of HPI Nozzles (One on Each Cold Leg Pipe) — Lowered-Loop 177-FA Plants

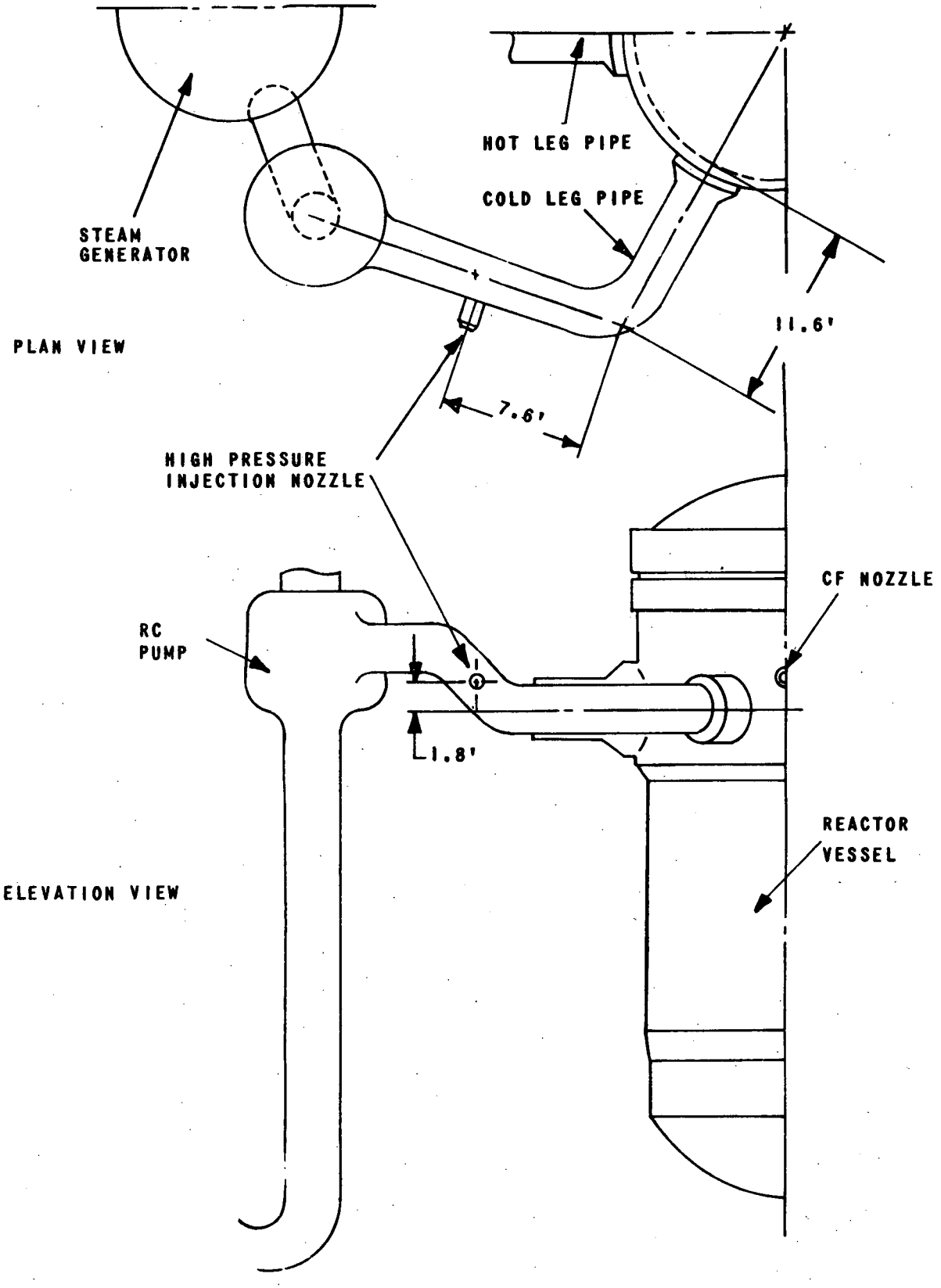

Figure 3-3. Locations of HPI Nozzles (One on Each Cold Leg Pipe) — Raised-Loop 177-FA Plants

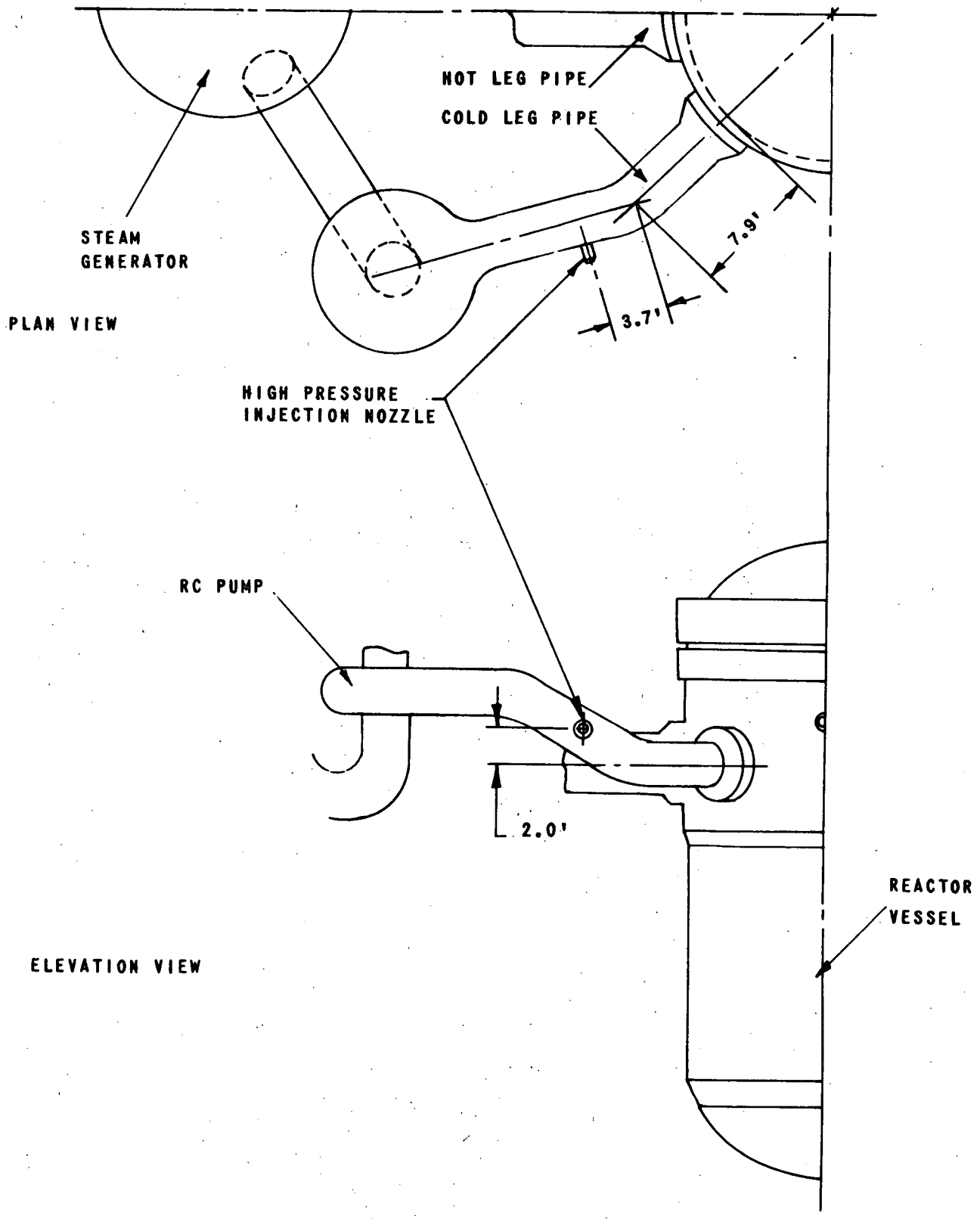

Figure 3-4. Downcomer Fluid Temperature Profiles — HPI Temperature 40F, VV Temperature 540F, $(\dot{M}_{HPI}/\dot{M}_{VV}) \sim 1.5$

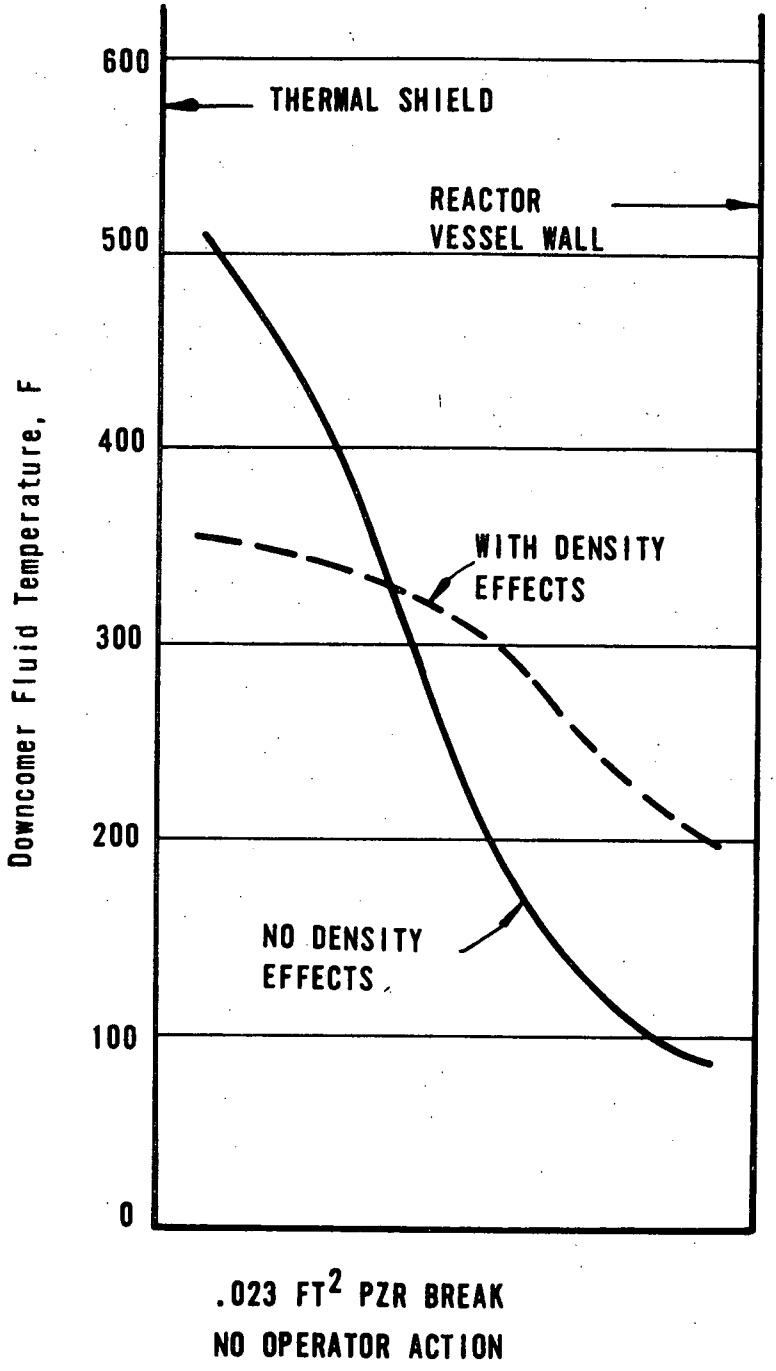

Figure 3-5. Downcomer/Cold Leg Velocities Without Density Effects

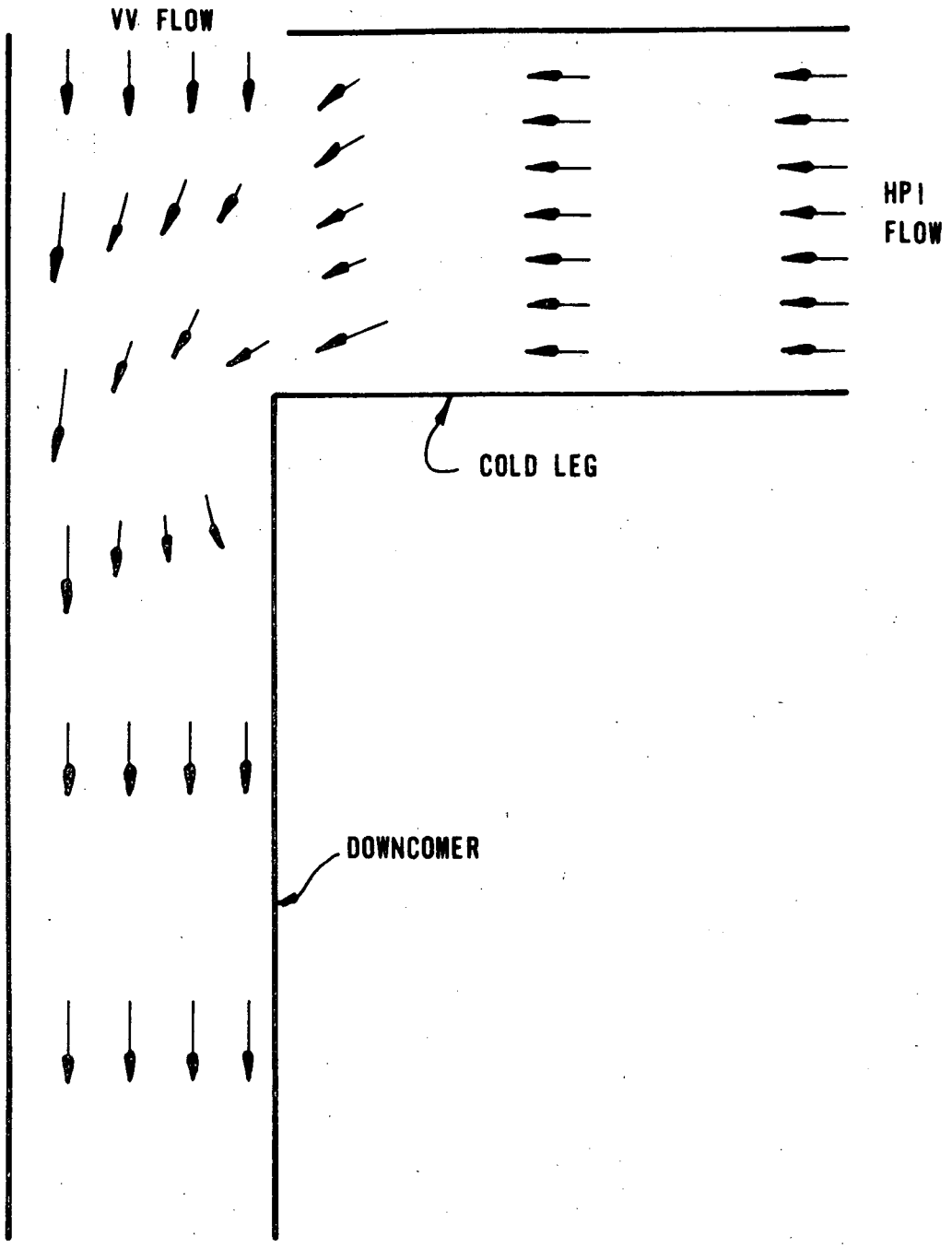

Figure 3-6. Downcomer/Cold Leg Velocities With Density Effects

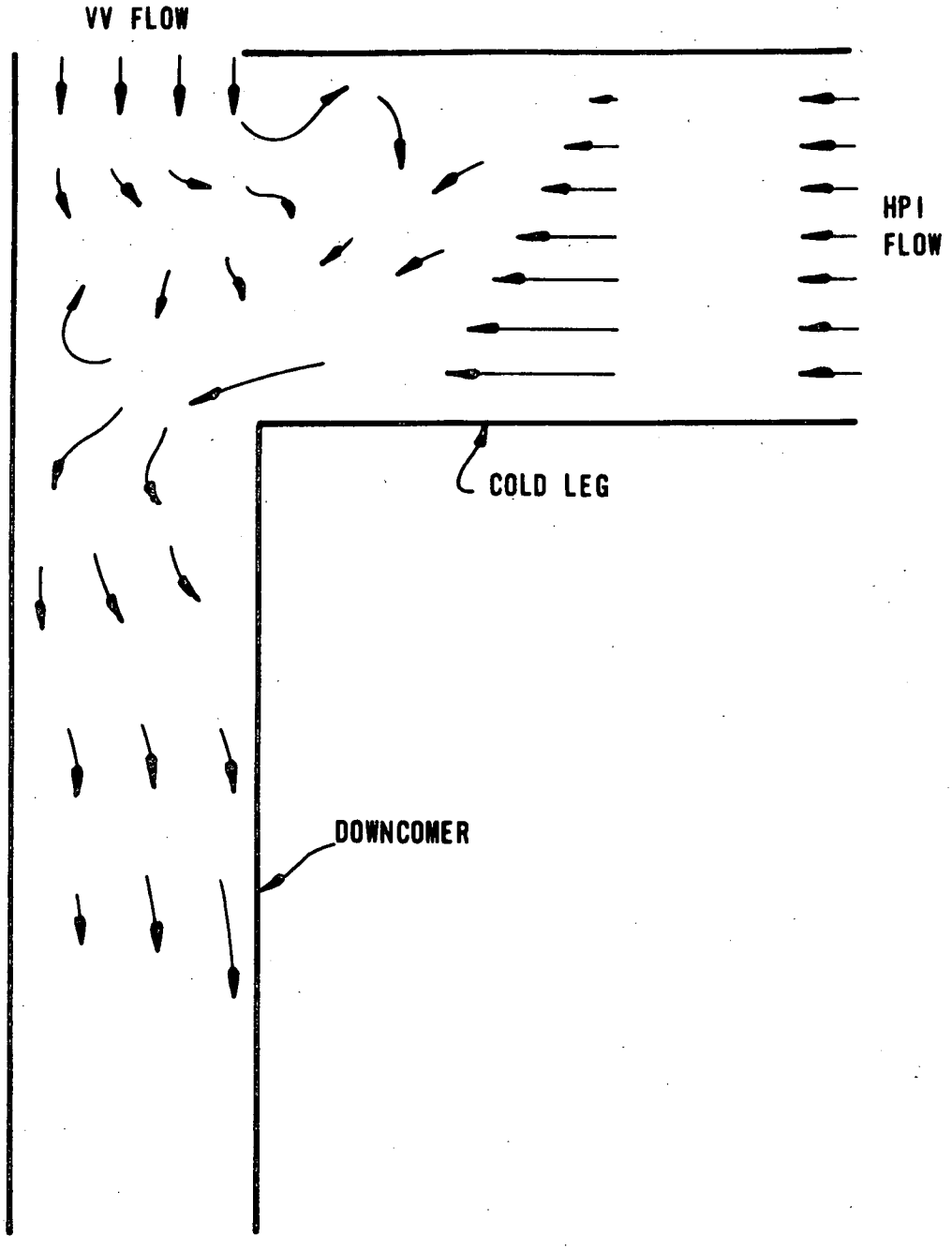

Figure 3-7. Downcomer Fluid Temperature at the RV Wall, 0.023-ft$^2$ Pressurizer Break With Operator Action, MIX2 Results

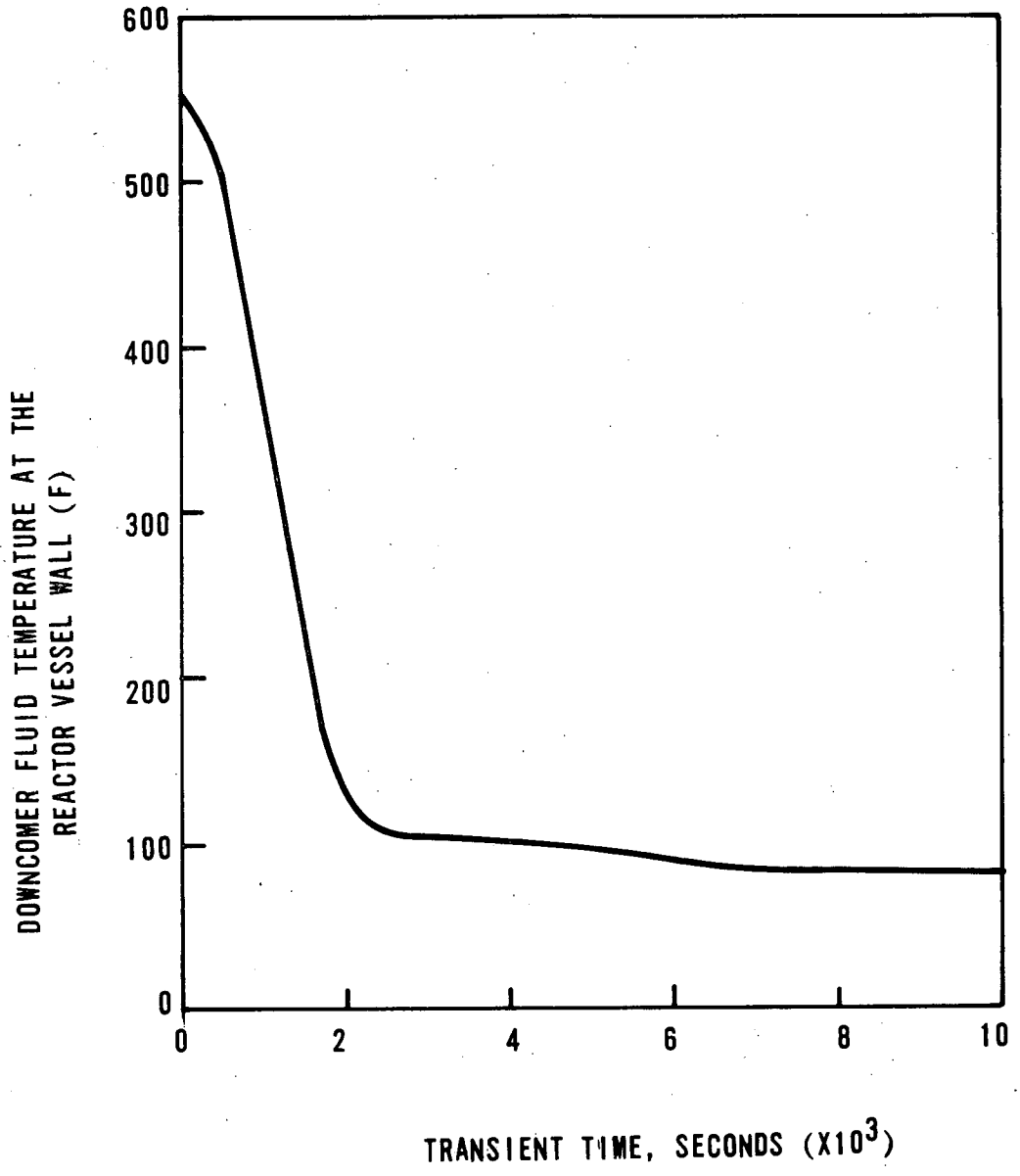

# 4. REACTOR VESSEL COOLDOWN ANALYSES

Once the downcomer fluid temperature next to the reactor vessel wall is determined using the methods described in section 3, the temperature profile in the reactor vessel versus time must be calculated. These reactor vessel cooldown analyses are described in this section.

## 4.1. 0.007-ft$^2$ Pressurizer Break Without HPI Throttling (Case 1, Table 1-1)

The initial analysis performed to evaluate the thermal shock concern was the 0.007-ft$^2$ pressurizer break without HPI throttling (case 1). The downcomer fluid temperature used in this analysis was the CRAFT determined mixed mean temperature, as described in section 3.1. The reactor vessel cooldown analysis performed for case 1 employed the BEFRAN[3] computer code. This analysis uses a one-dimensional, cylindrical heat transfer calculation which assumes a constant film coefficient. Subsequent reactor cooldown analyses (cases 2-4) used a more detailed calculation, as described below.

## 4.2. 0.007- and 0.023-ft$^2$ Pressurizer Breaks With Operator Action to Throttle HPI Flow (Cases 2-4, Table 1-1)

As mentioned in section 2.3 and described in detail in section 5, fracture mechanics analyses performed on the 0.007-ft$^2$ break without operator action to throttle HPI flow produce unacceptable results after several hours. As a result, analyses which included operator action were performed (cases 2-4, Table 1-1). The reactor vessel cooldown analyses performed on these cases is described herein. The downcomer fluid temperatures versus time used as input to cases 2 and 3 were the MIX2 results described in section 3.2. The downcomer fluid temperature versus time used in case 4 represents an extremely conservative bounding analysis. Except for the differences in the downcomer fluid temperature used as input, the reactor vessel cooldown analyses performed for cases 2-4 employ the same techniques. The bounding analysis (case 4) is described in detail in this section.

### 4.2.1. Bounding Reactor Vessel Cooldown Analyses (Case 4, Table 1-1)

As previously discussed, uncertainties exist in determining the extent of water mixing in the reactor vessel downcomer; therefore, to bound the overall concern, some conservative analyses were conducted. Four analyses assuming no HPI-vent valve flow mixing were performed to determine the RV thermal gradients versus time. These situations could be perceived as HPI flowing into the RV downcomer and then streaming down along the RV wall with no mixing with vent valve flow. For these analyses complete mixing was assumed in the RV downcomer while RC loop flow existed. Once the RC loop flow stopped, the RV downcomer temperature was rapidly dropped over 50 seconds to the assumed HPI temperature and then sustained there (Figure 4-1). In one analysis, the final downcomer temperature was assumed to be 40F, which corresponds to the minimum BWST temperature. In the other three analyses, the final downcomer temperatures were 90, 120, and 150F, which reflect various amounts of mixing.

Reactor vessel temperatures during a 0.023-$ft^2$ break with operator action were calculated. Fluid conditions were taken from the analyses described in section 2.3. Wall surface heat transfer is obtained from the larger of (turbulent) forced and free convection heat transfer. The transient one-dimensional wall energy transfer problem was solved using the explicit Euler technique. Wall temperatures and temperature gradients are obtained for nominal conditions, for varying injection temperatures, and (by separate analysis) with allowances for azimuthal conduction in the wall.

#### 4.2.1.1. Assumptions

1. Fluid Heating — After loop flow stagnates, the downcomer bulk fluid temperature is set arbitrarily to temperatures of 40, 90, 120, or 150F.
2. Initial Temperatures — Gamma and neutron flux attenuation in the wall are used to set the initial temperature distribution in the reactor vessel.
3. Vessel Outer Surface — The outer surface of the RV is assumed to be perfectly insulated.
4. Film Heat Transfer — Film heat transfer variations in opposing mixed convection are ignored. The film heat transfer coefficient (HTC) is set to the larger of the (pure, turbulent) forced and free HTCs.

4.2.1.2. Conditions

1. Geometry — The vessel wall is 8.4375-inch SA-508 class 2 steel, clad on the inner face with 0.1875-inch stainless steel; the inside diameter is 170.625 inches. The inner boundary of the downcomer is the thermal shield, with a 151-inch outer diameter. The heated length is 15 feet (but is of no consequence here, without fluid heating).

2. Initial Conditions — Initial conditions are those of an operating 177-FA plant at full power. Coolant flow is 131 mlbm/h at 555.4F and 2200 psia. Flux attenuation in the vessel wall generates 24 kBtu/h-ft$^4$ at the inner surface, attenuating approximately exponentially with wall depth (with a linear attenuation coefficient of 8.4/ft). Film heat transfer is by forced convection, and the total temperature rise across the vessel wall is 17F.

4.2.1.3. Analyses

1. Fluid Conditions — Fluid conditions are used as input except that loop flow from CRAFT is added to injection flow after HPI initiation at 140 seconds, and HPI flow is multiplied by 4.5 to account for fluid streaming after loop flow stagnates at T=540 seconds (the ratio of downcomer circumference to inlet nozzle diameter is 4.5).

2. Film Heat Transfer — In opposing flow, with forced convection downward along a vertical heated wall, heat transfer may differ from either pure forced or pure free convection. In laminar flow, opposing heat transfer is usually degraded from pure (forced or free) convection, but this influence in turbulent flow is unknown. Thus, the film heat transfer herein is estimated by evaluating the pure forced convection HTC and selecting the larger of the two, Figure 4-2. The forced convection HTC is as follows[4]:

$$H_{forced} = 0.023\ K/D\ Re^{0.8}\ Pr^{0.43}\ (Btu/h\text{-}ft^2\text{-}F)$$

where

K = fluid thermal conductivity, Btu/h-ft-F,

D = hydraulic diameter, ft (D $\sim$ 2W where W = downcomer width),

Re = Reynolds number, the ratio of inertial to viscous forces, Re = VD/$\nu$.

$V$ = fluid velocity, fps,

$\nu$ = kinematic viscosity, $ft^2/s$,

Pr = Prandtl number, the ratio of storage to conduction energy transfer, $Pr = C_p \mu/K$,

$C_p$ = specific heat, Btu/lbm-F,

$\mu$ = dynamic viscosity, lbm/h-ft.

Because $H_{forced}$ is proportional to $V^{0.8}$, it decreases abruptly as loop flow stagnates (Figure 4-2).

The free (or natural) convective HTC is[5]

$$H_{free} = 0.094\ K/L\ (Gr\ Pr)^{1/3}$$

where

$L$ = heated length, ft,

Gr = Grashof number, the ratio of buoyant to inertial force, $Gr = g\beta\Delta TL^3/\nu^2$,

$g$ = gravitational acceleration, 32 $ft/s^2$,

$\beta$ = fluid thermal expansivity, $\beta = 1/\rho\ \partial\rho/\partial T\ (1/F)$,

$\Delta T$ = governing temperature difference, wall to fluid, F.

Notice that (turbulent) $H_{free}$ is apparently independent of heated length, Also, as $H_{forced}$ decreases, the wall-to-fluid temperature difference increases, as does $H_{free}$ (Figure 4-2).

3. Vessel Wall Heat Transfer — The energy equation in the wall:

$$\rho C_p \frac{\partial T}{\partial t} = K\left(\frac{\partial^2 T}{\partial r^2} + \frac{1}{r}\frac{\partial T}{\partial r}\right),$$

with

$T = T(r,t)$ and boundary conditions (inner surface convection), $K\ \partial T/\partial r\ (r = r_i) = H[T(r = r_i) - T_{bulk}]$, and (insulated outer surface) $\partial T/\partial r\ (r = r_o) = 0$,

is solved by discretization in space and application of the Euler explicit method to solve the approximate system of ordinary differential equations. Temperature-dependent properties are employed,[6,7] as are the HTC modeling techniques previously described.

The solution of the energy equation is verified by comparing it to the slab approximation (valid for large inner radius):

$$\rho C_p \frac{\partial T}{\partial t} = K \frac{\partial^2 T}{\partial x^2}$$

The adequacy of the temporal incrementation is verified by doubling the number of time steps and comparing the standard and refined solutions. Spatial and temporal increments of $\Delta r$ = 1/8 inch and $\Delta T$ = 1/10 second are used.

4.2.1.4. Results

The resultant film HTC changes from forced to free at 7 minutes into the transient (Figure 4-2). Thus, free convection governs the bulk of the transient and ranges from h $\tilde{=}$ 200 Btu/h-ft$^2$-F at t=10 minutes to h $\tilde{=}$ 100 at t=1 hour, decreasing with wall surface temperature. Wall temperature profiles respond to downcomer temperatures (Figure 4-3); as loop flow stagnates, the downcomer temperature approaches the injection temperature, and wall surface heat transfer increases markedly. By t=10 minutes, the inner surface temperature approaches that of the injected fluid, but the outer wall temperatures have barely changed.

The assumed downcomer temperature was varied to assess its impact. As expected, the resultant wall temperature profiles are less sloped with raised downcomer temperatures, especially at later transient times (Figure 4-3).

Tangential conduction was investigated using FELCON, a transient, two-dimensional, finite element conduction code.[8] The wall temperature response without tangential conduction was obtained by setting the entire inner surface to 40F at t > 0. Tangential conduction effects were then introduced by setting 2 feet of the inner surface to 40F, while retaining the remaining 8 feet at 550F, and extracting the wall temperature profiles in the cooled region. As with increased HPI temperatures, tangential conduction decreases the wall temperature gradient, particularly at later transient times (Figure 4-4).

As discussed earlier, these results are very conservative and present a bounding case to the thermal shock question. The results of the fracture mechanics analysis for these cases are discussed in section 5.

Figure 4-1. Downcomer Fluid Temperature, 0.023-ft$^2$ Break (Typical Case 4, Table 1-1)

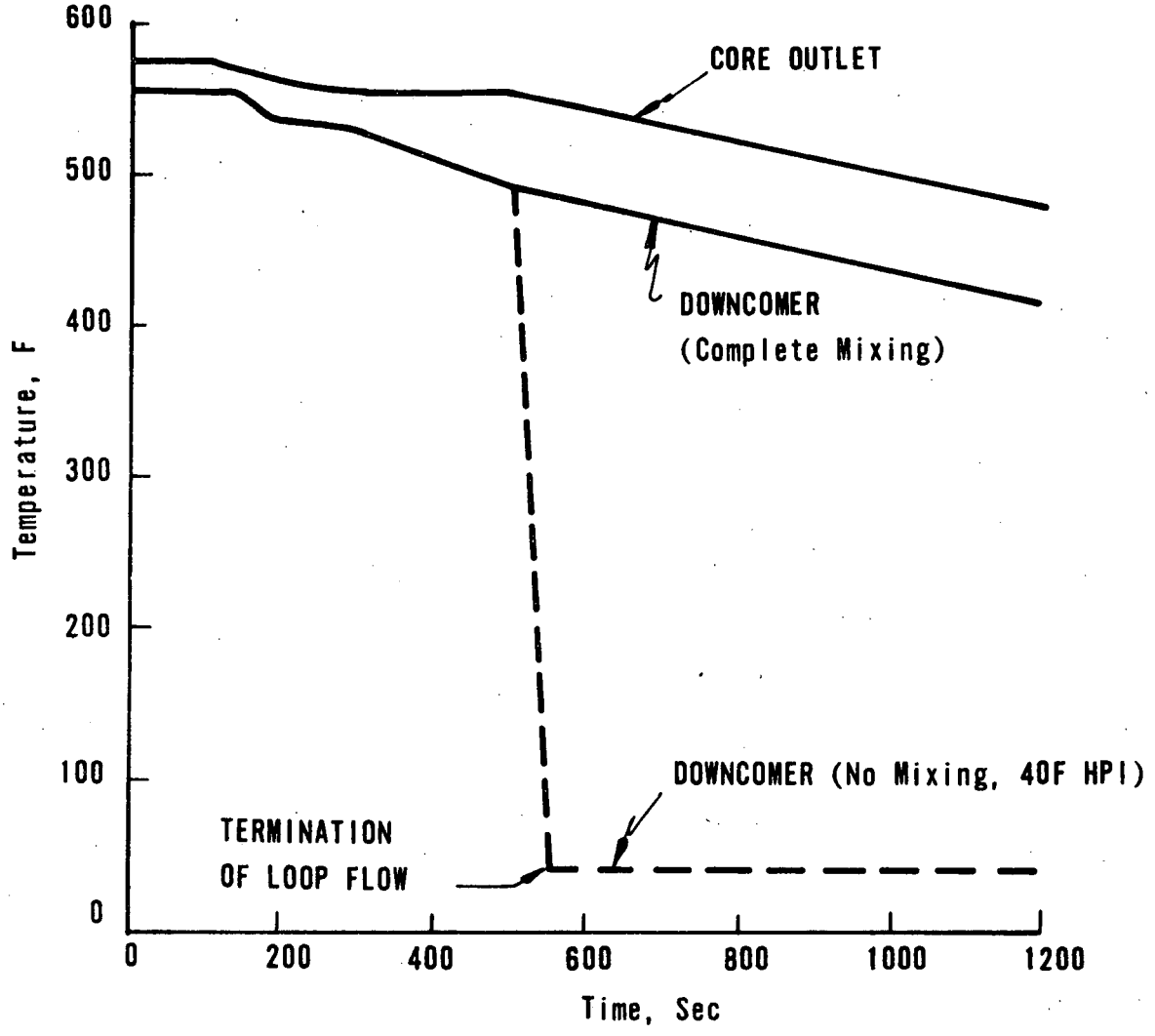

Figure 4-2. Heat Transfer Coefficient Vs Time
(Typical Case 4, Table 1-1)

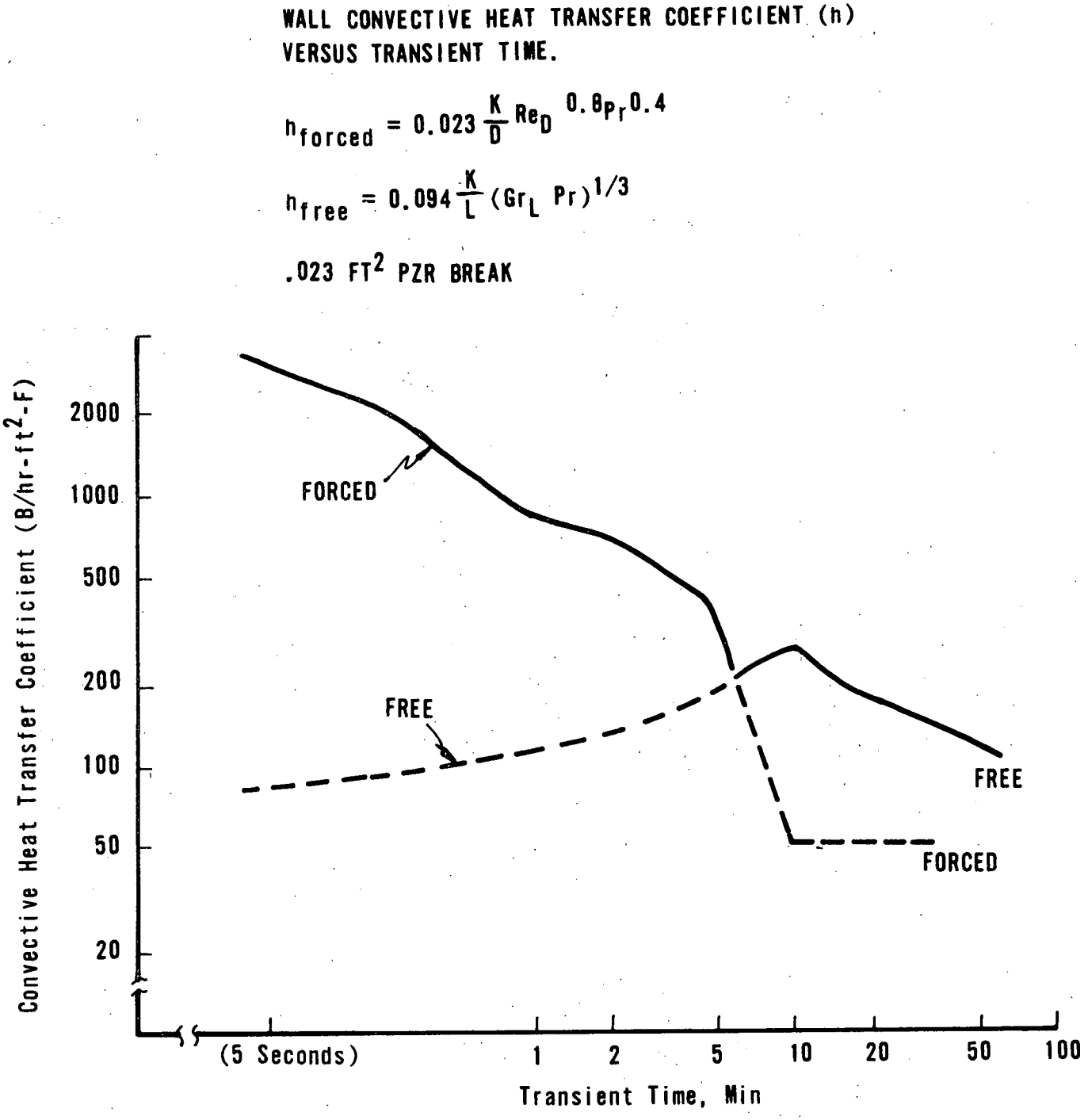

Figure 4-3. Transient Wall Temperature Profiles, 0.023-ft$^2$ Pressurizer Break (Typical Case 4, Table 1-1)

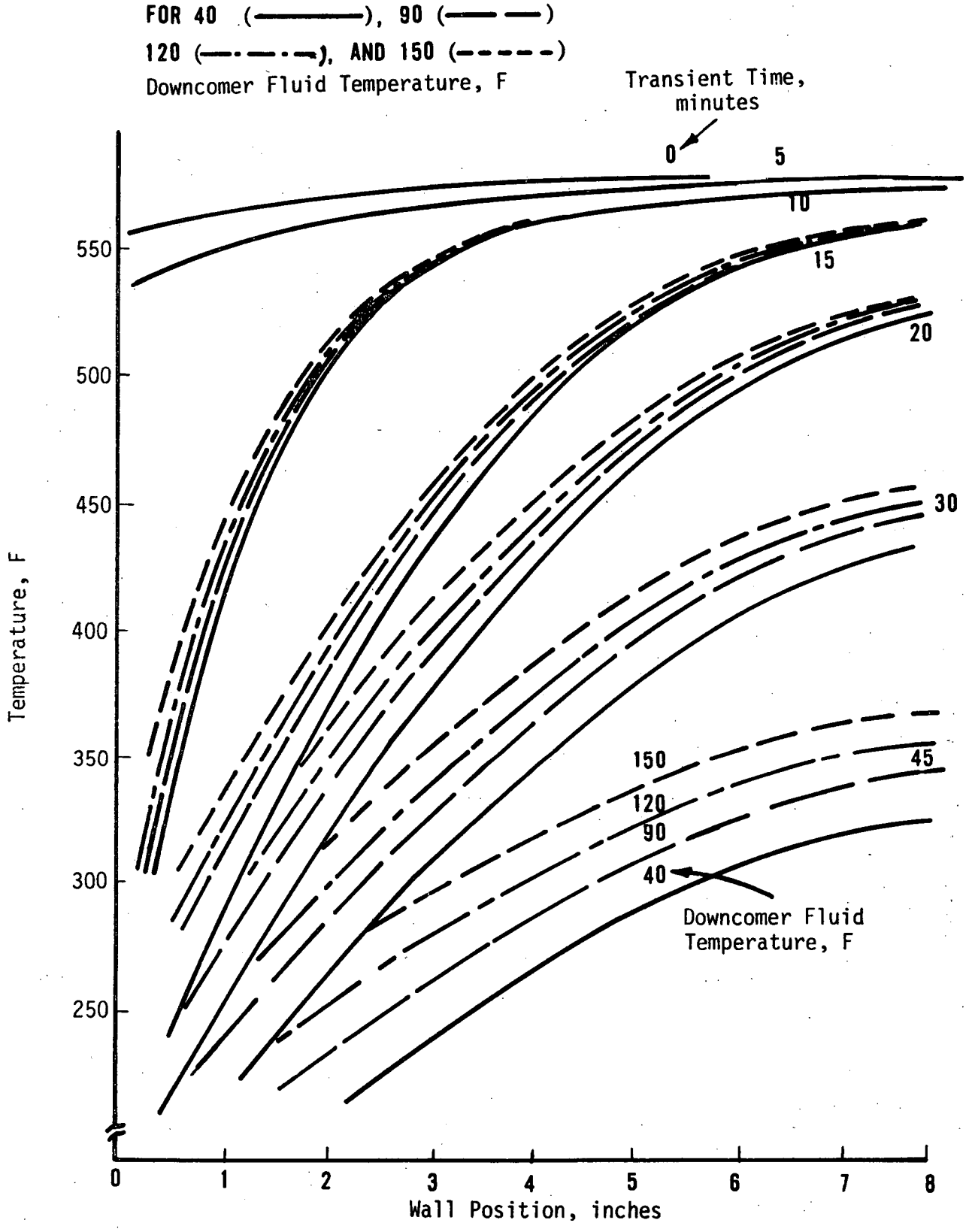

Figure 4-4. Tangential Conduction

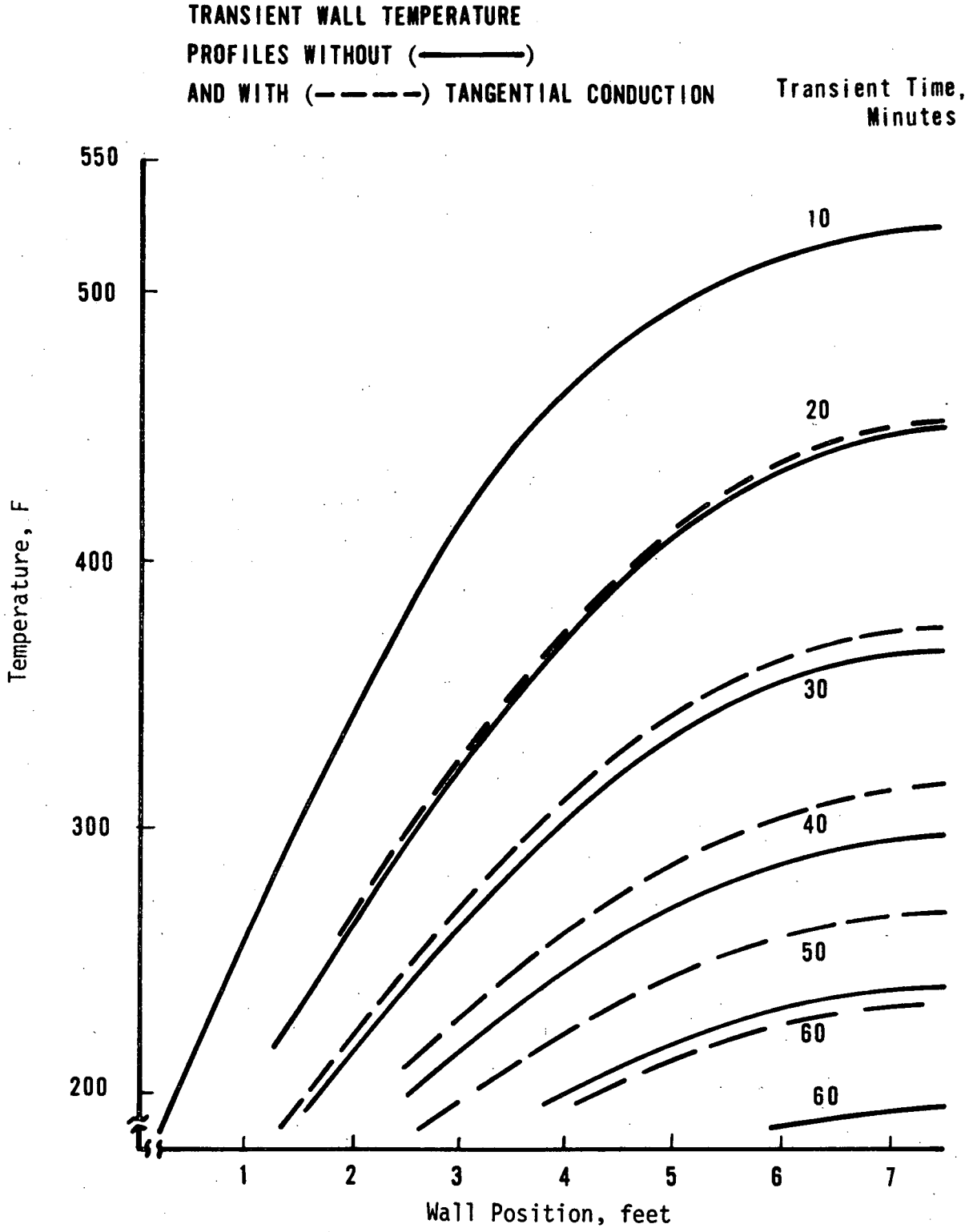

# 5. FRACTURE MECHANICS ANALYSES

The transient cases summarized in Table 1-1 have been evaluated to determine whether crack initiation is predicted. Subsequent crack arrest and the possiblity of warm prestressing are also evaluated.

## 5.1. Methodology

The linear elastic fracture mechanics (LEFM) analytical technique has been used to evaluate both types of transients discussed above. The validity of LEFM for predicting crack initiation and arrest has been demonstrated by the thermal shock experiments conducted in the HSST Program at the Oak Ridge National Laboratory.

### 5.1.1. Thermal Stress Intensity Factors

The thermal stresses due to the temperature gradient through the thickness of the vessel are computed from the following general relationship:

$$\sigma_r = \frac{\alpha E}{1-\nu}\frac{1}{r^2}\left[\frac{r^2-a^2}{b^2-a^2}\int_b^a Trdr - \int_a^r Trdr\right],$$

$$\sigma_\theta = \frac{\alpha E}{1-\nu}\frac{1}{r^2}\left[\frac{r^2+a^2}{b^2-a^2}\int_a^b Trdr + \int_a^r Trdr - Tr^2\right],$$

$$\sigma_z = \frac{\alpha E}{1-\nu}\left[\frac{2}{b^2-a^2}\int_a^b Trdr - T\right]$$

where

$\alpha$ = coefficient of thermal expansion,

$E$ = elastic modulus,

$\nu$ = Poisson's ratio,

$\sigma_r, \sigma_\theta, \sigma_z$ = stress components,

$r, \theta, z$ = reactor vessel axes.

The temperature distribution through the wall can be assumed to be approximately parabolic. The stress equations are evaluated by assuming the following general representation of the temperature distribution through the vessel.

$$T = A(b - r)^2$$

where

T = temperature,

r = vessel radial direction.

A,b = constants.

The stress intensity factors are then computed by the following generalized relationship[11]:

$$K_I = \sqrt{\pi c}\left(N_0F_1 + \frac{2c}{\pi}N_1F_2 + \frac{c}{2}N_2F_3 + \frac{4}{3}\frac{a^3}{\pi}N_3F_4\right)$$

where

c = crack depth, radially,

$N_0,N_1,N_2,N_3$ = coefficients of crack opening stress polynomial,

$F_1,F_2,F_3,F_4$ = geometry magnification factors depending on crack depth.

5.1.2. Pressure Stress Intensity Factors

The components of stress in the RV beltline region due to pressure are computed as follows:

$$\sigma_r = Pi \text{ at } r = a,$$

$$\sigma_z = \frac{a^2Pi}{b^2 - a^2},$$

$$\sigma_\theta = \frac{a^2Pi}{b^2 - a^2}\left(1 + \frac{b^2}{r^2}\right)$$

where

$\sigma_r,\sigma_z,\sigma_\theta$ = radial, axial, and hoop stresses,

r, z, $\theta$ = reactor vessel coordinate axes.

The stress intensity factors are computed from the same generalized relationship presented in section 5.1.1.

5.1.3. Welding Residual Stress Intensity Factors

The residual stresses due to welding are computed on the basis of the evaluation of residual stresses in heavy weldments conducted by Feril, Juhl, and

Miller.[9] The residual stress distribution through the vessel thickness is given below for three types of weld geometry shown in Figure 5-1.

Longitudinal welds: $\sigma(x)/S_y = 0.12 - 0.36x + 0.18x^2$

Circumferential welds:

Type 1: $\sigma(x)/S_y = -0.06 + 0.18x^2$ (Single V)

Type 2: $\sigma(x)/S_y = 0.12 - 0.72x + 0.72x^2$

where $\sigma(x)$ = residual stress distribution with directions as shown in Figure 5-1,

$S_y$ = yield stress,

$x = a/t$ (t - thickness), $o \leq a \leq t$.

The stress intensity factors are computed from the generalized relationship presented in section 5.1.1.

5.1.4. Material Fracture Toughness Data

The material fracture toughness data were obtained from the reference curves of the ASME Boiler & Pressure Vessel Code, Section XI, Appendix A.[10] Figure A-4200-1 gives lower bound static crack initiation toughness, $K_{IC}$, and crack arrest toughness, $K_{IA}$, as functions of metal temperature and material reference temperature, $RT_{NDT}$.

The material reference temperature, $RT_{NDT}$, is adjusted to account for irradiation embrittlement effects. The amount of adjustment to be added to the initial reference temperature is computed from USNRC Regulatory Guide 1.99. The adjustment is a function of the material's weight percent of copper and phosphorus and the accumulated neutron fluence, $n/cm^2$. The peak neutron fluence for the beltline region on the vessel inner surface is adjusted to account for specific weld locations axially and circumferentially. The neutron fluence attenuation through the vessel thickness is also taken into account.

Taking these factors into consideration, the controlling material was found to be the longitudinal weld seam, WF-70, in the lower shell of the Rancho Seco vessel. The properties of this material have been used as the base case for which all results have been quantified. The applicability of the results to reactor vessels other than that of the Rancho Seco plant and with lower irradiation levels is discussed in section 5.4.

Case 1 presented below (section 5.3.2.1) was analyzed using base material properties (Rancho Seco) and an accumulated neutron fluence corresponding to 6.0 EFPY* as a basis. (As of November 3, 1980, Oconee 1, the lead B&W plant, had accumulated 4.5 EFPY. Rancho Seco had accumulated 3.2 EFPY as of the same date.) The peak neutron fluence for the beltline region on the vessel inner surface corresponding to 6.0 EFPY is $4.0 \times 10^{18}$ n/cm$^2$. The computed adjusted reference temperature on the inner surface was 246F.

Cases 2 (section 5.3.2.2) and 4 (section 5.3.2.3) presented below were performed using base material properties (Rancho Seco) at an accumulated neutron fluence corresponding to 3.8 EFPY. The corresponding vessel beltline inner surface peak neutron fluence and computed adjusted reference temperature were $2.5 \times 10^{18}$ n/cm$^2$ and 200F, respectively.

Case 3 (section 5.3.2.2) presented below was analyzed using base material properties at both the 3.8 EFPY irradiation values of Cases 2 and 4 and using values corresponding to 4.8 EFPY. The vessel beltline inner surface peak neutron fluence and computed adjusted reference temperature corresponding to 4.8 EFPY were $3.1 \times 10^{18}$ n/cm$^2$ and 220F, respectively.

## 5.2. Flaw Parameter Assumptions

The reactor vessels in question have not operated long enough to have been subjected to an inservice inspection. Based on the shop inspections and the ASME Section XI baseline inspections, there is no evidence of flaws in any of these vessels. However, in order to perform the fracture mechanics analysis, the existence, location, orientation, and size of flaws were assumed. Surface flaws with the major axis oriented longitudinally and the minor axis oriented radially were postulated in the controlling weld metal. While the critical flaw size in the radial direction was a product of the fracture mechanics analysis, the aspect ratio for the initial flaw was assumed to be 6:1 as recommended by Section III, Appendix G of the ASME Code, and the aspect ratio for arrest and subsequent initiations was assumed to be infinitely long. This assumption is consistent with the crack propagation results from the thermal shock experiments conducted in the HSST Program.

- - - - -

*EFPY: effective full-power year.

Since the "critical" flaw size was unknown, a spectrum of sizes ranging from 0.21 to 3.0 inches with several aspect ratios were evaluated. Results showed that for the slower temperature changes (lesser degree of thermal shock — case 1, Table 1-1) deep flaws were critical but did not become limiting until several hours into the transient. However, for the fast transients (severe thermal shock — cases 2-4, Table 1-1) the shallow flaws were critical because they became "cold" at much higher stresses early in the transient. For the specific transients shown in Figures 5-2, 5-3, and 5-4 the 0.5-inch flaw provided the smallest pressure margins between allowable and actual transient pressure.

## 5.3. Results

### 5.3.1. Fracture Mechanics Evaluation Criteria

The transients evaluated here are considered to be accident conditions. Therefore, vessel integrity must be maintained to facilitate safe reactor shutdown. Crack initiation can be allowed provided the cracks can be arrested. The criterion for precluding crack initiation is as follows:

$$K_{IT} + K_{IP} + K_{IW} < K_{IC} \quad \text{at flaw size } a_1,$$

and cracks are arrested provided

$$K_{IT} + K_{IP} + K_{IW} < K_{IA} \quad \text{at flaw size } a_2$$

where

$K_{IT}$ = applied stress intensity factor due to thermals,
$K_{IP}$ = applied stress intensity factor due to pressure,
$K_{IW}$ = applied stress intensity factor due to residual stresses,
$K_{IC}$ = static crack initiation toughness,
$K_{IA}$ = crack arrest toughness.

The existence and applicability of warm prestressing is also evaluated. Warm prestressing exists provided crack initiation does not occur prior to or at the maximum applied load. If the load decreases continuously from the point of maximum load, subsequent predictions of crack initiation by LEFM are conservative for the following reasons:

1. The introduction of compressive residual stresses at the crack tip due to unloading.
2. Work-hardening in the plastic zone around the crack tip.
3. Blunting of the crack tip by plastic flow.

### 5.3.2. LEFM Results

As detailed in other sections of this report, transient cases were analyzed for break sizes of 0.007 $ft^2$ (stuck-open PORV), 0.015 $ft^2$, and 0.023 $ft^2$ (stuck-open safety relief valve). The LEFM results for the 0.007- and 0.023-$ft^2$ cases are presented in this section. The 0.015-$ft^2$ results are bounded by these cases. These transients were analyzed using three conditions of mixing. The first case (case 1, Table 1-1) is complete, perfect mixing which uses the downcomer reactor coolant temperature transient directly from CRAFT. The second mixing condition (cases 2 and 3, Table 1-1) employed MIX2 results of vent valve/HPI mixing (section 3). This second mixing condition represents an intermediate model as compared to complete mixing in CRAFT and the third mixing condition used, no mixing (case 4).

#### 5.3.2.1. 0.007-$ft^2$ Pressurizer Break Without HPI Throttling, Complete Mixing (Case 1, Table 1-1)

These transients are considered to be acceptable because crack initiation is not predicted before several hours into the event. However, a warm prestressing situation clearly exists. The operator should take action to depressurize the plant (throttle HPI) since the applied K exceeding $K_{IC}$ cannot be tolerated indefinitely. Again, these results are applicable to the base case (Rancho Seco) at 6 EFPY.

On the basis of this analysis, it was decided that subsequent analyses would be performed assuming operator action to throttle HPI (cases 2-4).

#### 5.3.2.2. 0.007- and 0.023-$ft^2$ Pressurizer Break With HPI Throttling, MIX2 Mixing (Cases 2 and 3, Table 1-1)

The allowable and actual transient pressure curves are shown in Figure 5-2 for the analyses corresponding to 3.8 and 4.8 EFPY. Again, these data represent the base case (Rancho Seco) analysis using 40F HPI temperature. Only the data for the 0.023-$ft^2$ break (case 3, Table 1-1) is illustrated since it was shown to be the worst transient; the downcomer temperature transient being more severe than that of the 0.007-$ft^2$ break (case 2, Table 1-1). Clearly, actual pressures remain below allowable, indicating no brittle fracture concern exists since crack initiation is not predicted. Again, a warm prestressing situation clearly exists.

### 5.3.2.3. 0.023-ft$^2$ Pressurizer Break With HPI Throttling, No Mixing (Case 4, Table 1-1)

In order to evaluate the required amount of water mixing in the downcomer, a series of thermal shock transients using hypothetical, worst-case downcomer conditions was analyzed. These temperature transients are 550-40, 550-90, 550-120, and 550-150F; the results of the 550-90F transient are shown, along with actual system pressure in Figure 5-3. Again, the results shown are for the base case (Rancho Seco) at 3.8 EFPY. The actual system pressure remains below allowable, indicating no brittle fracture concern exists since crack initiation is not predicted. Again, a warm prestressing condition clearly exists.

The 550-40F transient resulted in actual system pressure exceeding allowable at about 25 minutes into the transient. Crack propagation without arrest would be predicted under these hypothetical conditions.

The mixing required to heat 40° BWST water to 90°F at the RV wall in the downcomer during the critical times in the transient is slightly less than that predicted by the MIX2 model, which uses concentrated HPI flowing down the reactor vessel wall as a model (section 3.2). As previously described, Figure 3-7 shows the downcomer temperature results of the vent valve/HPI mixing predicted by MIX2 for the 0.023-ft$^2$ pressurizer break with HPI throttling. Figure 3-7 indicates that the 40F HPI fluid is warmed to approximately 90 to 100F at the RV wall by the mixing. A comparison of the allowable pressures in Figure 5-2 which assumes mixing and assumes 3.8 EFPY irradiation with Figure 5-3 which shows the results of the bounding analysis using 90° BWST fluid shows that there is another effect besides the no mixing assumption which results in lower allowable pressures for the 550-90F bounding analysis. This other hypothetical assumption is that the downcomer temperature is dropped from 550 to 90F over 50 seconds in the bounding analysis whereas if mixing occurs (Figure 3-7), this drop takes place over approximately 1 hour. Therefore, if the bounding analysis indicates 90F results are acceptable, then lesser temperatures (i.e., lesser mixing) would be acceptable using the mixing assumption.

In addition, assuming 40F HPI fluid temperature in these analyses is conservative. Borated water storage tank temperatures must be maintained between 40 and 90F during operation. Therefore, it may be possible to vary the BWST temperature within that range to assist in mitigating the thermal shock concern.

For breaks smaller than 0.023-$ft^2$, the actual transient pressures are somewhat higher. However, it takes longer before loop flow would completely stop. Therefore, the times at which the critical pressure for crack initiation without arrest exceeds the actual pressure are longer for breaks smaller than the 0.023-$ft^2$ break.

## 5.4. Applicability of Base Case (Rancho Seco)

The limiting welds with respect to brittle failure of the reactor vessel are longitudinal welds. This is true since for circumferentially oriented flaws in circumferential welds the allowable pressure would be twice that for a comparable longitudinal weld due to the differences in stress normal to the flaw orientation. Also, for longitudinal flaws in circumferential welds the base metal has substantially lower $RT_{NDT}$ thus higher toughness which prevents the flaw aspect ratio from becoming large. (Allowable pressures for flaws with a 1:1 or 2:1 aspect ratio are higher than flaws with a 6:1 aspect ratio.) Because of these inherent differences between flaws oriented in longitudinal and circumferential welds, the base analysis is only applicable to plants with longitudinal weld seams. As indicated in Table 5-1, these plants are Oconee 1, TMI-1, TMI-2, Crystal River 3, Arkansas Nuclear One (ANO-1), and Rancho Seco. The potential for cold water at the weld location would be most likely to exist only on plants with welds under or near cold leg nozzles. The locations of the longitudinal welds with respect to the cold leg nozzles are shown in Figures 5-5 through 5-10. In addition, the locations and dimensions of core flood nozzles, vent valves, and hot and cold leg pipes and nozzles are provided in Figures 5-11 and 5-12. As can be seen from these figures, the only plants with longitudinal welds under or near the cold leg nozzles are Oconee 1, ANO-1, and Rancho Seco. Welds for the other plants would be subjected to substantially higher water temperatures. Hence, the base analysis is very conservative for the other units.

The results of a bounding (no mixing, case 4) analysis using Oconee 1 material properties and an accumulated neutron fluence corresponding to 4.9 EFPY as a basis (Oconee 1 irradiation as of November 3, 1980 was 4.5 EFPY) produced acceptable results for all of the assumed BWST temperatures, including 40F. Figure 5-4 shows these results for the 550-40 and 550-90F transients.

Similar analyses showed even greater improvement for ANO-1. Clearly, Rancho Seco — which has the least irradiation — has the most restrictive allowable pressures.

In summary, significant variations in weld material, weld types, and irradiation times exist between plants, thus making the bounding analyses very conservative for some plants.

## 5.5. Conservatisms

It is felt that the fracture mechanics analysis described above has a number of inherent conservatisms. Without elaboration or quantification, these conservatisms are listed below.

1. Flaw size, shape, orientations, and location.
2. $K_{IC}$ and $K_{IA}$ lower bound toughness curves.
3. Adjusted $RT_{NDT}$ from upper bound of Regulatory Guide 1.99.
4. Applicability of LEFM to stresses above yield as in the case of severe thermal shock with pressure.
5. No credit for warm prestressing.

Table 5-1. Comparison of Reactor Vessel Materials[a]

| | | Adjustment $RT_{NDT}$, F |
|---|---|---|
| **Controlling Longitudinal Welds** | | |
| Oconee 1 (5.998 EFPY) | SA-1493 | 184[b] |
| Oconee 2 (5.528 EFPY) | NA[c] | NA |
| Oconee 3 (5.393 EFPY) | NA | NA |
| TMI-1 (5.516 EFPY) | SA-1526 | 198 |
| TMI-2 | SA-1493 | 160 |
| Crystal River 3 | WF-18/8 | 144 |
| ANO-1 | WF-18 | 160 |
| Rancho Seco | WF-70 | 222[b] |
| Davis-Besse 1 | NA | NA |
| Midland 1 | NA | NA |
| Midland 2 | BAB-243 | 39[d,e] |
| **Controlling Circumferential Welds** | | |
| Oconee 1 | SA-1229 | 171 |
| Oconee 2 | WF-25 | 223 |
| Oconee 3 | WF-67 | 173 |
| TMI-1 | WF-25 | 220 |
| TMI-2 | WF-193 | 158 |
| Crystal River 3 | WF-70 | 184 |
| ANO-1 | WF-112 | 195 |
| Rancho Seco | WF-154 | 187 |
| Davis-Besse 1 | WF-233 | 128 |
| Midland 1 | WF-70 | 151 |
| Midland 2 | BAB-243 | 39[d] |

(a) Reference: January 1, 1980 plus 2 EFPY adjustment to $RT_{NDT}$ from Regulatory Guide 1.99.

(b) These longitudinal welds are in the upper shell and underneath an inlet nozzle.

(c) NA: not applicable.

(d) The material listed is upper shell material, which is controlling over the weld material.

(e) Not a longitudinal weld.

Figure 5-1. Types of Weld Orientations

LONGITUDINAL WELD

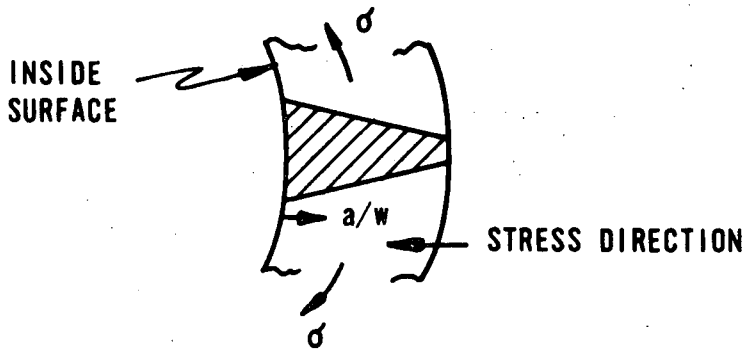


CIRCUMFERENTIAL WELD

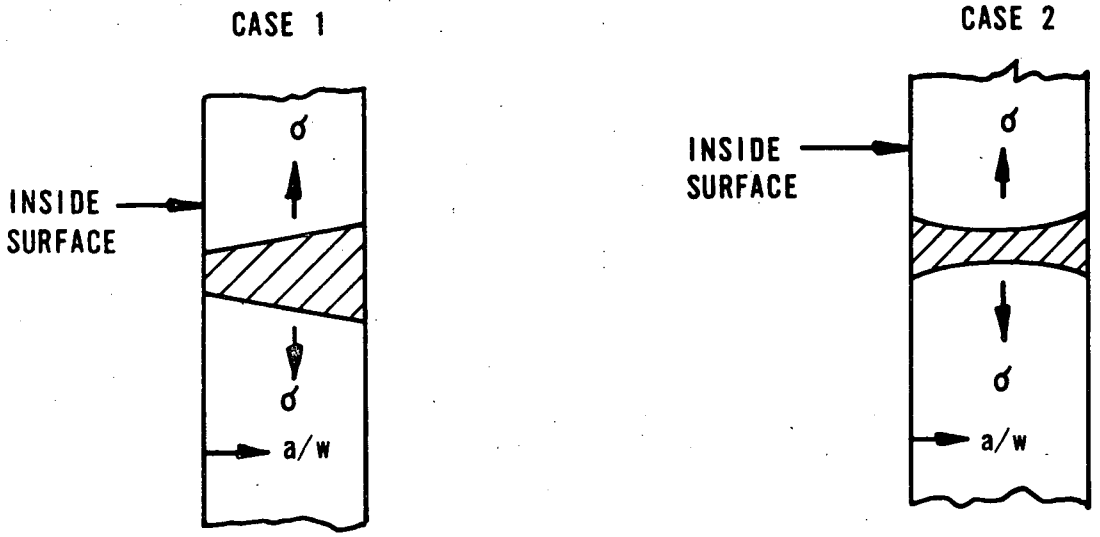

Figure 5-2. Allowable and Actual Pressures Vs Time, 0.023-ft$^2$ Pressurizer Break With Operator Action, Rancho Seco, 40F BWST, MIX2 (Case 3, Table 1-1)

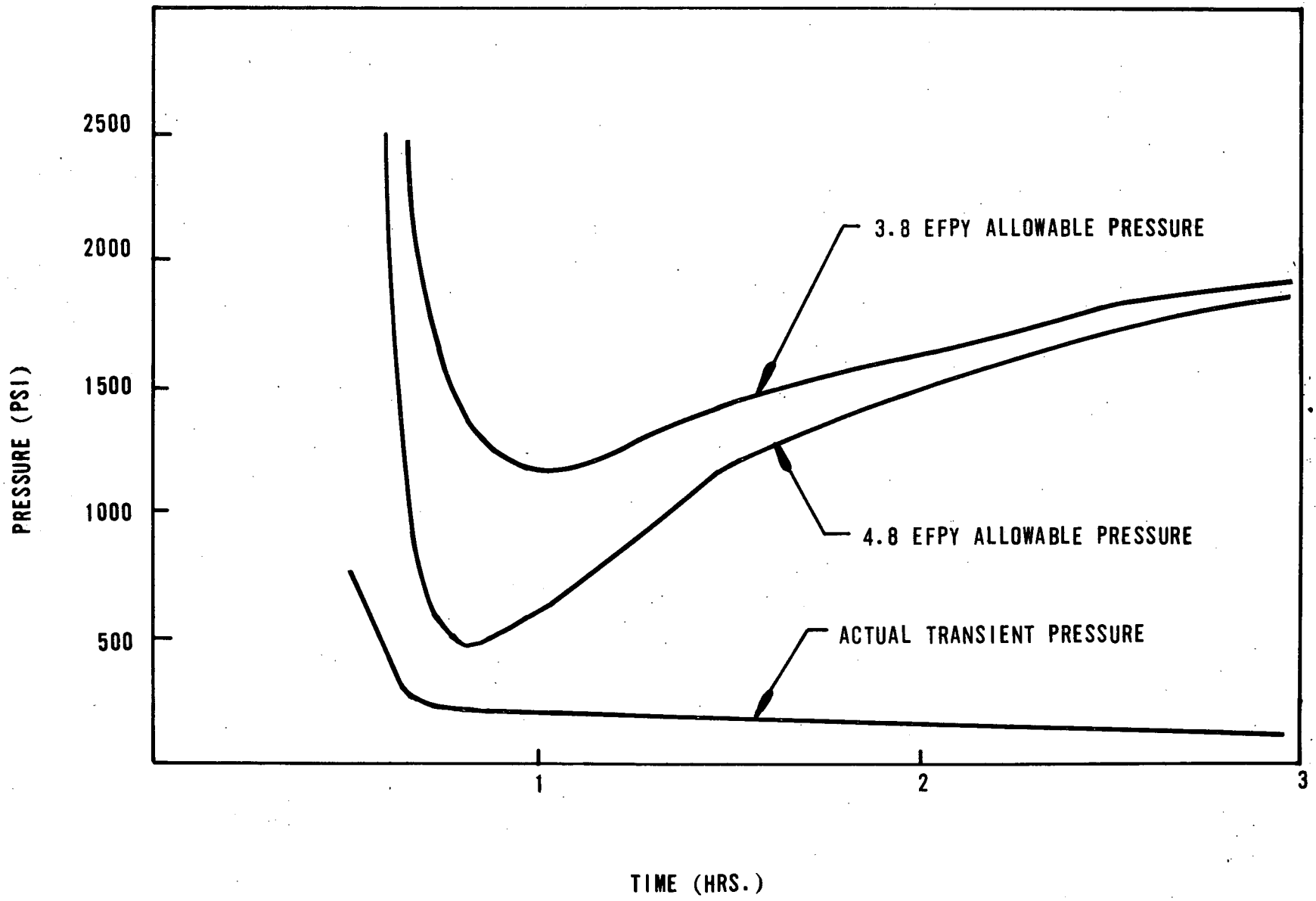

Figure 5-3. Allowable and Actual Pressure Vs Time, 0.023-ft$^2$ Pressurizer Break With Operator Action, Rancho Seco, 550-90F Transient, Bounding Analysis, 3.8 EFPY (Case 4, Table 1-1)

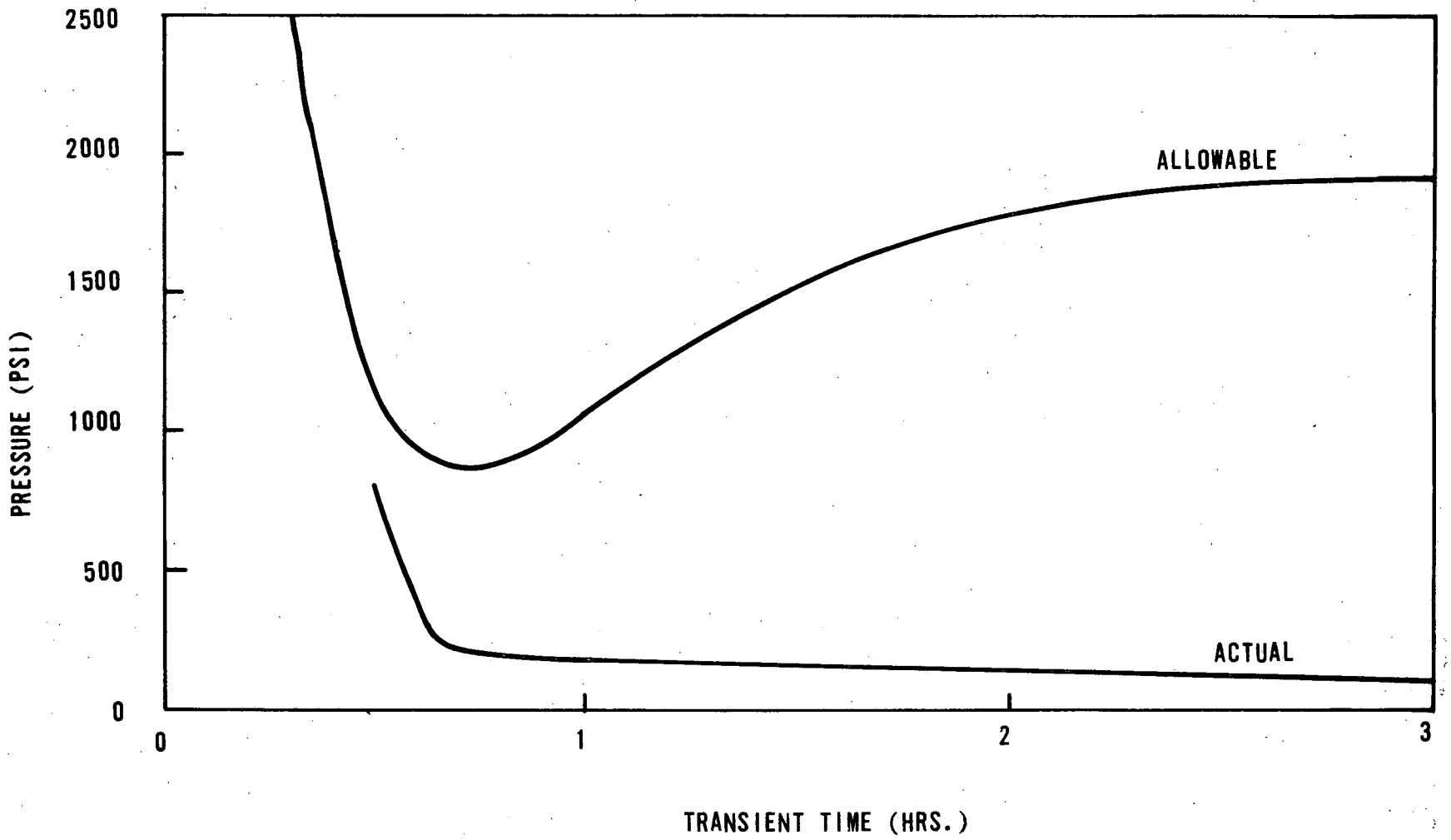

Figure 5-4. Allowable and Actual Pressure Vs Time, 0.023-ft$^2$ Pressurizer Break With Operator Action, Oconee 1, 550-90 and 550-40F Transient, Bounding Analysis, 4.9 EFPY (Case 4, Table 1-1)

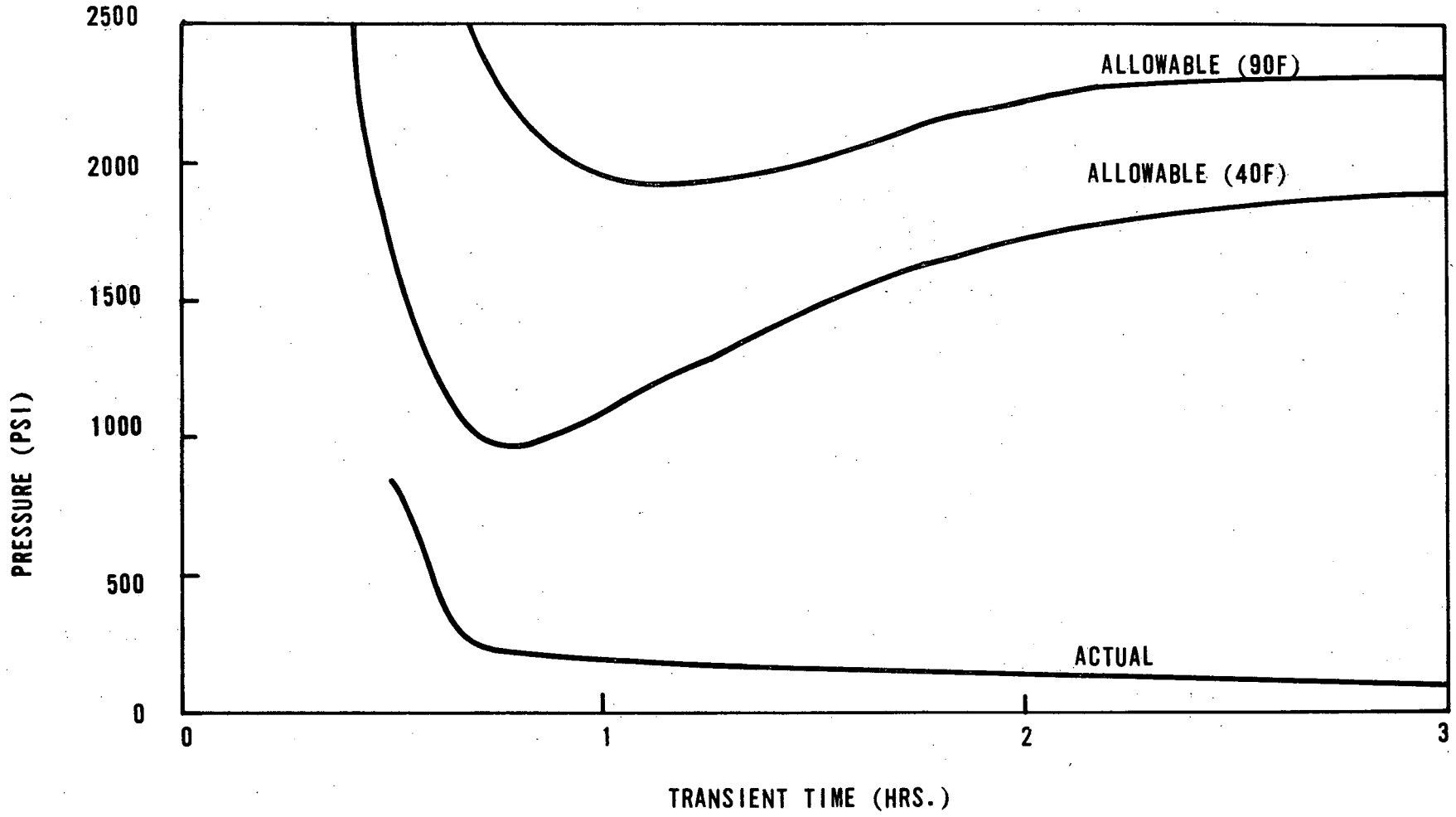

Figure 5-5. Oconee 1 Inside Surface Reactor Vessel — Weld Locations of Interest

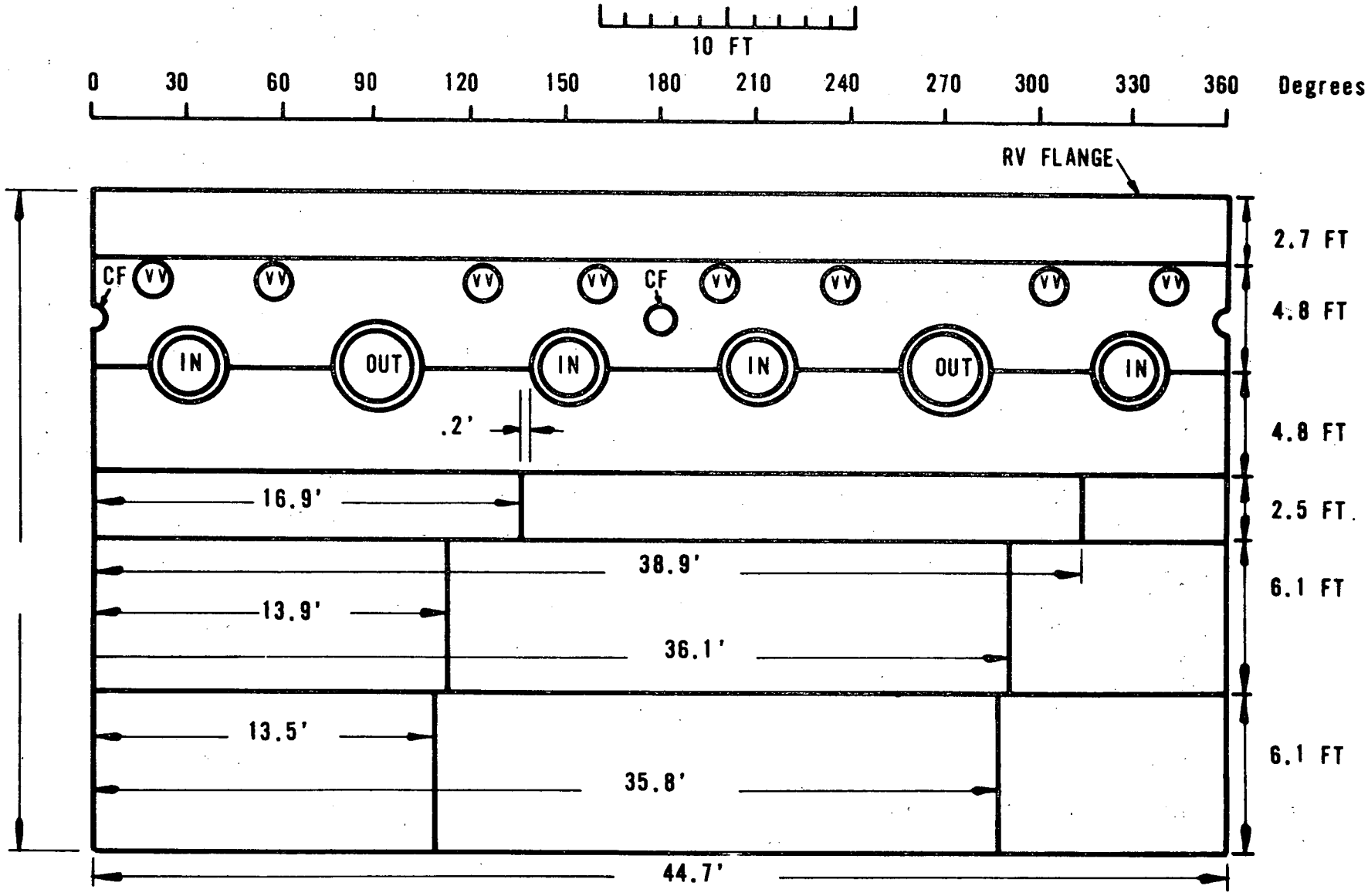

Figure 5-6. TMI-1 Inside Surface Reactor Vessel — Weld Locations of Interest

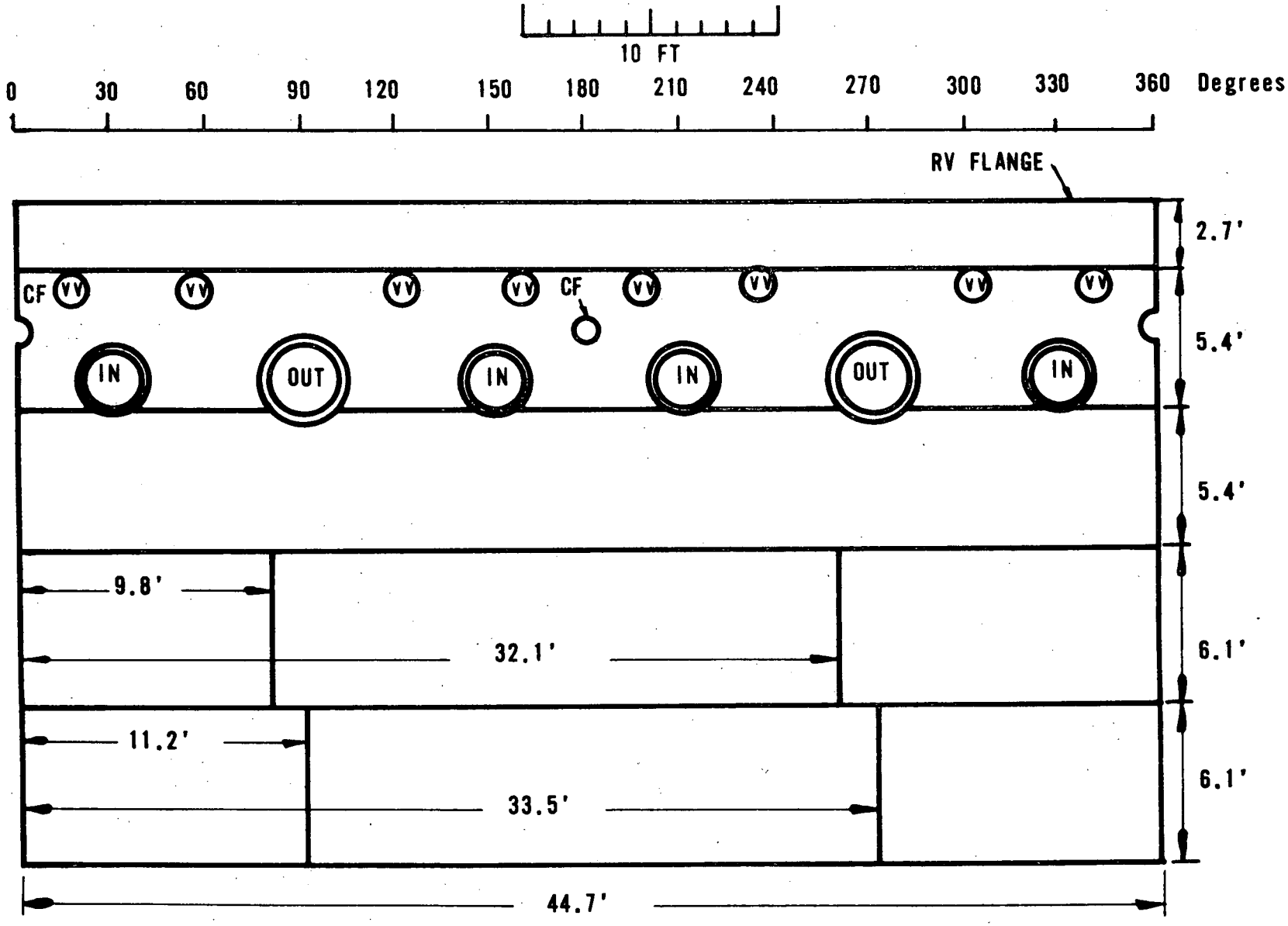

Figure 5-7. TMI-2 Inside Surface Reactor Vessel — Weld Locations of Interest

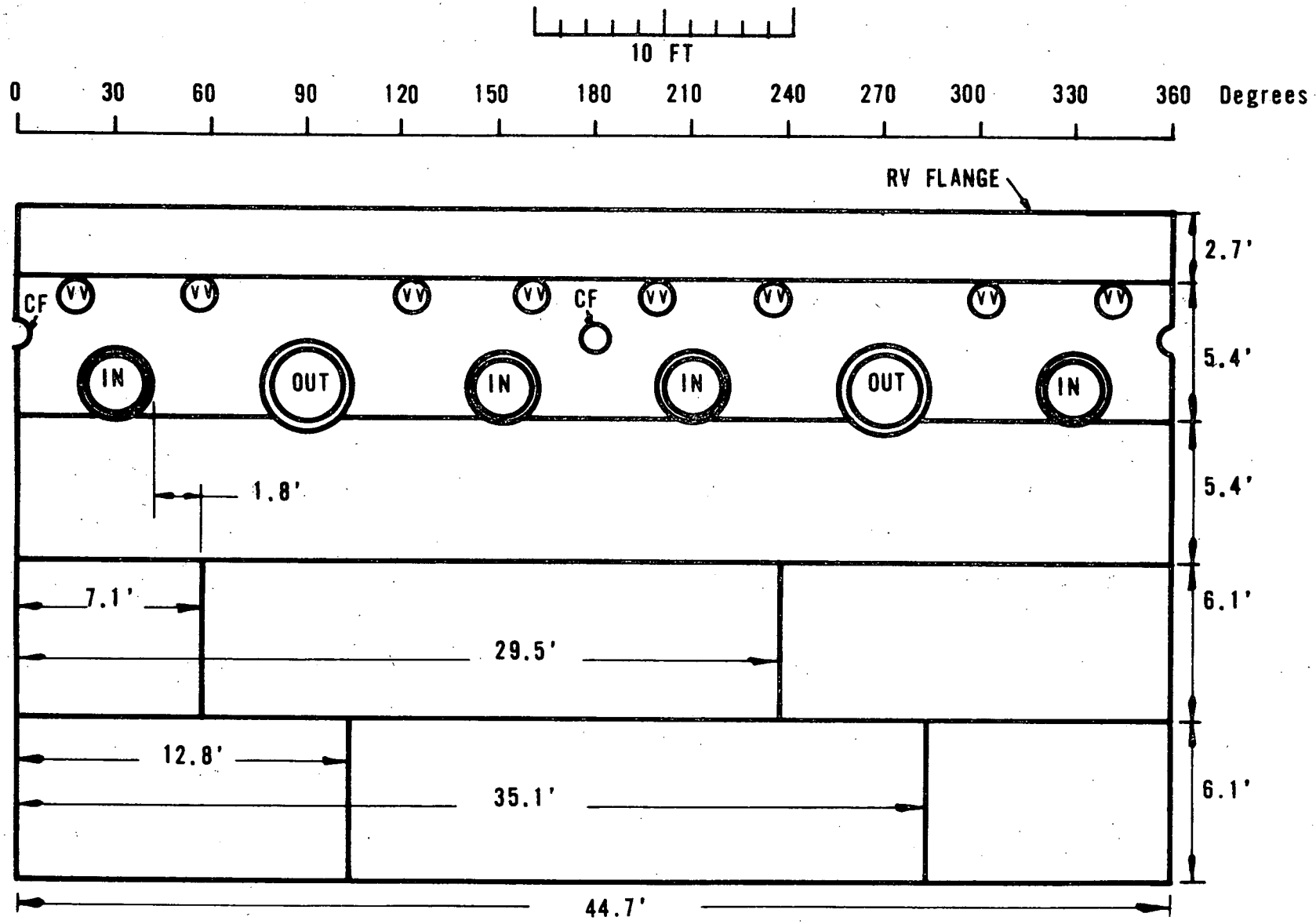

Figure 5-8. Crystal River 3 Inside Surface Reactor Vessel — Weld Locations of Interest

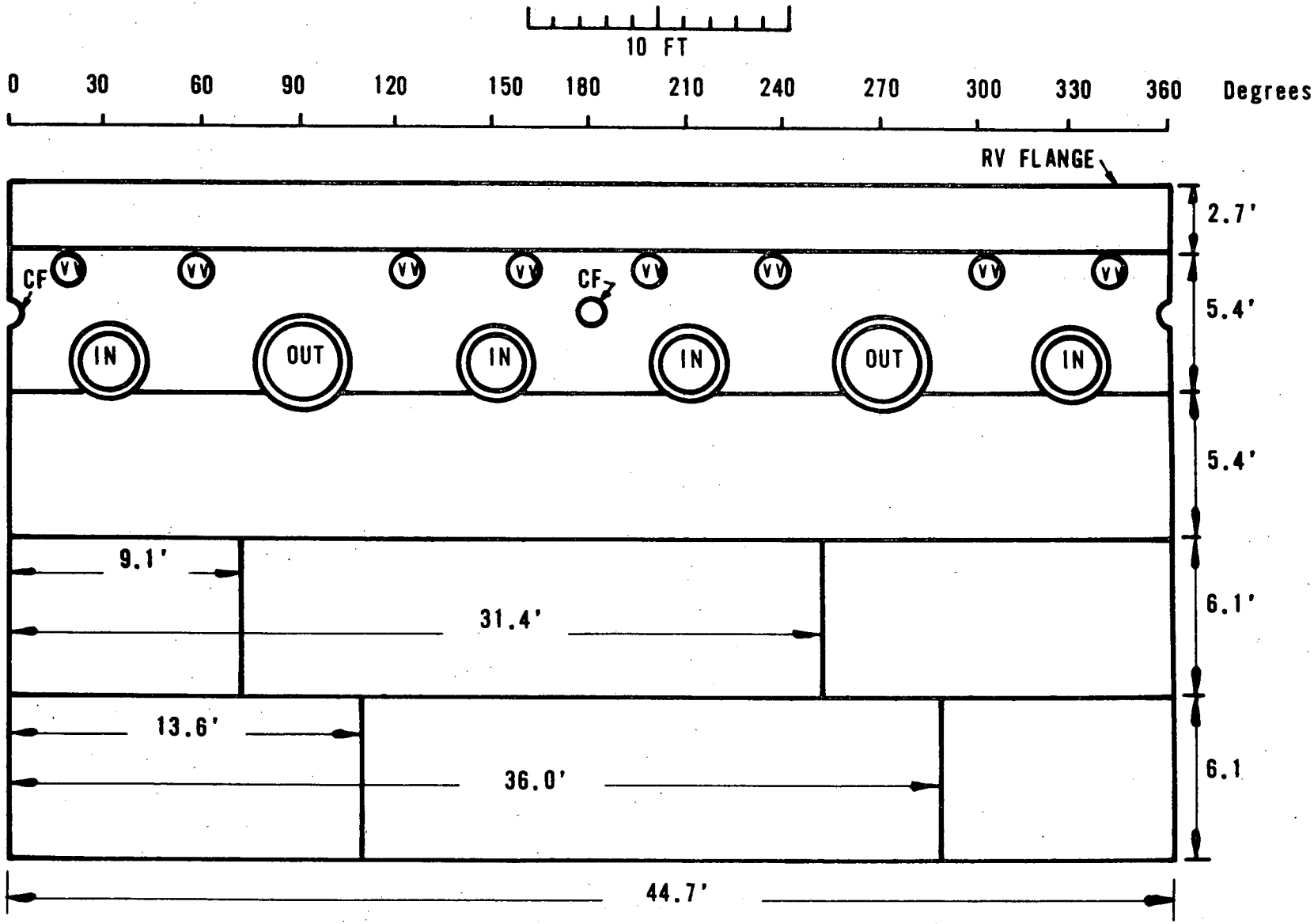

Figure 5-9. ANO-1 Inside Surface Reactor Vessel — Weld Locations of Interest

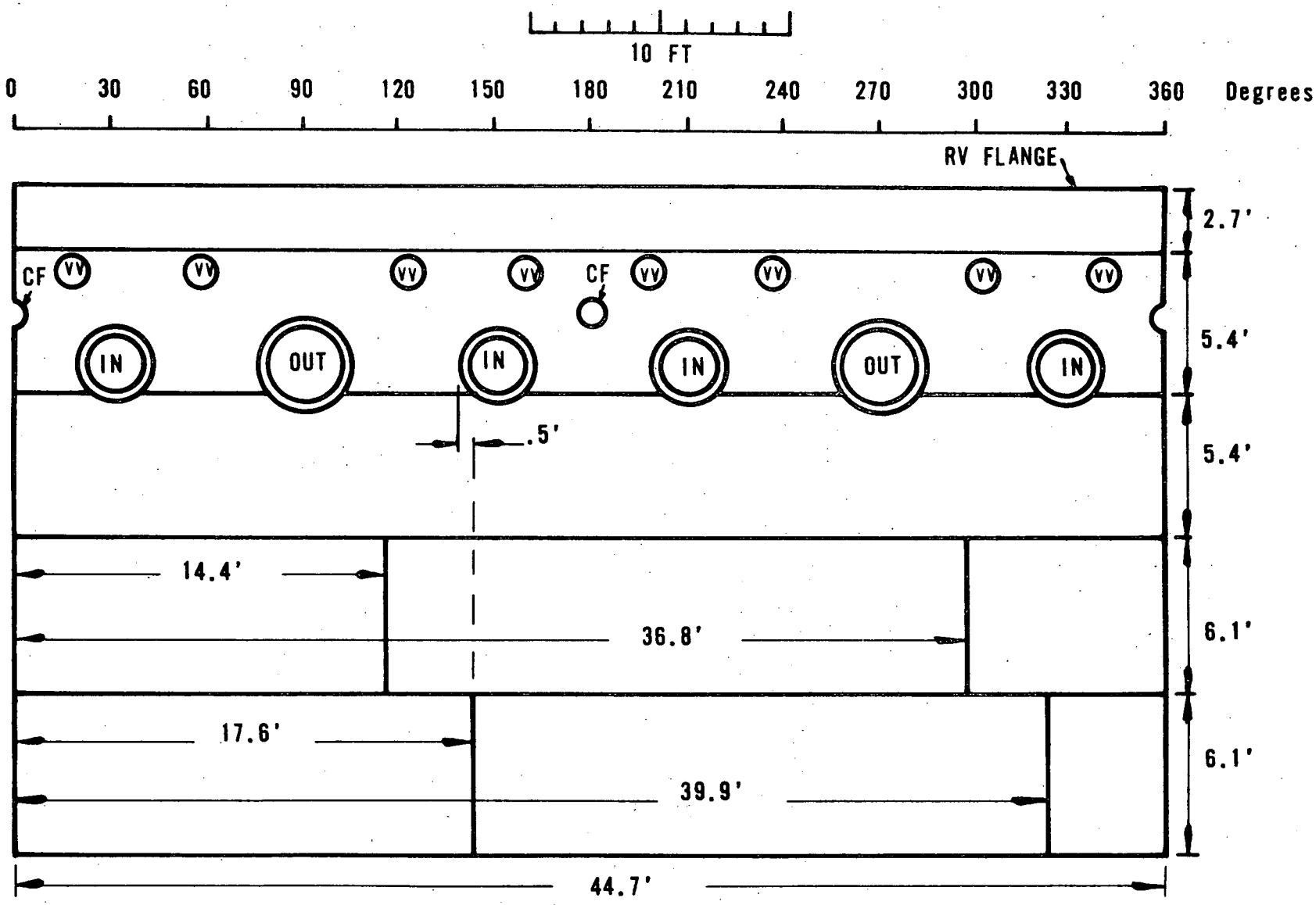

Figure 5-10. Rancho Seco Inside Surface Reactor Vessel — Weld Locations of Interest

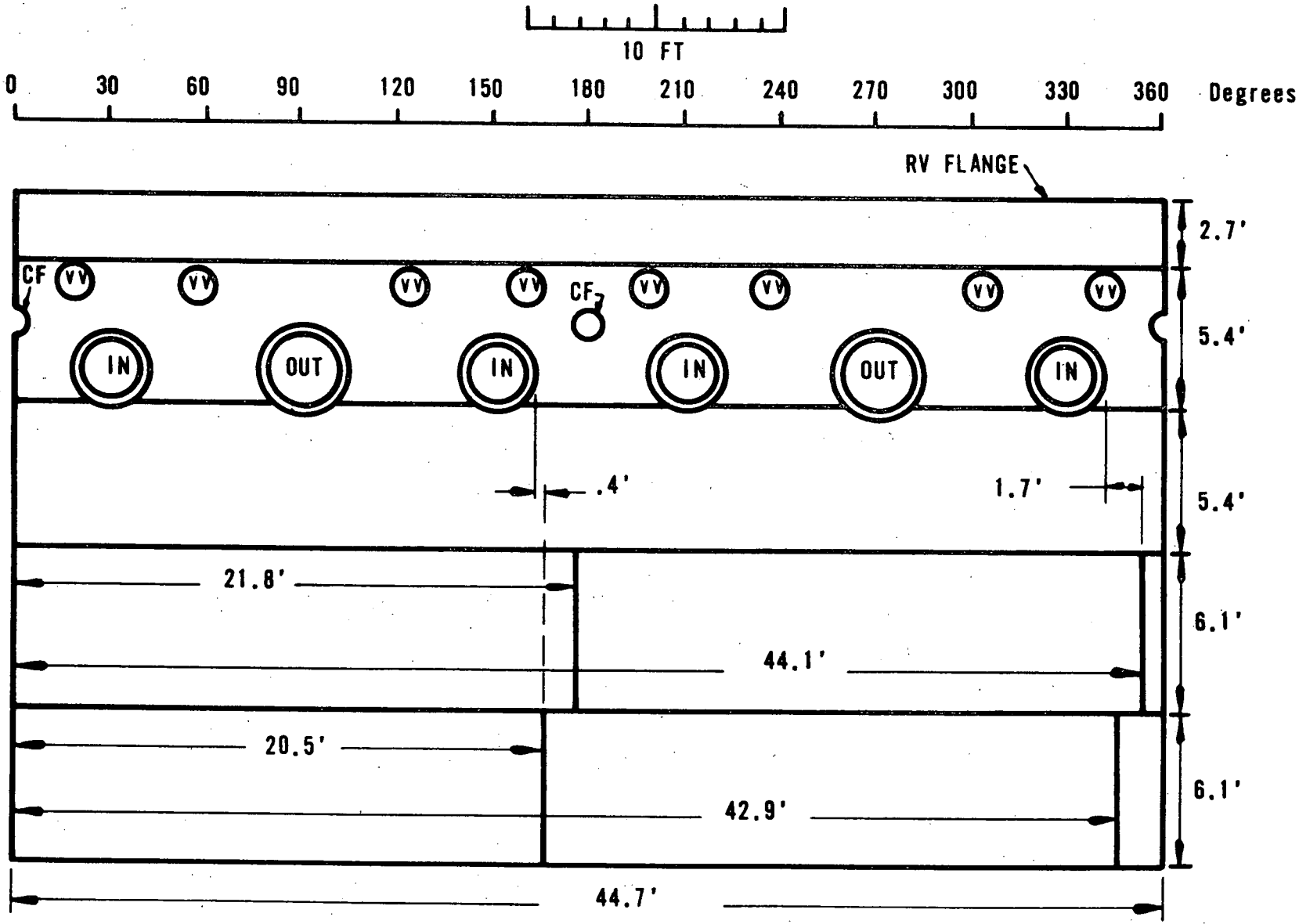

Figure 5-11. Reactor Vessel Nozzle Locations — Inside Surface, Typical 177-FA Lowered-Loop Plant

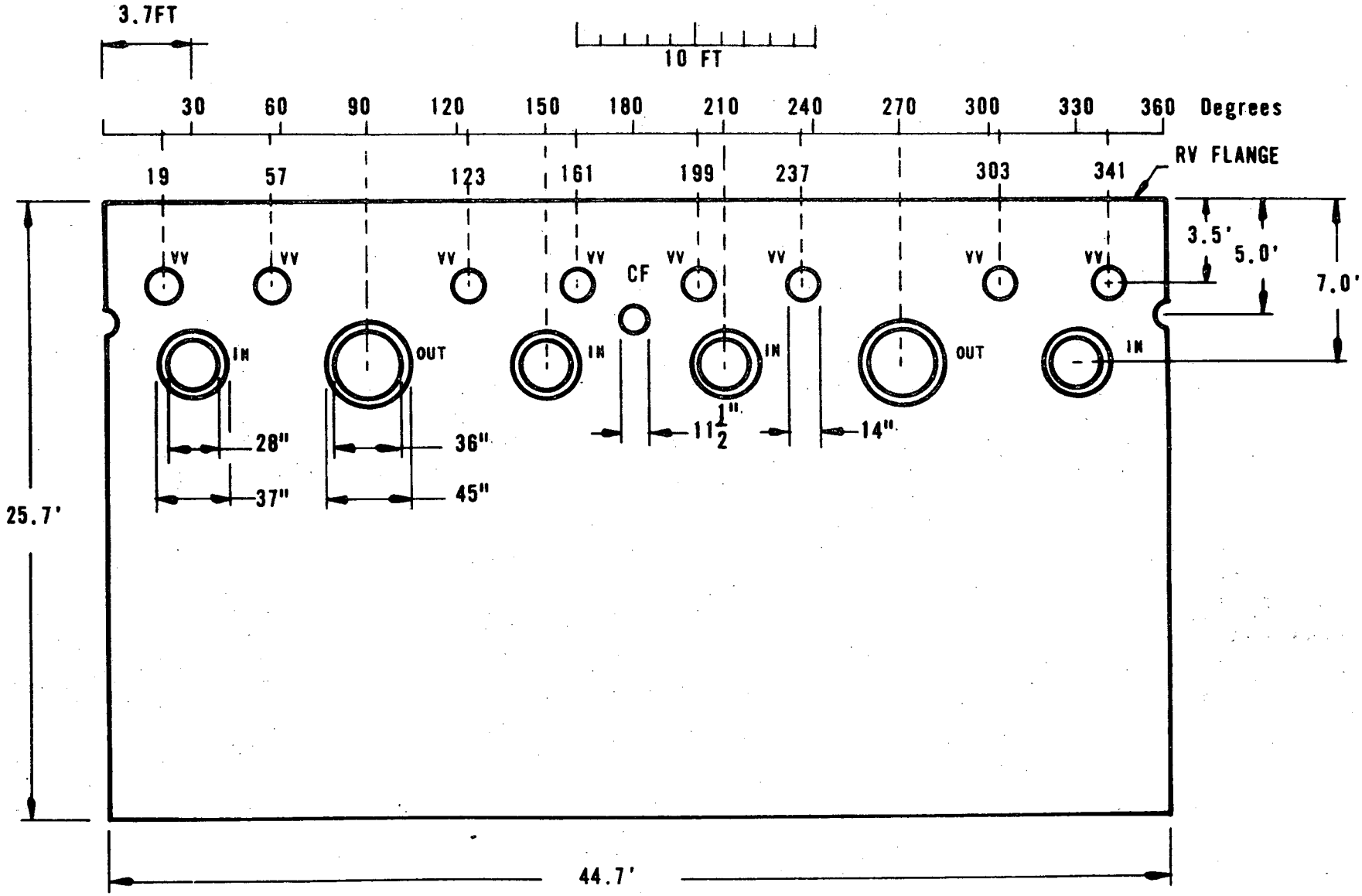

Figure 5-12. Reactor Vessel Nozzle Locations — Inside Surface, Typical 177-FA Raised-Loop Plant (Davis-Besse 1)

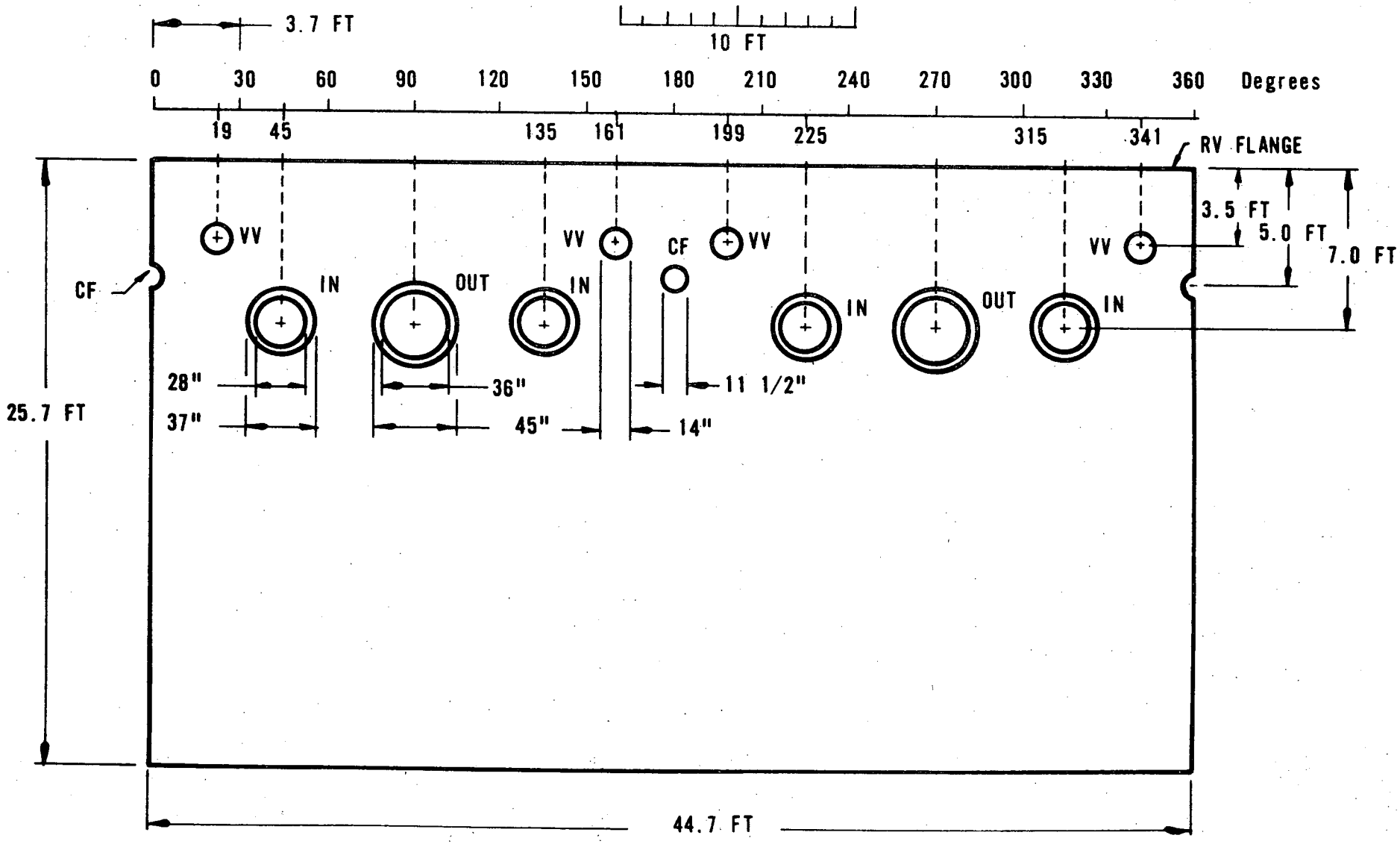

# 6. SUMMARY AND CONCLUSIONS

The investigations and analyses described in this report were performed to evaluate the concern of brittle fracture following a small LOCA, assuming an extended loss of feedwater and an extended loss of forced reactor coolant system flow. This is in response to the NRC's information request of July 12, 1979.

## 6.1. Analyses Performed

LOCA analyses were performed for break sizes of 0.007-, 0.015-, and 0.023-$ft^2$ assuming no feedwater to the steam generators. Each break size was analyzed assuming (1) no operator action and (2) the operator throttles HPI flow to maintain approximately a 100F subcooling margin at the core outlet. The purpose of the LOCA analyses was to determine the HPI flow rate, vent valve flow rate and temperature, and RCS pressure.

A very conservative evaluation was developed to define the worst case bounding downcomer temperature conditions used for the LEFM analyses. The bounding case assumed the HPI flowing into the downcomer flows down along the RV wall without spreading out circumferentially and with no mixing with the vent valve fluid. Resulting downcomer fluid bulk temperatures of 40, 90, 120, and 150F were assumed for inputs to the worst case LEFM calculations (case 4, Table 1-1).

Other, more realistic downcomer analyses were performed which included gravity effects, circumferential distribution of the vent valve flow, and mixing with the concentrated HPI flow stream (cases 2 and 3, Table 1-1).

Linear elastic fracture mechanics analyses were performed for each break size, with and without operator action to throttle HPI flow, for different mixing assumptions.

## 6.2. Conclusions

The analyses reported in other sections of this report result in the following conclusions.

### 6.2.1. General Conclusions

1. Vent valve flow occurs for the entire duration of the small break LOCA transients analyzed (Figure 2-30).
2. As long as forced flow exists (reactor coolant pumps are operating), the incoming HPI water will mix with water returning from the steam generators and no reactor vessel brittle fracture concern exists.
3. In the case in which no loop flow is present, vessel downcomer local wall temperatures will depend on the interaction of many factors including the flow rate and temperature of the HPI water, the flow rate and temperature of the vent valve return flow, and the degree of mixing between them.
4. Welds likely to experience the most rapid cooldown are those vertically below the cold leg nozzles into which HPI water is injected. The limiting welds with respect to brittle failure of the reactor vessel are longitudinal welds. Only in the Oconee 1, ANO-1, and Rancho Seco reactor vessels do longitudinal welds exist under or near the cold leg nozzles. Hence, the analysis of the longitudinal welds on Oconee 1, ANO-1, and Rancho Seco is conservative for the other welds (other operating B&W units).
5. The controlling RV material (weld and base material) with the lowest $RT_{NDT}$ was found to be the longitudinal weld seam, WF-70 in the lower shell of the Rancho Seco vessel. The properties of this material are used as the base case for generic enveloping analyses of all reactor vessels.
6. Throttling of HPI to reduce system pressures will be required to help alleviate the brittle fracture concern.

### 6.2.2. Specific Conclusions

As of November 3, 1980, Oconee 1, the lead B&W plant, had accumulated 4.5 EFPY. Rancho Seco had accumulated 3.2 EFPY. The following conclusions are burnup and mixing-model dependent. As discussed throughout this report, all of the analyses leading to these conclusions are performed using input assumptions which conservatively envelop all B&W operating plants.

1. Results of a base case (Rancho Seco) analysis corresponding to 6 EFPY and assuming complete HPI/vent valve fluid mixing (case 1, Table 1-1) are considered acceptable because crack initiation is not predicted before several hours into the event. The operator should take action to depressurize the plant (throttle HPI).

2. Base case (Rancho Seco) analyses at 3.8 and 4.8 EFPY which assume operator action to throttle HPI to maintain approximately 100F subcooled conditions at the core outlet and which assume HPI/vent valve fluid mixing as determined using MIX2 (section 3) show acceptable results (Figure 5-2). No brittle fracture concern is indicated since crack initiation is not predicted (cases 2 and 3, Table 1-1). The calculated margins between actual and allowable pressure indicate operation for some time beyond the 4.8 EFPY actually analyzed would be acceptable. A worst-case (40F) HPI temperature was assumed.

3. Base case (Rancho Seco) analyses at 3.8 EFPY which assume operator action to throttle 40F HPI to maintain approximately 100F subcooled conditions at the core outlet and which assume no HPI/vent valve mixing following loss of natural circulation (case 4, Table 1-1) result in allowable pressures being exceeded at about 25 minutes into the transient. Crack initiation without arrest would be predicted for this hypothetical case. (The no HPI/vent valve mixing assumption means the RV downcomer fluid temperature at the RV wall changed from 550 to the HPI temperature of 40F in 50 seconds when RC loop flow (natural circulation) stopped.) Analysis of the same transient assuming 90F HPI water gives acceptable results (Figure 5-3).

   The same transient using 40F HPI water (worst case) was analyzed using Oconee 1 data at 4.9 EFPY. Oconee 1 is the second most limiting reactor vessel. The results (Figure 5-4) are acceptable indicating no brittle fracture concern for all reactor vessels except Rancho Seco using any BWST temperature including the worst case (40F). Crack initiation is not predicted. Similar analyses using ANO-1 data indicated even greater margins. Again, the calculated margins between actual and allowable pressure indicate operation for some time beyond the irradiation actually analyzed would be acceptable.

4. State-of-the-art methods do not presently support highly accurate analytical predictions of the three-dimensional fluid mixing in the downcomer. Until the amount of mixing between HPI fluid and vent valve fluid is better defined, the exact amount of margin, the length of time that margin exists, or the adequacy of operation action to eliminate any brittle fracture concern cannot be rigorously determined. Certainly the analyses reported herein are in many respects conservative with what the actual situation is expected to be. The major arguments supporting this are

   - An extended total loss of feedwater or extended loss of loop flow is unrealistic.
   - Some mixing and heating of the HPI will occur.
   - Warm prestressing benefits are present.

## 7. REFERENCES


[1] CRAFT — Fortran Program for Digital Simulation of a Multinode Reactor Plant During LOCA, BAW-10092, Babcock & Wilcox, Lynchburg, Virginia, April 1975.

[2] D. F. Ross (NRC) to J. H. Taylor (B&W), letter, "Information Request on Reactor Vessel Brittle Fracture," July 12, 1979.

[3] P. K. Nair, S. B. Skaar, and D. E. Smith, BEFRAN-1 Beltline Fracture Analysis, NPGD-TM-498, Babcock & Wilcox, Lynchburg, Virginia, May 1979

[4] F. W. Dittus and L. M. K. Boelter, University Publications in Engineering, Vol 2 (1930), p 443.

[5] G. C. Vliet and D. C. Ross, "Turbulent Natural Convection ...," ASME J. Heat Transfer, November 1975, pp 549-555.

[6] Nuclear Systems Material Handbook, Vol 1 (1978), TID-26666, Hanford Engineering Development Laboratory, Richland, Washington (1978).

[7] ASME Boiler and Pressure Vessel Code, Section III, Appendixes (1977).

[8] D. T. Buchanan and Y. H. Hsii, FELCON — General Purpose Program for Solving Thermal Conduction Problems, NPGD-TM-268, Rev. 1, Babcock & Wilcox, Lynchburg, Virginia, February 1979.

[9] D. A. Ferril, P. B. Juhl, and D. R. Miller, "Measurement of Residual Stresses in a Heavy Weldment," Welding Journal, WRG Supplement, Vol 45, No. 11, November 1966.

[10] ASME Boiler & Pressure Vessel Code, Section XI, Appendix A.

[11] P. K. Nair, Accident Transients Fracture Analysis for 177-FA Reactor Vessel Beltline Region, BAW-1605, Babcock & Wilcox, Lynchburg, Virginia, January 1980.

LOCA REPRESSURIZATION DUE TO LOSS OF STEAM CONDENSING SURFACE IN SG'S

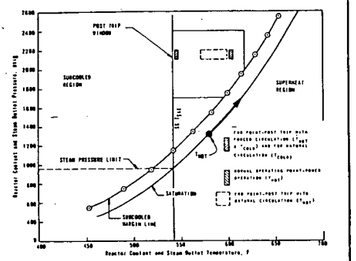


NOTES: 1. PR IS AVAILABLE TO AT LEAST 150.

REVERSE HT TRANSFER DUE TO RCS DEPRESSURIZATION

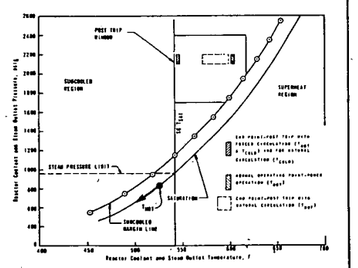


NOTES: 1. $P_{RCS} < P_{SG}$

LACK OF PRIMARY TO SECONDARY HT TRANSFER

TREAT LACK OF ADEQUATE SUBCOOLED MARGIN -

IS ONE SG LEVEL INC. TO 95% OR OP RANGE
YES | NO

NO HEAT TRANSFER DUE TO LOSS OF STEAM CONDENSING SURFACE OR RCS DEPRESSURIZATION

NO HT TRANSFER DUE TO LOSS OF SEC. INVENTORY

REVERSE HT. TRANSFER*
YES | NO

LOWER STEAM PRESSURE UNTIL ($T_{SAT}$) SO IS EQUAL TO (Th - 50F)

HEAT TRANSFER*
YES | NO

GO TO COOLDOWN PROCEDURE FOR SATURATED CONDITIONS WITH A SMALL BREAK

IS REVERSE HT TRANSFER RE-ESTABLISHED*
YES | NO

GO TO LONG TERM COOLING FOLLOWING A MAJOR LOCA

CAN RC PUMPS BE STARTED*
YES | NO

LOWER STEAM PRESSURE UNTIL ($T_{SAT}$) SG IS EQUAL TO (Th-50)
NOTE: IF $P_{RCS}$ > 1500 PSIG NO REDUCTION IN STEAM PRESSURE IS REQUIRED

BUMP AN RC PUMP & LET SYSTEM STABILIZE (SEE BEST METHODS FOR EQUIPMENT OPERATION)

HEAT TRANSFER TO ONE OR TWO SG*
NO | YES

WAIT 15 MIN
OPEN PORV - IF $P_{RCS}$ > 2300 CLOSE PORV WHEN PRCS < $P_{SG}$ + 100

HAVE 4 RC PUMPS BEEN BUMPED*
NO | YES

LOWER STEAM PRESSURE UNTIL ($T_{SAT}$) SG = (Th - 100)

START AN RC PUMP & LET IT CONTINUE TO RUN

GO TO COOLDOWN PROCEDURE FOR SATURATED CONDITIONS WITH A SMALL BREAK

IF $P_{RCS}$ > 2300 PSIG OPEN PRV; CLOSE PRV WHEN PRCS < $P_{SG}$ + 100 PSIG

HEAT TRANSFER*
YES | NO

SUBCOOLED MARGIN
YES | NO

GO TO PLANT COOLDOWN PROCEDURE FOR SUBCOOLED CONDITIONS AND A SMALL BREAK

GO TO HPI COOLING

START HPI COOLING
- OPEN PRV & MAINTAIN MAX HPI -

RESTORE FEEDWATER (MAIN OR EMERGENCY) & RAISE LEVEL TO 95% OR OP RANGE

IS F/R RESTORED TO AT LEAST ONE SG*
NO | YES

GO TO HPI COOLING

HEAT TRANSFER TO OPERATIVE SG(s)
YES | NO

STOP HPI COOLING (CLOSE PRV)

SUBCOOLED MARGIN*
YES | NO

THROTTLE HPI

GO TO COOLDOWN PROCEDURE FOR SUBCOOLED CONDITIONS WITH SMALL BREAK

GO TO COOLDOWN PROCEDURE FOR SATURATED CONDITIONS WITH A SMALL BREAK

LOCA REPRESSURIZATION DUE TO NO FEEDWATER

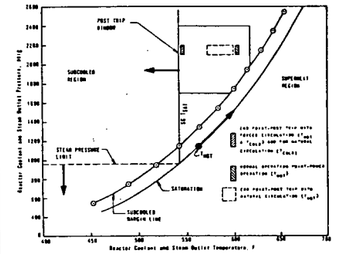


NOTES:
1. NO FW IS "ON": SG LEVEL IS LOW OR ZERO.
2. SEE FIGURE F-8 AND F-10 FOR TYPICAL LOCA EXAMPLES

Figure 6
POST-LOCA CORRECTIVE ACTION FOR LACK OF PRIMARY TO SECONDARY HEAT TRANSFER

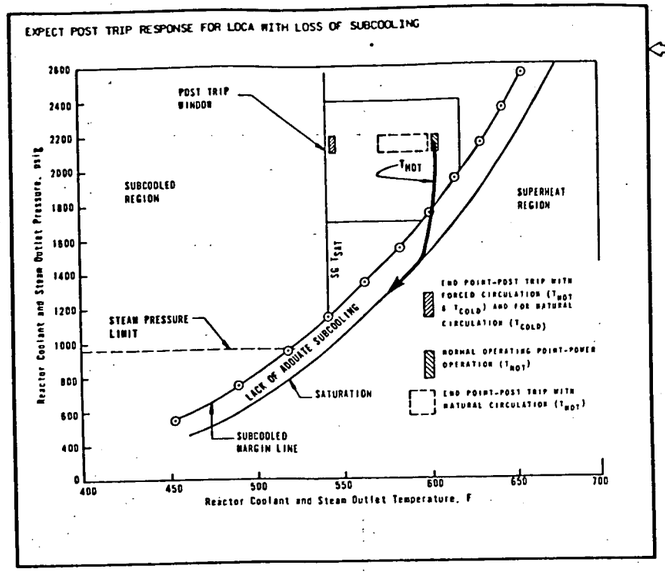


LACK OF ADEQUATE SUBCOOLED MARGIN

*1. TRIP RC PUMPS

*2. CONFIRM 2-HPI ON AT MAX. CAPACITY & BALANCE FLOWS

*3. CONFIRM EFW 'ON' & RAISE LEVEL TO 95%

4. ATTEMPT TO LOCATE AND ISOLATE THE LOCA

SUBCOOLED MARGIN?

| YES | NO |
|---|---|

THROTTLE HPI

ABNORMAL SYMPTOMS? (OVERHEATING OR OVERCOOLING)

| NO | YES |
|---|---|

GO TO PLANT COOLDOWN PROCEDURE FOR SUBCOOLED CONDITIONS WITH A SMALL BREAK

TREAT OVERCOOLING OR OVERHEATING PER PROCEDURE

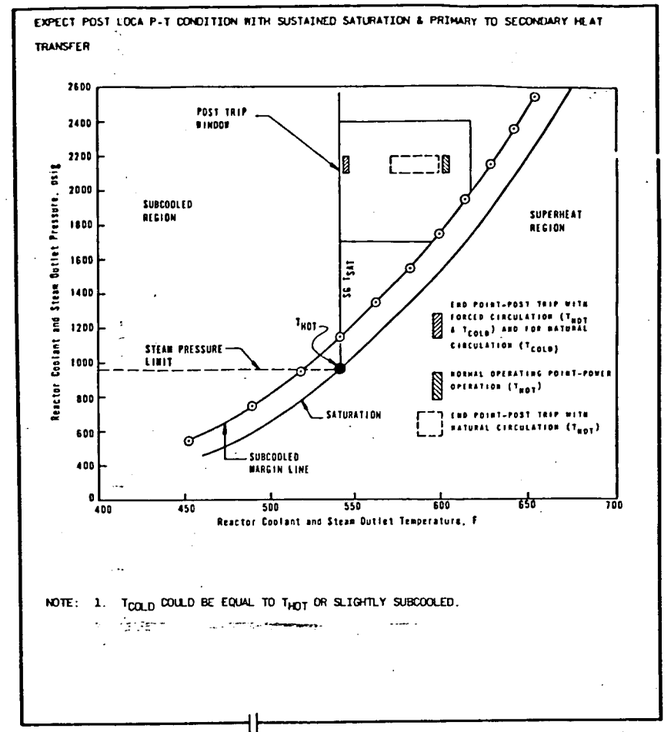


NOTE: 1. $T_{COLD}$ COULD BE EQUAL TO $T_{HOT}$ OR SLIGHTLY SUBCOOLED.

HEAT TRANSFER IN BOTH SG?

| YES | NO |
|---|---|

GO TO PLANT COOLDOWN PROCEDURE FOR SATURATED CONDITION WITH A SMALL BREAK

GO TO LACK OF PRIMARY TO SECONDARY HT. TRANSFER

*FOR MORE DETAILS, GO TO ATOG PART II BEST METHODS OF EQUIPMENT OPERATION.

Figure 5

POST-LOCA CORRECTIVE ACTION FOR LACK OF ADEQUATE SUBCOOLED MARGIN

## CORRECTIVE ACTIONS FOR LOW MAIN FEEDWATER TEMPERATURE

## CORRECTIVE ACTIONS FOR HIGH STEAM GENERATOR LEVEL

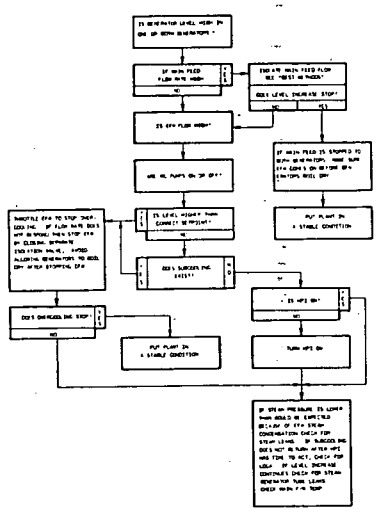

## CORRECTIVE ACTIONS FOR LOW STEAM PRESSURE

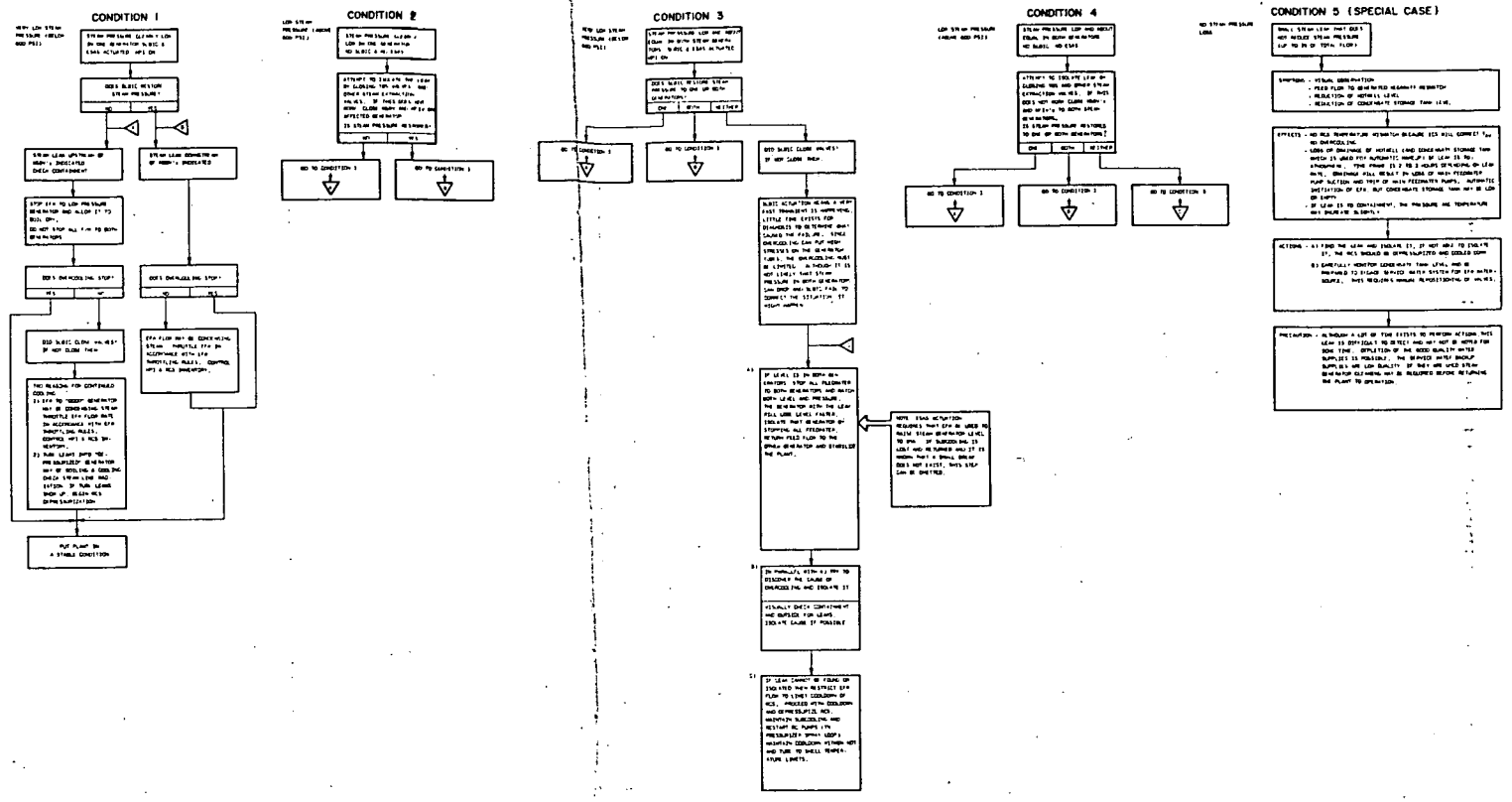


## FIGURE 3 OVERCOOLING DIAGNOSIS CHART

### TYPICAL P-T DIAGRAM

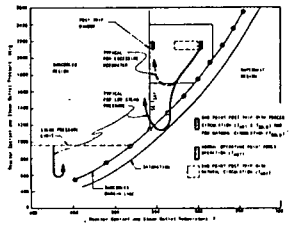

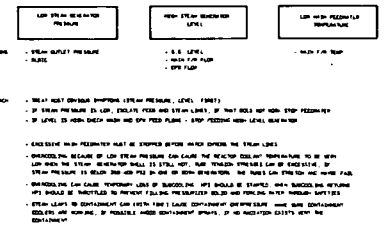

# TABLE 4 SYMPTOMS FOR LOCA'S THAT CAN BE LOCATED OR ISOLATED

THIS CHART WILL AID IN LOCATING SOME BREAKS; ALL BREAKS CANNOT BE LOCATED. SOME BREAKS WHICH CAN BE LOCATED CAN ALSO BE ISOLATED AND THE LOCA CAN BE STOPPED. IT MAY BE DIFFICULT TO DISTINGUISH SMALL STEAM LINE LEAKS INSIDE CONTAINMENT FROM LOCA'S; BUILDING ENVIRONMENT WILL CHANGE FOR BOTH AND THE STEAM PRESSURE WILL NOT ALWAYS BE LOW. HOWEVER, A LOCA WILL CHANGE BUILDING RADIATION LEVELS; AND THE REACTOR WILL REPRESSURIZE AND REGAIN FULL SUBCOOLING WITH A STEAM LINE BREAK.

## SYMPTOMS FOR LOCA'S THAT CAN BE ISOLATED

(Symptoms or alarms most likely to show location are underlined)

| FAILURE | LOCATING SYMPTOMS | ISOLATING HARDWARE |
|---|---|---|
| Makeup and purification system outside containment and letdown coolers | - Low makeup tank level<br>- High ICW radiation<br>- High ICW surge tank level (for breaks in letdown cooler)<br>- Local sump levels, radiation alarms | Letdown valve **1) upstream of coolers |
| Seal return line and seal return cooler outside containment | - Low makeup tank level<br>- High ICW radiation<br>- High ICW surge tank level (for breaks in seal return cooler)<br>- Local sump levels, rediation alarms<br>- High seal return flow | Seal return**1) isolation valve |
| Pressurizer electromatic relief valve | - Acoustic Monitor Alarm<br>- High quench tank level<br>- High quench tank temperature<br>(These will only be good when the quench tank rupture disk is good) | ERV isolation valve |
| Makeup-letdown imbalance (this is not a break, but is a loss of coolant) | - High makeup tank level<br>- Bleed holdup tank level<br>- Makeup flow rate (+) seal injection flow (-) letdown flow | Letdown control**1) valve |
| Decay heat removal line break outside containment (decay heat removal system in operation-plant is cooled down) | - High or low decay heat removal flow<br>- Low pump suction press.<br>- Local sump and local radiation alarms | Decay heat letdown**2) drop line valve |
| Decay heat cooler tube leak (decay heat removal sys. in operation- plant is cooled down) | - High ICW surge tank level<br>- High ICW radiation | Cooler isolation valves |

## SYMPTOMS FOR LOCA'S THAT CANNOT BE ISOLATED

(Symptoms or alarms most likely to show location are underlined)

| | |
|---|---|
| Steam Generator Tube(s) | - High steam line radiation<br>- High steam generator level |
| Pressurizer Safety Valves | - Acoustic Monitor Alarm<br>- High quench tank level<br>- High quench tank temperature<br>(These will only be good while the quench tank rupture disk is good) |
| HPI Injection Line Break | - Flow imbalance between injection**3) lines (High flow will be through broken line) |
| RC Pump Seal Failure | - High seal return temperature ($\sim 350^{o}F$) combined with: Low stage and upper stage pressures are equal and high |
| RCS Instrumentation Lines<br>- Pressurizer Level<br>- Pressures<br>- RC Flow | - False low level reading<br>- False low pressure<br>- False high or low flow compared with known pump operation |

**Footnotes:
1) Do not allow makeup tank to drain or operating makeup pump will lose suction and fail.
2) Inadequate Core Cooling Guidelines for loss of decay heat removal should be implemented.
3) Break cannot be isolated to prevent loss of reactor coolant, but HPI line can be closed to prevent loss of injection water